

THE ELECTRONIC STRUCTURE OF DISORDERED SYSTEMS

1976

P. M. DOOLEY

UMI Number: U431420

All rights reserved

INFORMATION TO ALL USERS

The quality of this reproduction is dependent upon the quality of the copy submitted.

In the unlikely event that the author did not send a complete manuscript and there are missing pages, these will be noted. Also, if material had to be removed, a note will indicate the deletion.



UMI U431420

Published by ProQuest LLC 2015. Copyright in the Dissertation held by the Author.
Microform Edition © ProQuest LLC.

All rights reserved. This work is protected against
unauthorized copying under Title 17, United States Code.



ProQuest LLC
789 East Eisenhower Parkway
P.O. Box 1346
Ann Arbor, MI 48106-1346



THESIS
521.925
31.3.77

x753016582

STATEMENT

The accompanying thesis submitted for the degree of Ph.D. entitled 'The Electronic Structure of Disordered Systems' is based on work conducted by the author in the Department of Physics of the University of Leicester mainly during the period between October, 1972 and September, 1975.

All the work recorded in this thesis is original unless otherwise acknowledged in the text or by references. None of the work has been submitted for another degree in this or any other university.

Signed: ..P..M..Dooley..... Date: 20..November...1976.

DEDICATION

To my mother and father for all they denied themselves over the past years so that this thesis could be written.

ACKNOWLEDGEMENTS

I wish to thank Professor John L. Beeby for encouragement, patience and excellent supervision over my three years with the physics department at the University of Leicester. I should also like to thank Dr. Peter Jewsbury for countless helpful discussions and guidance for part of the work presented in this thesis. Miss Janet Carbone, Mrs. Jacky Plews, and Mrs. Rosemary Littler are to be thanked for their preparation of the manuscript. I also wish to thank my wife Elizabeth for her support and encouragement at all times. Finally thanks are due to the University of Leicester for the receipt of a research demonstratorship during the period of this work.

CONTENTS

INTRODUCTION	i
CHAPTER I LIQUID ALLOYS	
1.1 Introduction	1
1.2 The 'Metallic' Alloys	3
1.3 The Liquid Semiconductors	9
1.4 The Liquid Semiconductor Problem	14
CHAPTER II CHARGE TRANSFER IN ORDERED AND DISORDERED ALLOYS	
2.1 Charge Transfer, Ionicity And Covalency	16
2.2 The Importance Of Charge Transfer In Disordered Alloys	19
2.3 Coherent Potential Approximation and Binary Disordered Alloys	22
2.4 Charge Transfer In Liquid Semiconductors	32
CHAPTER III CHARGE TRANSFER AND ELECTRONEGATIVITY DIFFERENCE	
3.1 Electronegativity Difference	37
3.2 Electrochemical Effects In Alloys Of Cadmium, Magnesium And Mercury	39
3.3 Electrochemical Effect In Simple Metal Alloys	47
CHAPTER IV CHARGE TRANSFER AND ATOMIC CELL SIZE	
4.1 The Problem	60
4.2 The Change In Atomic Cell Size With Charge Transfer	61
4.3 The One-Dimensional Binary Alloy	69
4.4 Three-Dimensions	74
CONCLUSION : PART I	77

CHAPTER V	THE HYDROGEN MOLECULE IN AN ELECTRON GAS	
5.1	Introduction	78
5.2	Hydrogen Molecule In An Electron Gas I	79
5.3	Hydrogen Molecule In An Electron Gas II	87
5.4	Conclusion	95
CHAPTER VI	THE CHEMICAL COMPLEX IN MOLTEN Mg-Bi AND Tl-Te	
6.1	Introduction	96
6.2	Thermodynamic Properties	97
6.3	Hall Effect, Conductivity and Energy Of Mixing	103
6.4	Conclusion	105
CHAPTER VII	MUFFIN-TINS : PHASESHIFTS	
7.1	Introduction	107
7.2	Construction Of The Muffin-Tin Potential	108
7.3	Single Scatterer: Phaseshifts	111
7.4	Local Electronic Density Of States: Scattering Path Operator	118
CHAPTER VIII	A CALCULATION ON THE SEMICONDUCTING MAGNESIUM- BISMUTH SYSTEM	
8.1	Introduction	121
8.2	Theoretical Approach	123
8.3	The Bottom Of The Band In A Liquid Alloy	126
8.4	Calculations And Results	129
8.5	Discussion	135
8.6	Behaviour Of Transport Properties	139
8.7	Summary	141
CONCLUSION	: PART II	142

Appendix I

Appendix II

Bibliography

INTRODUCTION

There is a class of binary liquid alloys whose electrical properties closely resemble those normally associated with solid semiconductors over a restricted range of compositions. They are often referred to as liquid semiconductors. These are low conductivity liquids, with conductivities which increase with temperature, and Hall coefficients that depart markedly from the free electron behaviour. Liquid Cu-Te, Ag-Te, Tl-Te, In-Te, Mg-Bi and all alloys involving selenium as one component are some of the alloys classified as semiconducting. This thesis constitutes a theoretical study of liquid semiconductors made up of components which are metallic in the pure liquid state (e.g., Mg-Bi, Li-Bi), since it is possible to continually follow the transition from the metallic to the semiconducting behaviour.

Chapter I introduces the electrical behaviour of liquid alloys posing the problems presented by the liquid semiconducting systems. The possibility of the formation of chemical complexes Mg_3Bi_2 , Li_3Bi in liquid semiconducting Mg-Bi, Li-Bi has been put forward (c.f. Enderby, 1974). Chapters II, III and IV look at charge transfer in ordered and disordered alloys as a means to understanding the nature of the bonding within such systems. The suitability of electronegativity difference as a meaningful parameter in determining the degree of ionicity within chemically bonded disordered alloy systems, as well as the problem of defining the atomic cell size, are considered in depth. Chapter V examines the binding of the hydrogen molecule in an electron gas serving as a basis for the

(ii)

treatment in Chapter VI of the covalently bonded Mg_3Bi_2 complex in molten Mg-Bi. The final chapters present a phenomenological study carried out on the Mg-Bi system using the multiple scattering techniques appropriate in the muffin-tin approximation for the atomic potentials. Chapter VII introduces the muffin-tin concept and that of associated scattering phaseshifts for the atomic potential, while Chapter VIII gives details of the calculation performed on the liquid Mg-Bi system. The conclusions reached represent a departure from the thinking of the previous chapters.

CHAPTER I

LIQUID ALLOYS

1.1 INTRODUCTION

The electrical behaviour of liquid alloys has been extensively studied by means of measurements of the conductivity (σ), the Hall coefficient (R) and the thermoelectric power (S). Several workers have been able to distinguish the existence of at least three groups of liquid alloys, each with its own characteristic electrical properties.

One group is made up of liquid alloys whose electron transport parameters are typical of the metallic state. The conductivity is in excess of $3000\Omega^{-1}\text{cm}^{-1}$, the thermopower less than $\pm 50\mu\text{V deg}^{-1}$, the Hall coefficient is approximately equal to R_0 , the free electron value, and $\frac{d\sigma}{dT}$ is always negative. Liquid Ag-Au, Mg-Cd, In-Tl, Pb-Sn, Bi-Sb are some of the alloys known to fall within this group.

A second group includes liquids with intermediate conductivities ($5000\Omega^{-1}\text{cm}^{-1} > \sigma > 1800\Omega^{-1}\text{cm}^{-1}$), positive values of $\frac{d\sigma}{dT}$, and metallic type Hall coefficients and thermoelectric powers. Liquid Cu-Sn, Bi-Te, Sb-Te, Au-Te, Cd-Sb are some of the alloys known to fall in this group.

The final group is made up of liquid alloys for which the transport parameters are substantially different from those typical of the metallic state over a restricted range of compositions. They are low conductivity liquids ($\sigma < 200\Omega^{-1}\text{cm}^{-1}$) with positive values of $\frac{d\sigma}{dT}$ and Hall coefficients which are quite distinct from those of normal liquid alloys. This final group includes liquid Cu-Te, Ag-Te,

Tl-Te, In-Te, Mg-Bi and all liquid alloys involving selenium as one component.

Enderby and Collings (1970) have classified liquid alloys into two groups, one appreciably more metallic in character than the other. Type I alloys are characterized by Hall coefficients, thermoelectric powers and conductivities which are essentially smooth functions of composition. The first group of liquid alloys above are type I, known as simple liquid alloys. The second group are type I alloys in which $\frac{d\sigma}{dT}$ is positive. There is good reason to believe (Enderby, 1974) that type I liquid alloy transport properties may be treated by the theoretical techniques of Faber and Ziman (1965). Alloys in the final group are type II liquid alloys, usually referred to as liquid semiconductors. Joffe and Regel (1960) first thought that alloys in the second group could also be classed as liquid semiconductors, but subsequent experimental evidence (Enderby and Simmons, 1969; Allgaier, 1969) ruled out such a classification, in spite of a positive $\frac{d\sigma}{dT}$. Type II alloys are characterized by Hall coefficients, thermoelectric powers and conductivities which vary sharply over a well defined composition range, deviating markedly from values typical of the metallic state. They are usually referred to as liquid semiconductors because they exhibit most of the properties associated with the solid semiconductors.

The second section of this chapter looks at the electrical behaviour of the type I, or more metallic, liquid alloys. The experimental features which characterize these systems, and the theoretical methods appropriate to their understanding, are

presented. The third section looks in detail at the electrical properties of the liquid semiconducting systems, while the final section spells out the problems they present. In order to make matters more definite these systems will be subdivided into five categories depending upon the electrical nature of the constituents of each alloy in the pure liquid state. Liquid Mg-Bi, for example, is made up of two components which are both metallic in the liquid state, hence this alloy system is a metal-metal liquid semiconductor. Particular attention is paid to the metal-metal liquid semiconductors since it is possible to follow the gradual transition from the metallic to the semiconducting state. The theoretical models offered for these systems are presented and criticised in subsequent chapters.

1.2 THE 'METALLIC' ALLOYS

1.2.1 Transport Properties

The nearly free electron theory expresses the conductivity (σ) of electrons in the form

$$\sigma = \frac{ne^2\tau}{m} \quad (1.2.1)$$

where n is the electron number density, e , the electron charge, m , the electron mass and τ , the mean free time between collisions.

This may readily be expressed in terms of the mean free path, L :

$$\sigma = \frac{e^2LS_F}{3\pi^2\hbar} \quad (1.2.2)$$

where $S_F \equiv$ area of Fermi surface $= 4\pi K_F^2$, with K_F the Fermi wavenumber.

If a is denoted as the average interatomic spacing, in the limit $L \gg a$, the so called weak scattering limit (c.f. Mott, 1973),

conductivities are in excess of about $3000\Omega^{-1}\text{cm}^{-1}$. This has been observed to be a regime into which many liquid metals and alloys fall, and it has been possible to evaluate the conductivity from (1.2.2) for pure metals (Ziman, 1961) and alloys (Faber-Ziman, 1965) using appropriate prescriptions for L . In this same limit, the thermoelectric power (S) is related to the conductivity through

$$S = \frac{\pi^2}{2} \frac{K_B^2 T}{e} \left[\frac{d \ln(\sigma)}{dE} \right]_{E=E_F} \quad (1.2.3)$$

This is often expressed in terms of the resistivity (ρ) through

$$S = \frac{\pi^2}{2} \frac{K_B^2 T}{e E_F} x$$

where $x = -E_F \left[\frac{\partial \ln(\rho)}{\partial E} \right]_{E=E_F} = -E_F \left[\frac{1}{\rho} \frac{\partial \rho}{\partial E} \right]_{E=E_F} = -E_F \left[\frac{1}{\rho} \frac{\partial \rho}{\partial K} \frac{\partial K}{\partial E} \right]_{E=E_F}$

$$(1.2.4)$$

Providing it is assumed that all valence electrons contribute to the conduction process, the Hall coefficient (R) is given by the elementary expression

$$R = \frac{1}{ne} \quad (1.2.5)$$

In the limit $L \lesssim a$ ($\sim 3 \text{ \AA}$), Mott postulates that conduction in disordered systems is still largely due to the extended electron states, with the conductivity strongly dependent on the density of states at the Fermi level. (1.2.2) has been generalised to give

$$\sigma = \frac{e^2 L S_F}{3\pi^2 \hbar} g^2 \quad (1.2.6)$$

where $g = \frac{n(E_F)}{n_0(E_F)}$ is in the range 1 to 0.3,

with $n(E_F)$, the real density of states, $n_0(E_F)$, the free electron density of states, both evaluated at the Fermi energy. In this regime, liquid conductivities fall between $3000\Omega^{-1}\text{cm}^{-1}$ and $200\Omega^{-1}\text{cm}^{-1}$. The thermopower is expressed in terms of the density of states at the Fermi energy

$$S = \frac{\pi^2}{3} \frac{K_B^2 T}{e} 2 \left[\frac{d \ln n(E)}{dE} \right]_{E=E_F} \quad (1.2.7)$$

It is not easy to go beyond free electron theory to obtain a sensible expression for the Hall coefficient.

Below a conductivity of $200\Omega^{-1}\text{cm}^{-1}$, Mott argues that conduction processes do not involve extended electron states.

1.2.2 Faber-Ziman Theory

The Faber-Ziman nearly free electron theory for liquid alloys determines the resistivity and thermoelectric power in terms of pseudopotentials through the structure factor, $a(q)$.

The structure factor is defined to be (Appendix 1):

$$\begin{aligned} a(q) &= \frac{1}{N} \sum_i \exp(-i \mathbf{q} \cdot \mathbf{r}_i) \\ &= 1 + \frac{N}{V} \int_0^\infty \{g(r)-1\} \frac{\sin qr}{qr} 4\pi r^2 dr \end{aligned} \quad (1.2.8)$$

where N is the number of scatterers, q , the wavenumber, \mathbf{r}_i , the position of the nuclei, V , the volume of the sample, and $g(r)$, the radial distribution function. The resistivity (ρ) is then given as

$$\rho = \frac{3\pi}{he^2} \frac{N}{V v_F^2} \langle v^2(q) a(q) \rangle \quad (1.2.9)$$

where $v(q)$ is the atomic pseudopotential, v_F , the Fermi velocity,

and

$$\langle F(q) \rangle \equiv \text{average over } q \text{ from } 0 \text{ to } 2K_F = \int_0^{2K_F} F(q) q^3 dq$$

In a liquid alloy there are three radial distribution functions g_{11} , g_{22} , g_{12} where the numbers 1 and 2 refer to the alloy components, and, consequently, there are three partial structure factors a_{11} , a_{22} , a_{12} . The partial structure factors are related to the radial distribution functions through

$$a_{\alpha\beta} = 1 + \frac{N}{V} \int_0^{\infty} \{g_{\alpha\beta}(r) - 1\} \frac{\sin qr}{qr} 4\pi r^2 dr \quad (1.2.10)$$

where $g_{\alpha\beta}$ represents the distribution of α -type atoms from a β -atom origin, α and β being dummy suffices which take on values 1 and 2.

The binary alloy resistivity is then given by

$$\begin{aligned} \rho_{\text{ALLOY}} &= \frac{3\pi}{\hbar e^2} \frac{N}{V v_F^2} \langle c(1-c)v_1^2 + c(1-c)v_2^2 - 2c(1-c)v_1v_2 \\ &\quad + c^2v_1^2a_{11} + (1-c)^2v_2^2a_{22} + 2c(1-c)v_1v_2a_{12} \rangle \\ \text{i.e. } \rho_{\text{ALLOY}} &= \frac{3\pi}{\hbar e^2} \frac{N}{V v_F^2} \langle v_1^2\{c(1-c) + c^2a_{11}\} + v_2^2\{c(1-c) + (1-c)^2a_{22}\} \\ &\quad + 2c(1-c)v_1v_2(a_{12}-1) \rangle \end{aligned} \quad (1.2.11)$$

where c is the concentration of component 1, v_1 , the pseudopotential of component 1, and v_2 , the pseudopotential of component 2.

A considerable simplification occurs in the case of an alloy in which the two constituents are so similar that they may be substituted one for the other. Provided

- (1) the scattering is weak,
- (2) $a_{11} = a_{22} = a_{12} = a$,
- (3) v_1, v_2 are concentration independent,

and (4) the Fermi wavenumber remains practically constant in the

alloying process,
the resistivity is given by

$$\rho_{\text{ALLOY}} = \frac{3\pi}{\hbar e^2} \frac{N}{v_F^2} \langle a\{c v_1^2 + (1-c)v_2^2\} + c(1-c)(1-a)(v_1 - v_2)^2 \rangle \quad (1.2.12)$$

(1.2.12) describes accurately the concentration dependence of the resistivity for the simple liquid alloys, Ag-Au and Na-K.

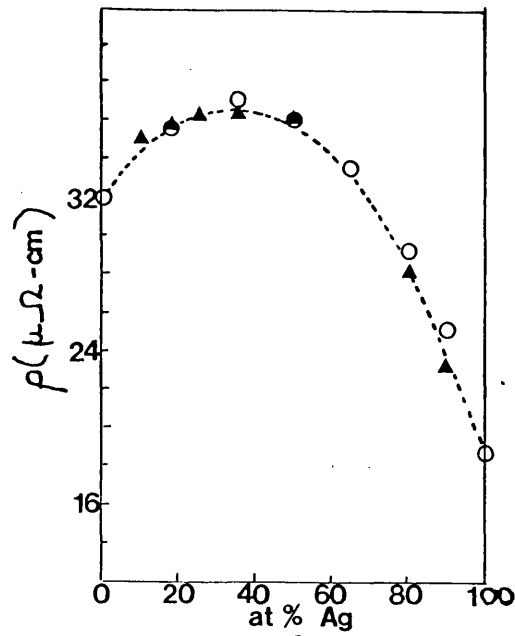
The thermopower parameter x from (1.2.4) can be expressed

$$x_{\text{ALLOY}} = \frac{E}{K} \frac{\partial K}{\partial E} \left| 2 \frac{K}{v} \frac{\partial v}{\partial K} + 4 - 4 \frac{F(2K_F, K)}{\langle F(2K_F, K) \rangle} - K \frac{\langle \frac{\partial}{\partial K} F(2K_F, K) \rangle}{\langle F(2K_F, K) \rangle} \right| \quad (1.2.13)$$

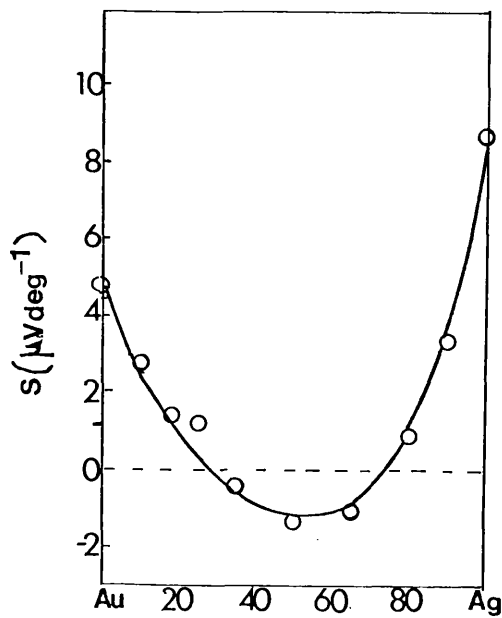
$$\text{where } \langle F(q, K) \rangle = \langle v_1^2 \{c(1-c) + c^2 a\} + v_2^2 \{(1-c)c + (1-c)^2 a\} + v_1 v_2 \{2c(1-c)(a-1)\} \rangle$$

1.2.3 Experiment and Theory: A Comparison

The metallic liquid alloys fall into two basic categories each characterized by Hall coefficients, thermoelectric powers and conductivities which are essentially smooth functions of composition. Liquid Ag-Au, Na-K, Mg-Cd, In-Tl, Pb-Sn, Bi-Sb are some of the alloys which belong to the first category, known as simple liquid alloys. With conductivities greater than $3000 \Omega^{-1} \text{cm}^{-1}$, thermopowers less than $+50 \mu\text{V deg}^{-1}$ and Hall coefficients not significantly different from the free electron value, these alloys possess transport parameters usually associated with liquid metals. Liquid monovalent Ag-Au was the first of these systems to be studied in which sound agreement was found between the Faber-Ziman theory and experiment (Howe and Enderby, 1967). The resistivity and thermopower curves are given in figure 1.2.1. Enderby et al (1968) went on to compare experimental data for Mg-Cd, In-Tl,



The resistivity of liquid Ag-Au at 1135°C. ○ Howe & Enderby, 1967
 ▲ Rall & Motz, 1957.



Thermopower of liquid Au-Ag at 1135°C ○ Howe & Enderby, 1967.
 — Theoretical curve derived from Faber-Ziman theory.

Fig. 1.2.1

Pb-Sn, Bi-Sb with theory and again found reasonable agreement (figure 1.2.2). Faber-Ziman theory appears to work well for the simple liquid alloys.

The second category of liquid alloys, considered more metallic in character by Enderby and coworkers, are distinctive in that they are alloys in which $\frac{d\sigma}{dT}$ is positive, for which reason they were once thought to be semiconducting (Joffe and Regel, 1960). Conductivities fall between $3000\Omega^{-1}\text{cm}^{-1}$ and $1800\Omega^{-1}\text{cm}^{-1}$, thermoelectric powers and Hall coefficients are metallic in character. Figure 1.2.3 presents the conductivity of liquid (a) ZnSb, (b) Bi_2Te_3 , (c) Sb_2Te_3 taken from Enderby and Walsh (1966). The smooth variation of conductivity with composition for molten Bi-Te at 585°C is depicted in figure 1.2.4. Systematic investigations of σ , S and R as functions of composition for the liquid Cu-Sn alloy have been carried out by Enderby and Howe (1968) and Enderby, Hasan and Simmons (1967). A Faber-Ziman nearly free electron picture is found to provide a good basis for understanding the electron transport phenomena. For the Hall coefficient in particular, Enderby et al suppose that R is always inversely proportional to the electron number density, n. However, as a result of the composition fluctuations in the liquid alloy, the effective valence of the Sn atoms is either two or four, depending upon the environment. In order to approximate this effect it is assumed that the effective valence of Cu is always one, while that for Sn varies linearly from two at the Cu-rich end to four at the Sn-rich end. The electron number density is thus given by

$$n = \frac{(1+c+2c^2)N_0}{c(M_1-M_0)+M_0} \quad (1.2.14)$$

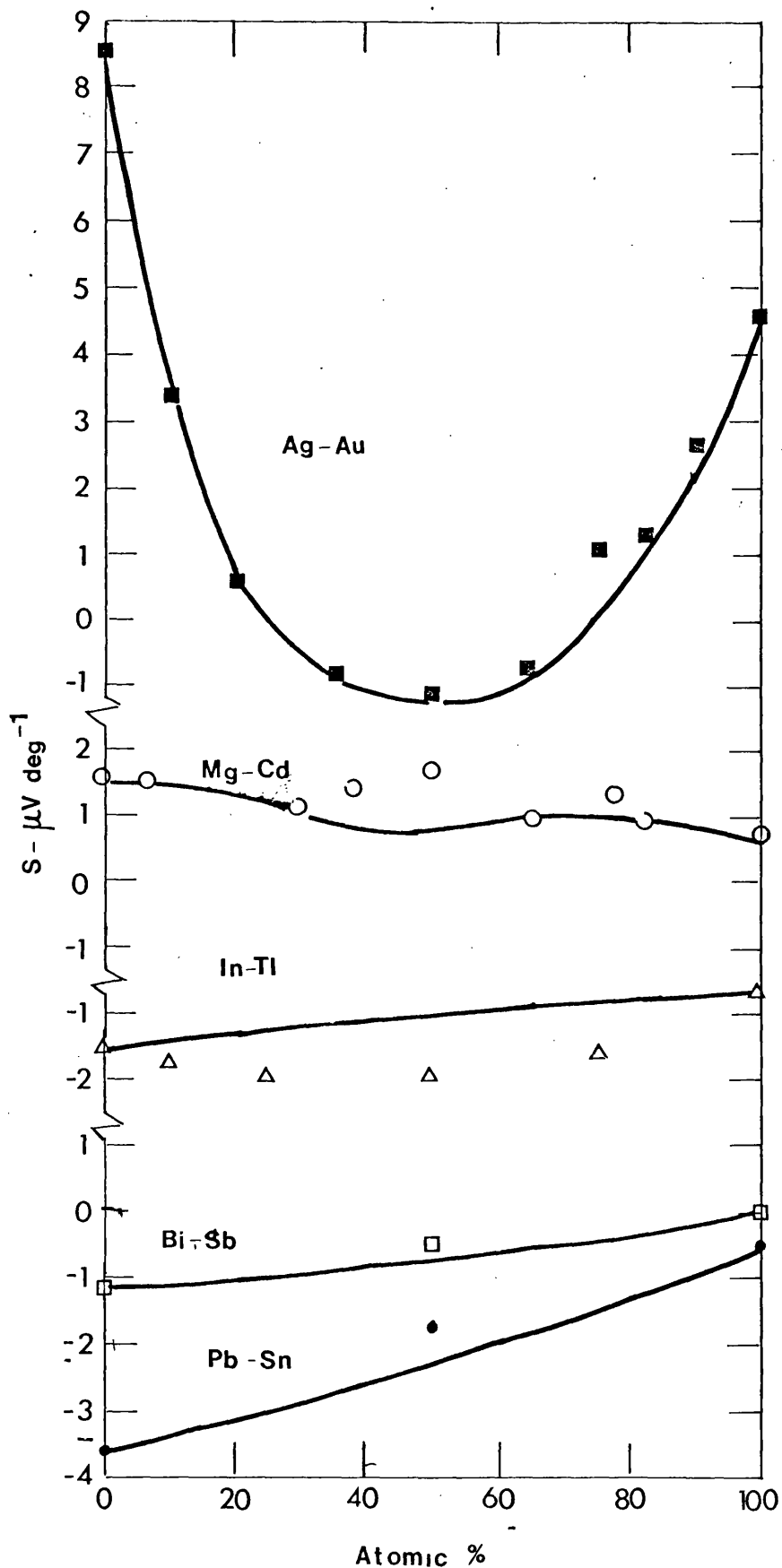


Fig 1.2.2

The thermopower of equivalence liquid alloys as a function of composition : ■ Ag-Au ; ○ Mg-Cd ; △ In-Tl ; □ Bi-Sb ; ● Pb-Sn [The first named is on the left of the diagram.]

— with energy dependent pseudopotentials

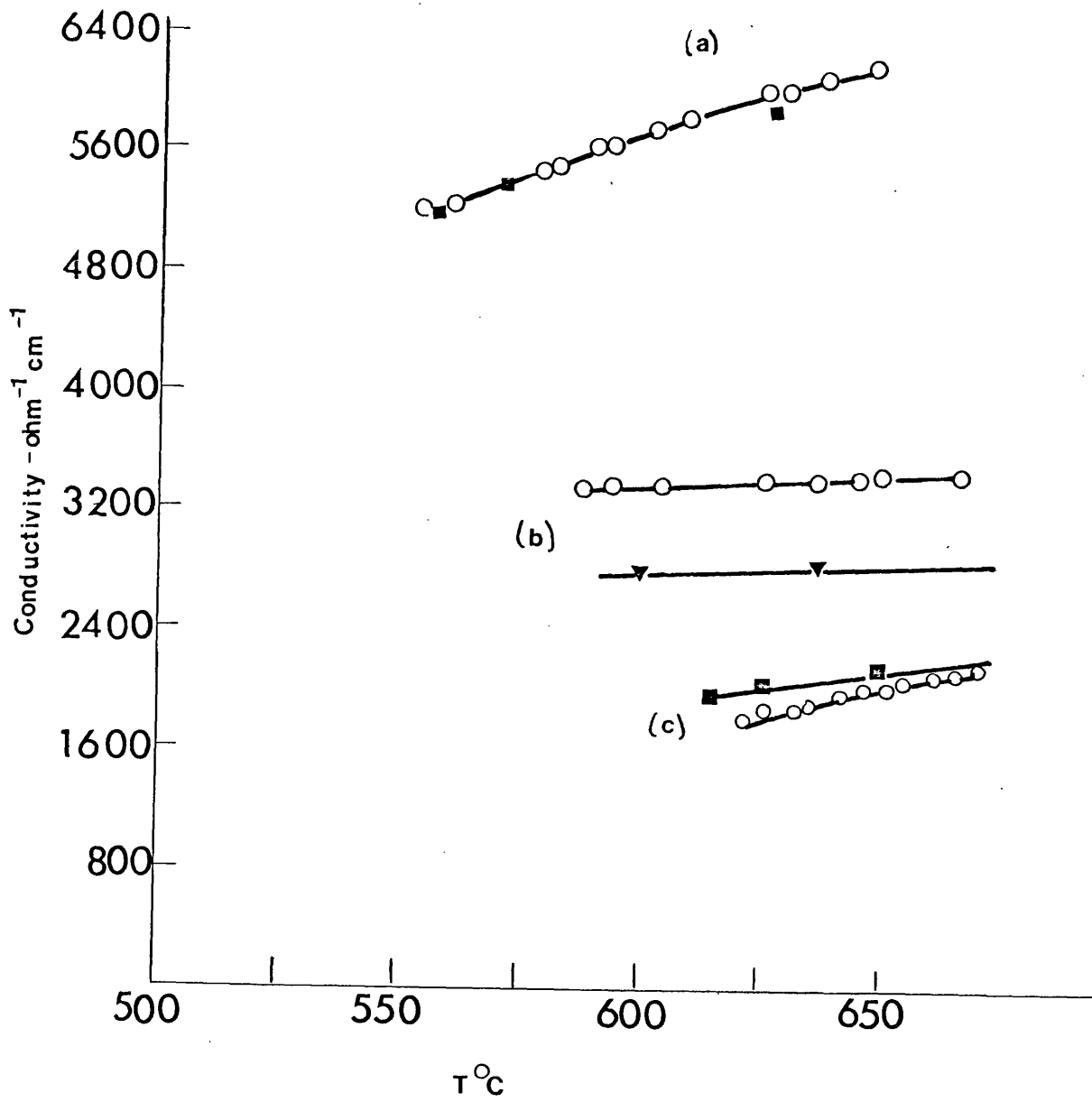


Fig. 1.2.3

The conductivity of liquid (a) ZnSb , (b) Bi_2Te_3 , (c) Sb_2Te_3

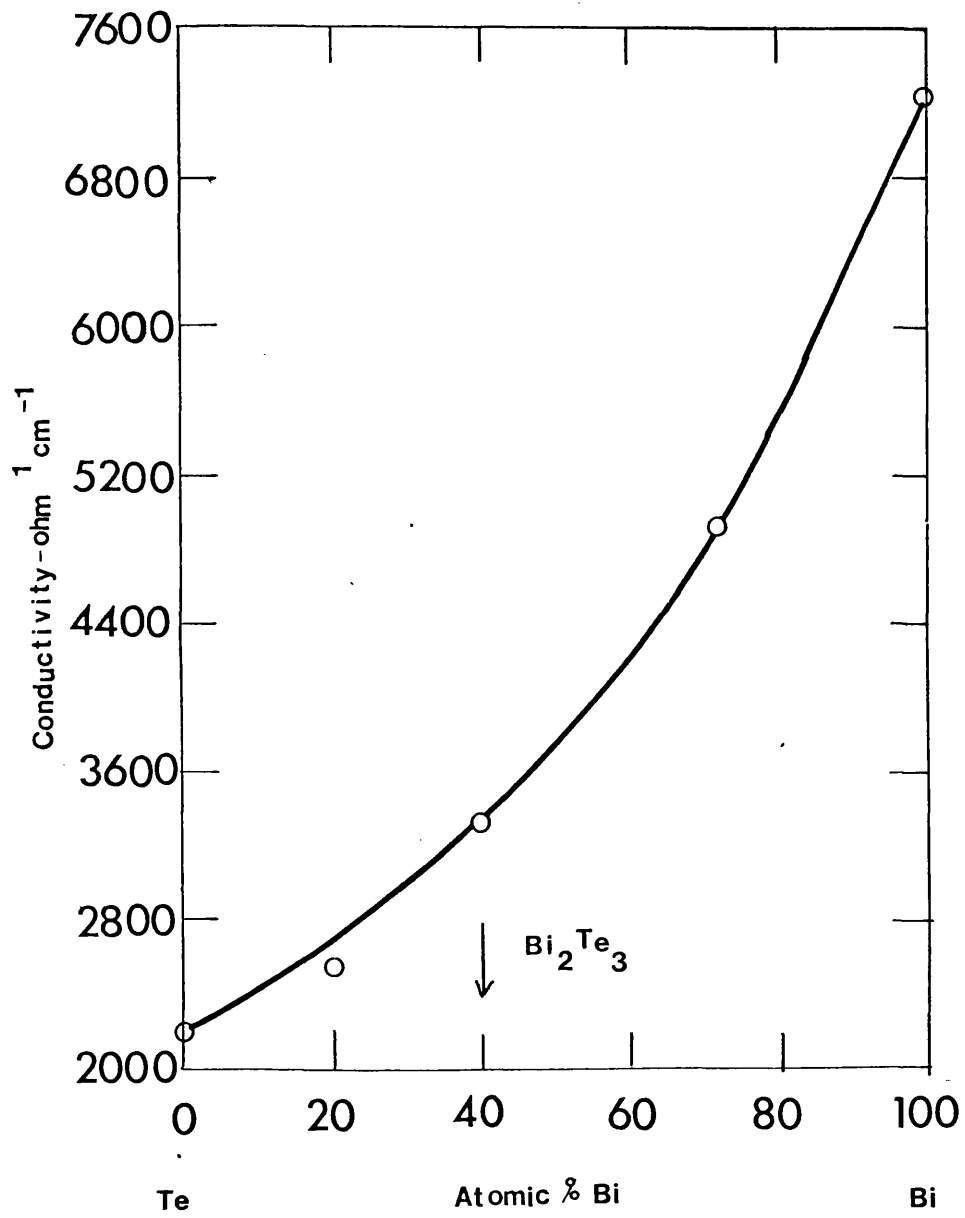


Fig.1.2.4

The electrical conductivity of liquid Bi₁Te at 585°C

where M_0 , M_1 are the atomic weights of Cu and Sn respectively, c is the concentration of Sn, N is Avogadro's number and ρ is the alloy density. The free electron Hall coefficient for Cu-Sn calculated from (1.2.5) and (1.2.14) can be seen from figure 1.2.5 to agree remarkably well with experiment.

A direct comparison between Faber-Ziman theory and experiment for those alloys in which $\frac{d\phi}{dT}$ is positive has not been carried out on a wide scale because the relevant partial structure factors are not known. On the strength of the reasonable agreement which exists for the Cu-Sn system, Enderby groups these alloys with the simple liquid alloys, stating that the positive $\frac{d\phi}{dT}$ arises from the temperature dependence of the partial interference functions without justification.

1.3 THE LIQUID SEMICONDUCTORS

1.3.1 Introduction

Several liquid alloys have very low electrical conductivities ($<200\Omega^{-1}\text{cm}^{-1}$) over a restricted range of concentrations. When none of the components is naturally a semiconductor or insulator in the liquid state then these concentration ranges are narrow and around well defined ratios of small integers. Alternatively, the conductivity can be low over a large range of concentrations if one of the pure liquid components has a low conductivity. Many other electronic properties, e.g. thermopower, Hall coefficient of such systems demonstrate an anomalous behaviour quite distinct from the properties of normal liquid alloys. These are all properties which are dependent on the electron

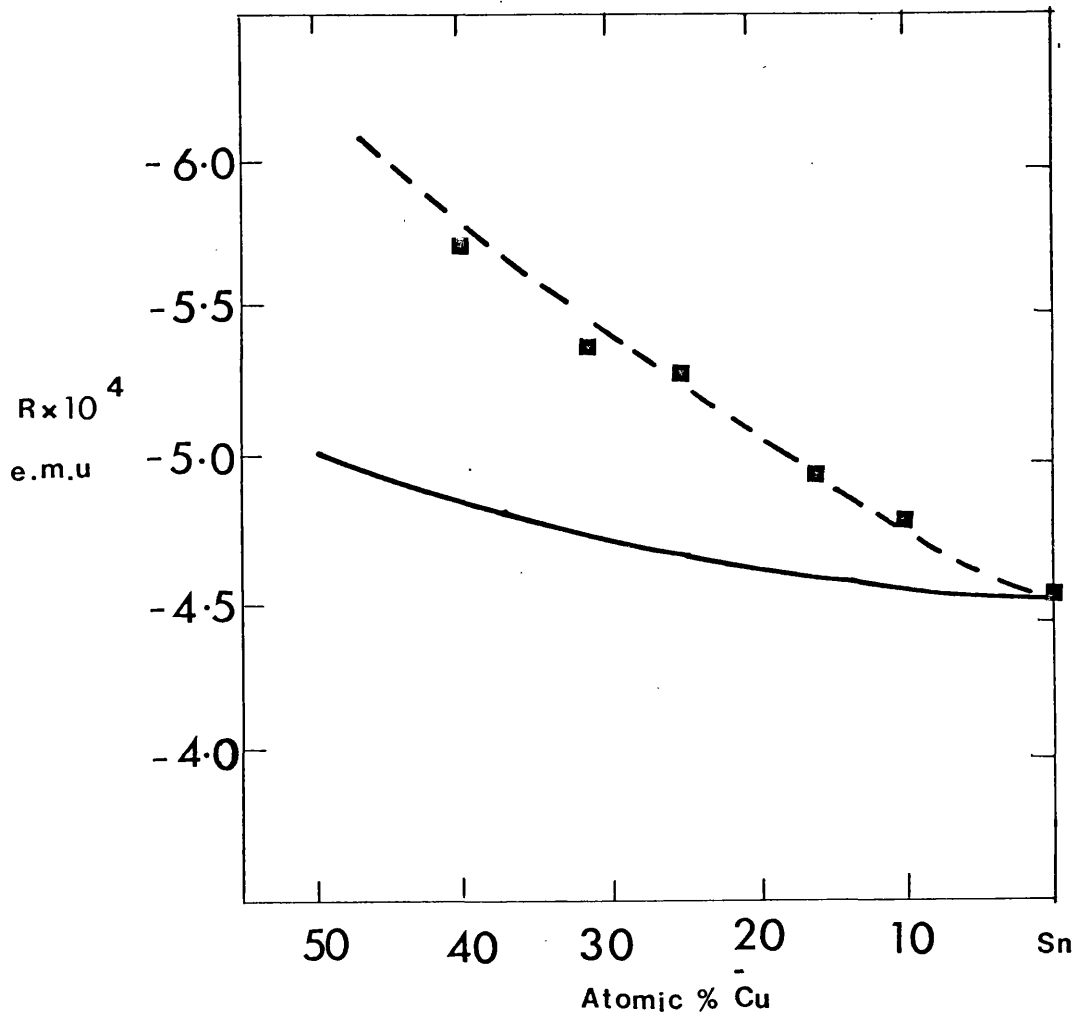


Fig.1.2.5

The Hall coefficient of liquid CuSn

- experimental observation
- free electron Hall coefficient
- - - calculated according to 1.2.14

distribution at the Fermi energy. As well as possessing very curious transport properties, these are also alloys in which $\frac{d\sigma}{dT}$ is positive. Such alloys are often referred to as liquid semiconductors because they exhibit most of the properties usually associated with conventional solid semiconductors. As far as is known all liquid semiconductors are also amorphous semiconductors, although the reverse is not true. Table 1.3.1 lists some of the alloy systems considered to be liquid semiconducting, together with their electrical conductivities at the critical composition.

In order to make matters more definite it is often convenient to subdivide the liquid semiconductors into five groups distinguished by the electrical nature of the alloy components in the pure liquid state:

- (i) metal-metal systems, e.g. Mg-Bi, Li-Bi
- (ii) metal-semimetal systems, e.g. Ag-Te, Cu-Te, Tl-Te
- (iii) metal-semiconductor systems, e.g. Ni-S, CoS
- (iv) semimetal-semiconductor systems, e.g. Te-Se
- (v) semiconductor-semiconductor systems, e.g. As-Se

The following sections will outline the experimental features of each group. Any explanations which have been offered for the semiconducting behaviour of certain systems will be briefly mentioned.

1.3.2 Metal-Metal Systems

Liquid Mg-Bi, Li-Bi, Mg-Sb alloys fall into this category. Although experimental studies on these systems are limited they are of special interest since it is possible to follow the gradual change from the metallic to the semiconducting state. The

TABLE 1.3.1

Liquid Semiconductors

LIQUID ALLOY	CRITICAL COMPOSITION	CONDUCTIVITY ($\Omega^{-1}\text{cm}^{-1}$)
S-Ag	Ag_2S	200
S-Pb	PbS	110
S-Cu	Cu_2S	50
S-Sn	SnS	24
S-Ge	GeS	1.34
S-Tl	Tl_2S_3	1.7×10^{-2}
	Tl_4S_3	6.5×10^{-3}
S-Sb	Sb_2S_3	1.5×10^{-2}
Te-Cu	Cu_2Te	200
Te-Ag	Ag_2Te	150
Te-Fe	Fe Te ₂	400
Te-Tl	Tl_2Te	70
Te-Cd	CdTe	40
Te-Zn	ZnTe	40
Te-In	In_2Te_3	25
Te-Ga	Ga_2Te_3	10
Bi-Mg	Mg_3Bi_2	45 ± 15
Bi-Li	Li_3Bi	?

References

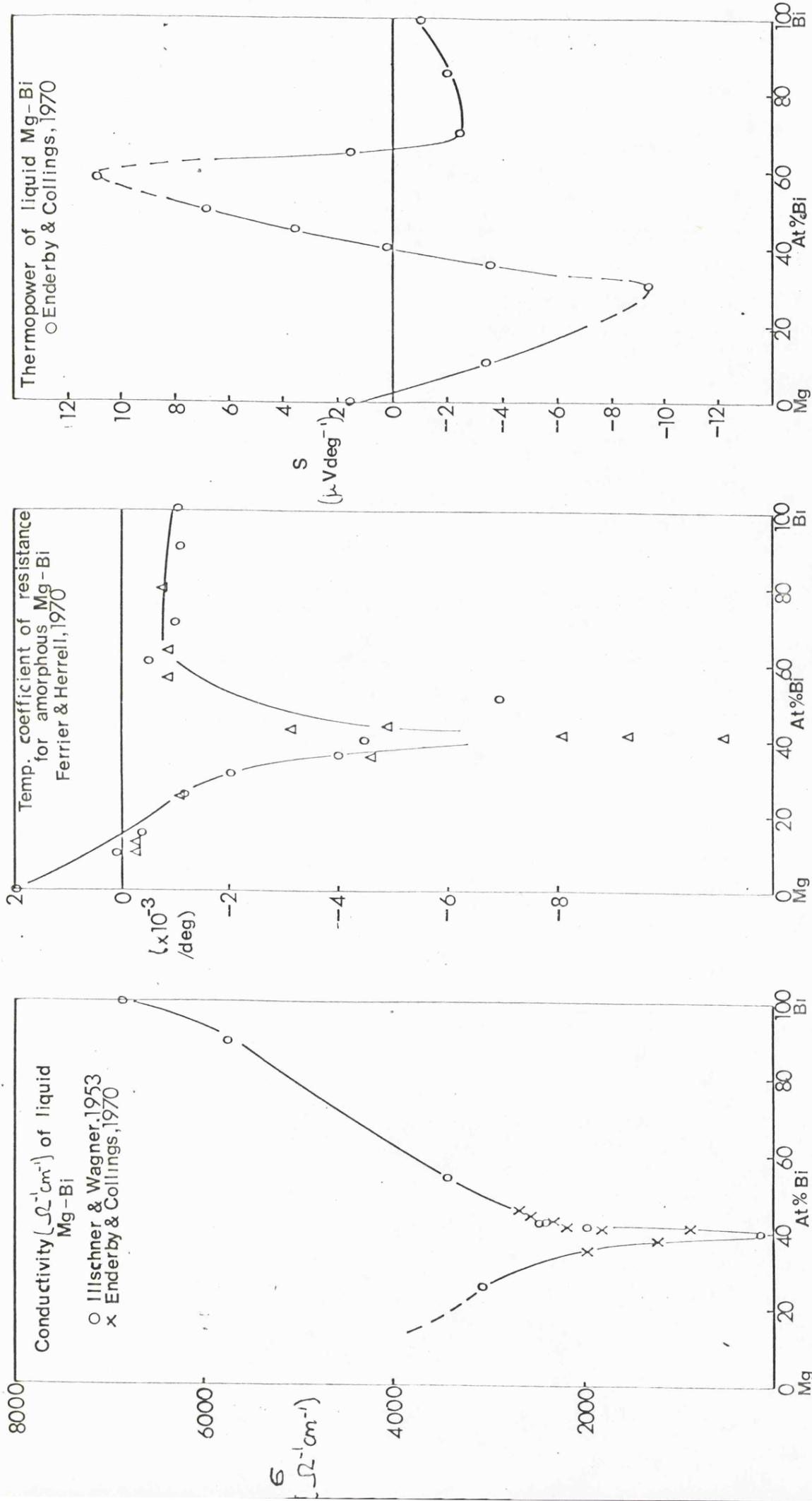
Allgaier (1969)
 Enderby and
 Collings (1970)

conductivity and thermopower of liquid Mg-Bi have been measured by Ilschner and Wagner (1953) and Enderby and Collings (1970) and are shown in figure 1.3.1 (a) and (c). The curves are striking: at the composition corresponding to Mg_3Bi_2 the conductivity drops dramatically, and the thermopower changes sign. Near this composition, the conductivity increases with increasing temperature. Phase diagrams for these liquid alloys are available, (Hanson, 1958). These, together with thermodynamic data (Hultgren et al, 1963), indicate that there is a major change in bonding as you go from pure liquid A to pure liquid B in these metal-metal semiconductors. Further discussion of the nature of the bonding is delayed until later chapters.

1.3.3 Metal-Semimetal Systems

This group includes liquid Ag-Te, Cu-Te, Ga-Te and Tl-Te. Selected experimental data on the conductivity, thermopower and Hall coefficient for the Tl-Te, Ag-Te, Cu-Te alloys are presented in figure 1.3.2 - 1.3.5, taken from Dancy (1965), Cutler and Mallon (1966), and Enderby and Simmons (1969). Phase boundaries for Tl-Te and Mg-Bi (the metal-metal system) are shown in figure 1.3.6, taken from Hanson (1958). The following remarks appear to be valid for the metal-semimetal semiconductors:

- (1) the alloys possess a two-phase liquid region in the range $0.7 < x < 1$, where x is the atomic percentage of the metallic component;
- (2) the Hall coefficient is negative at all compositions achieving a maximum at the composition where the conductivity is a minimum;

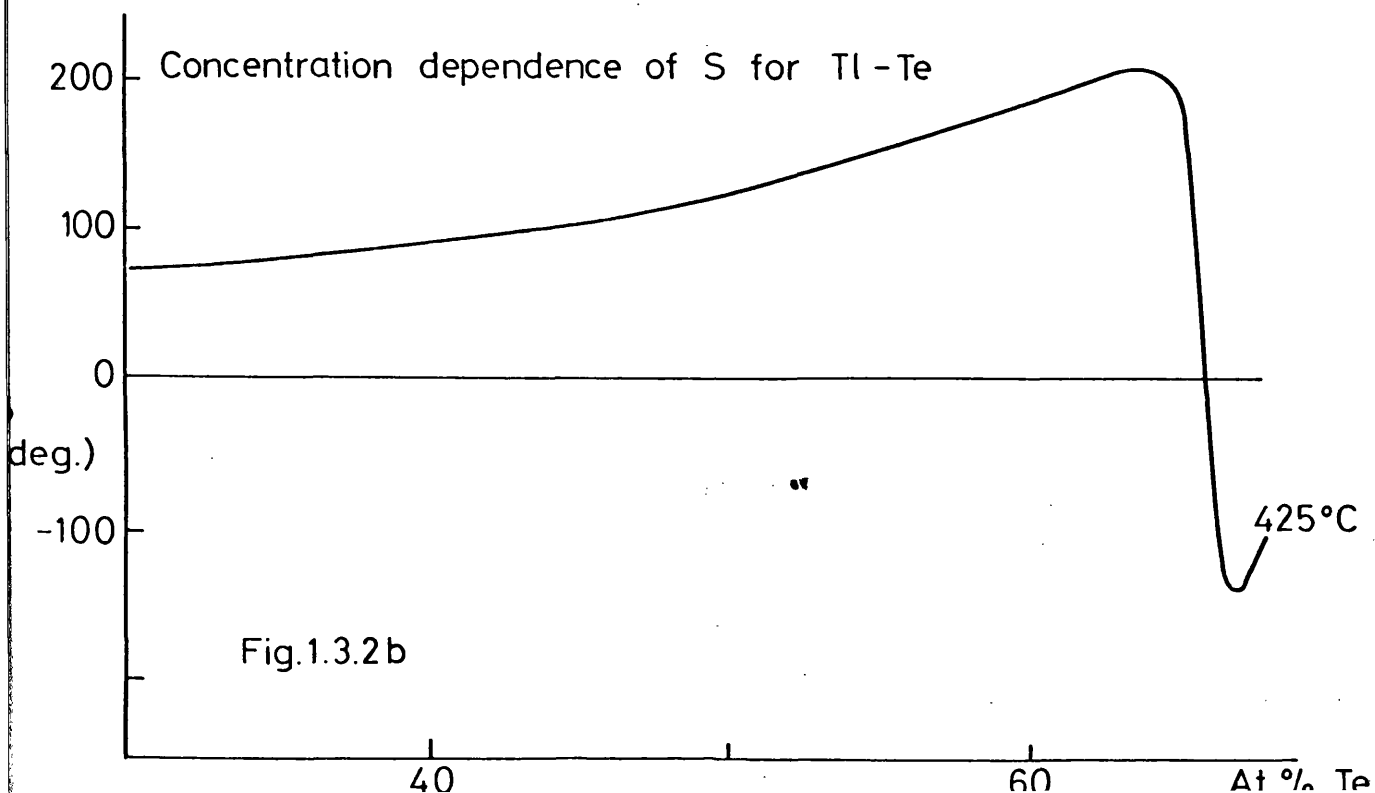
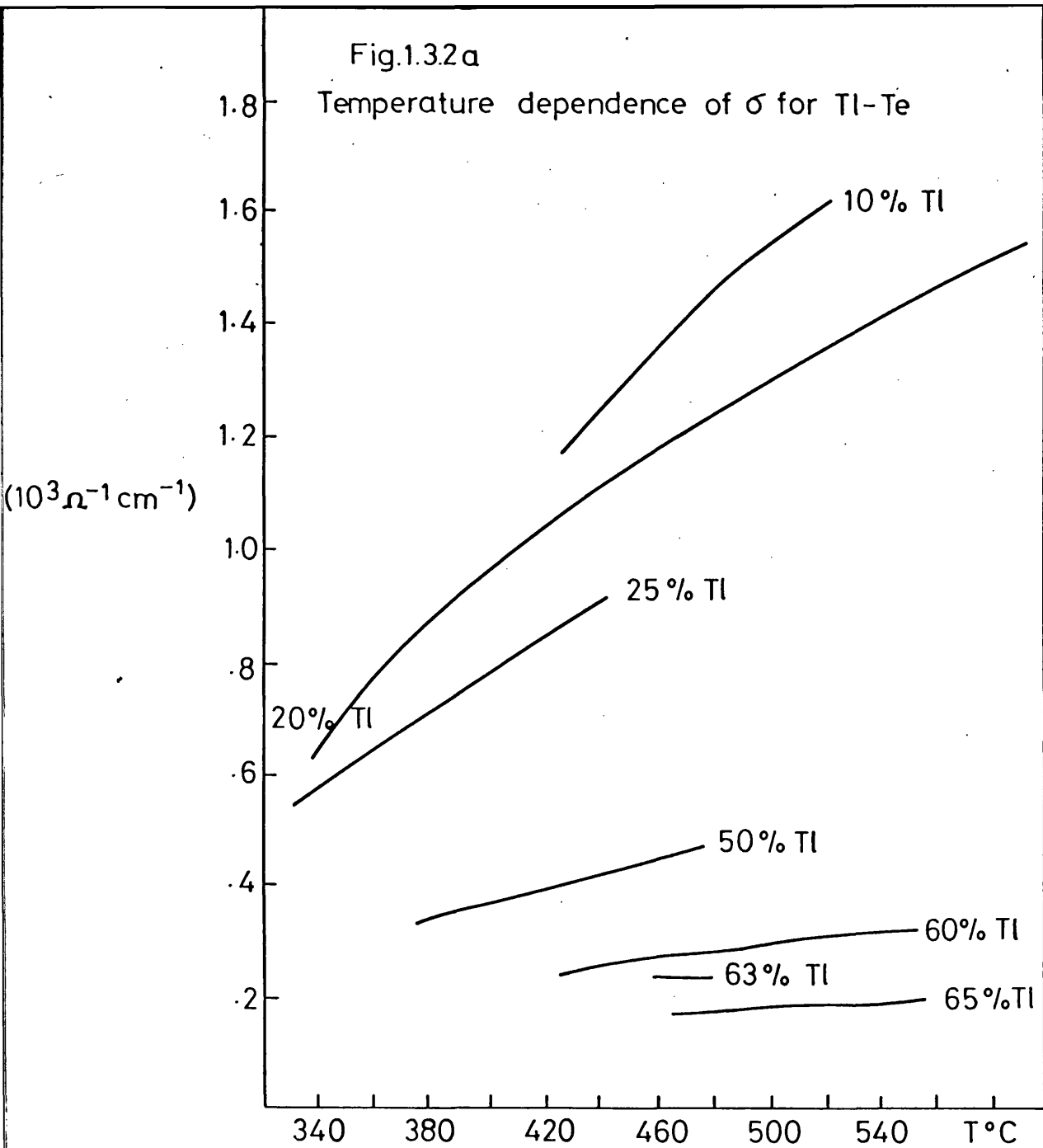


(a)

(b)

(c)

Fig. 1.3.1



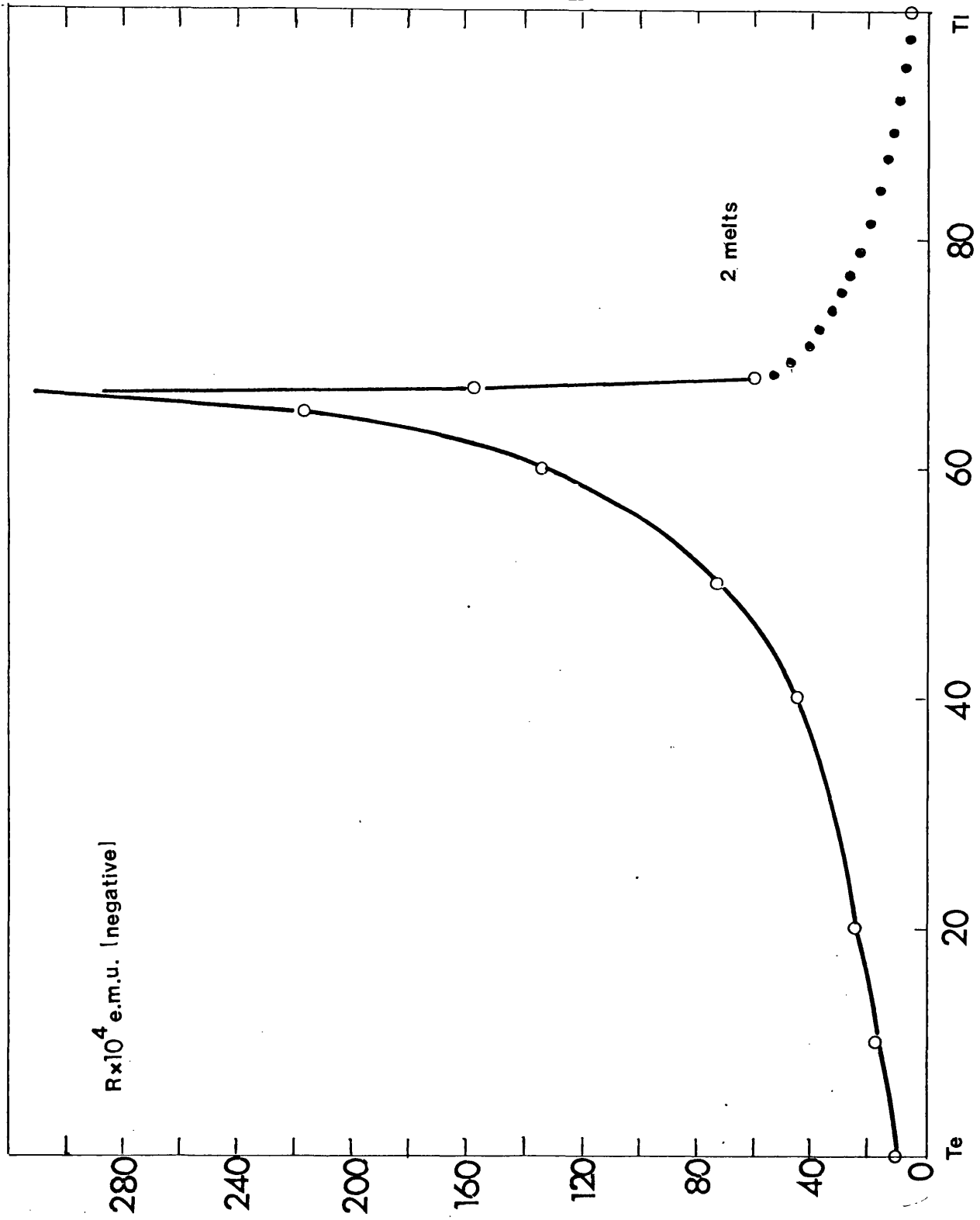


Fig 1.3.3

The Hall coefficient for
liquid Tl-Te at 585°C.

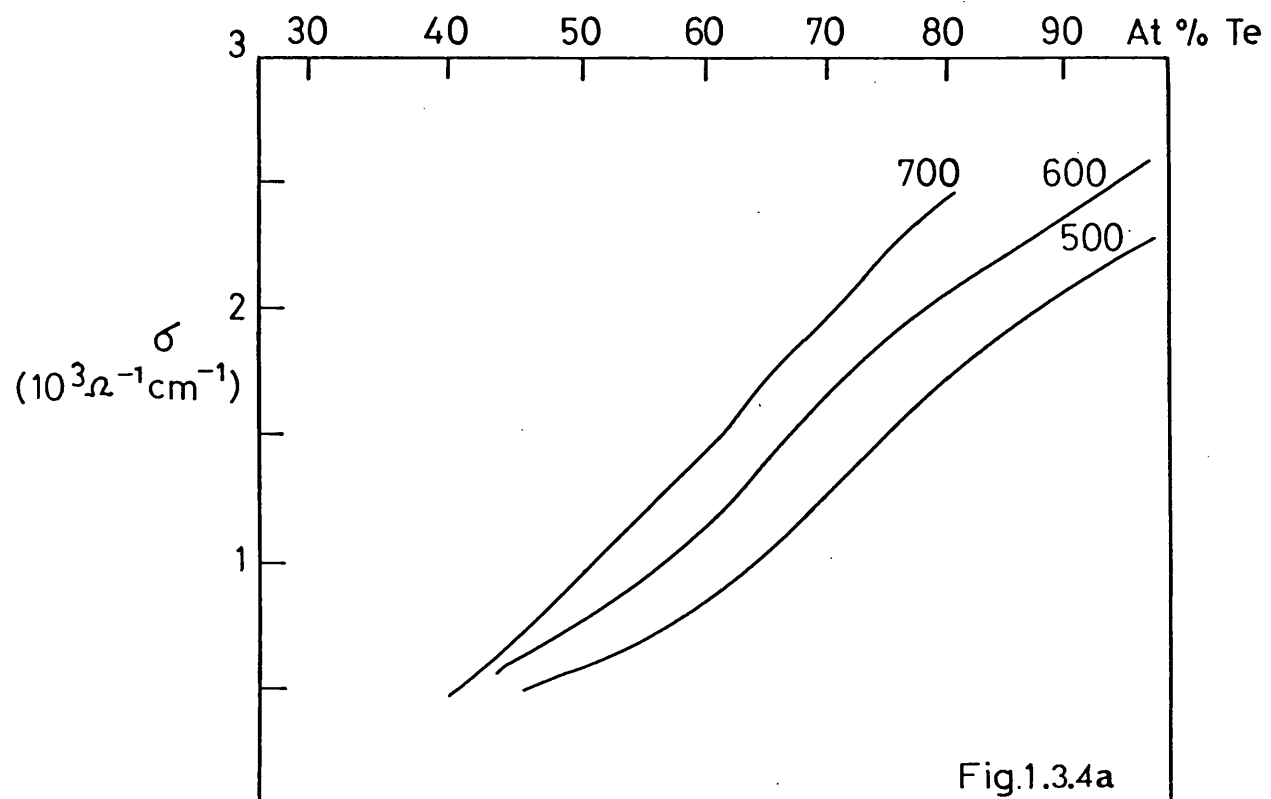


Fig.1.3.4a

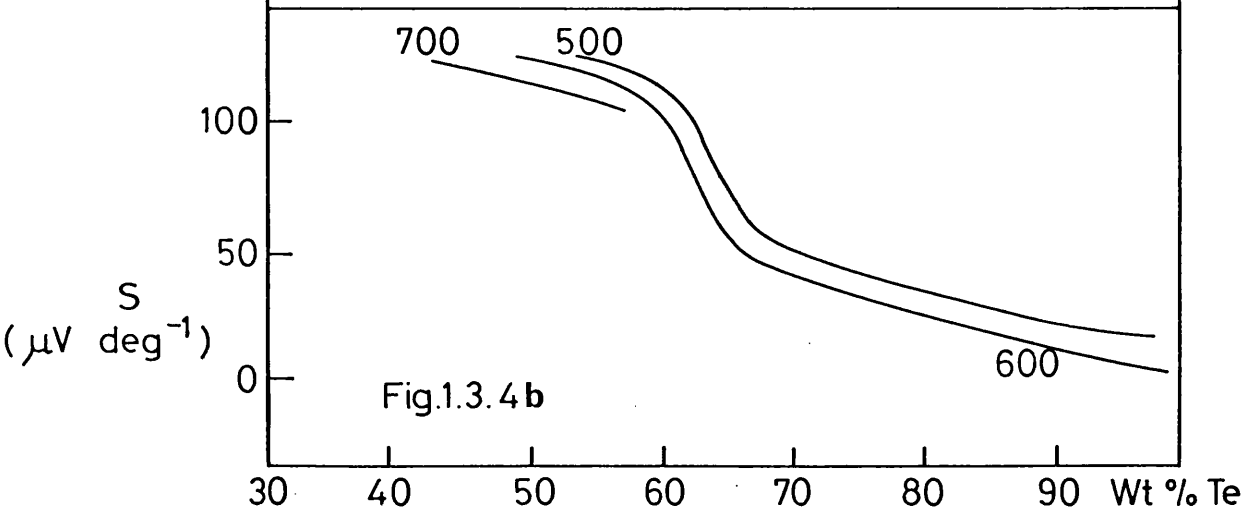


Fig.1.3.4b

Concentration dependence of S and σ for the alloy system Ag-Te

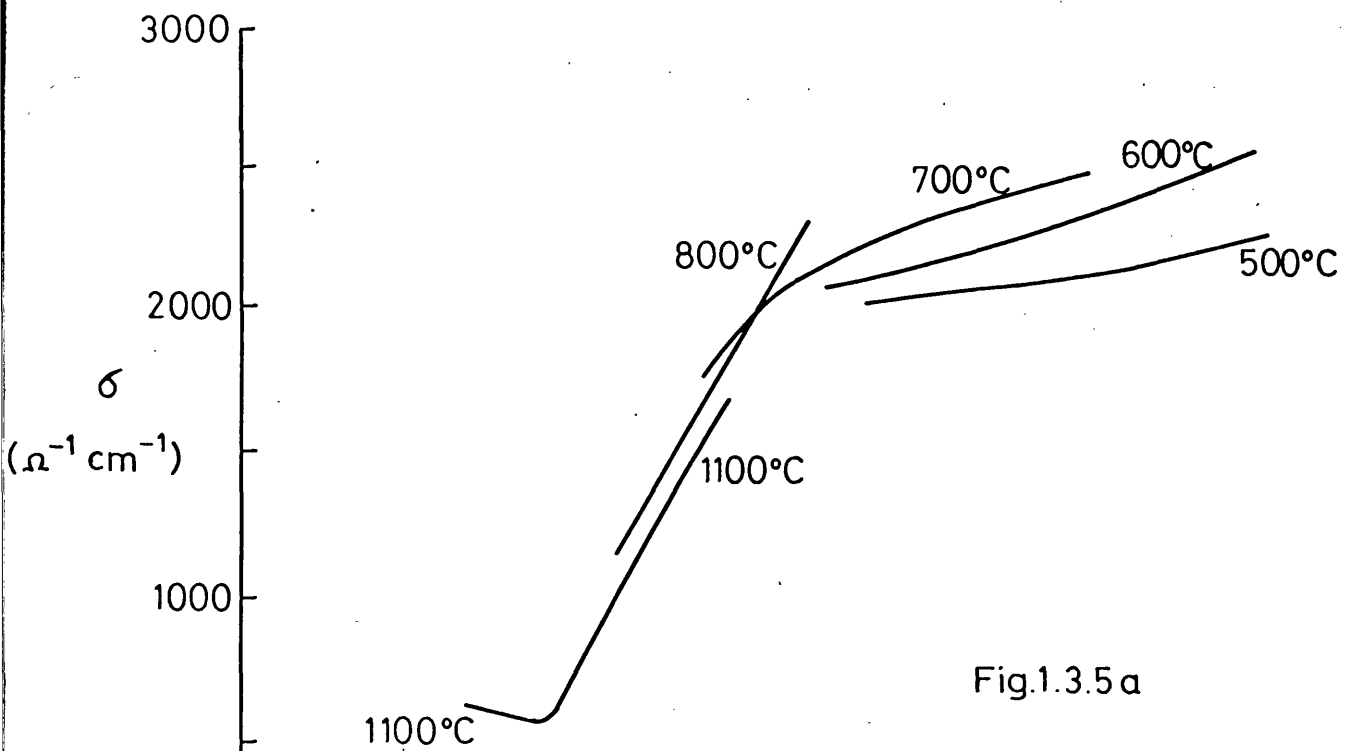


Fig.1.3.5a

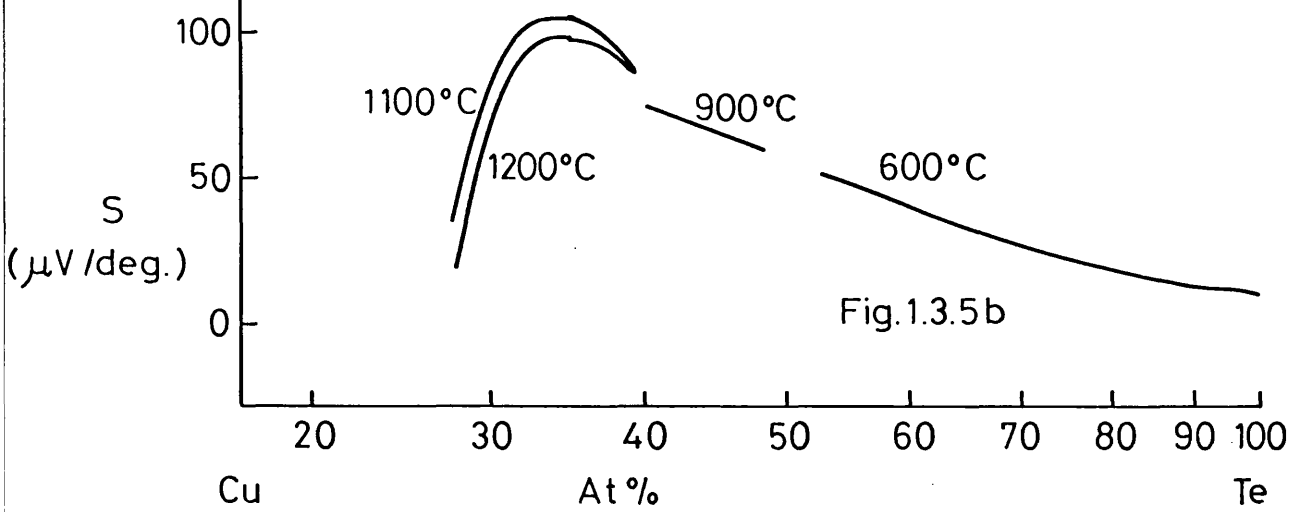


Fig.1.3.5b

Fig.1.3.5 ^a Concentration dependence of S for Cu-Te systems.

Fig.1.3.5 ^b Concentration dependence of σ for Cu-Te systems.

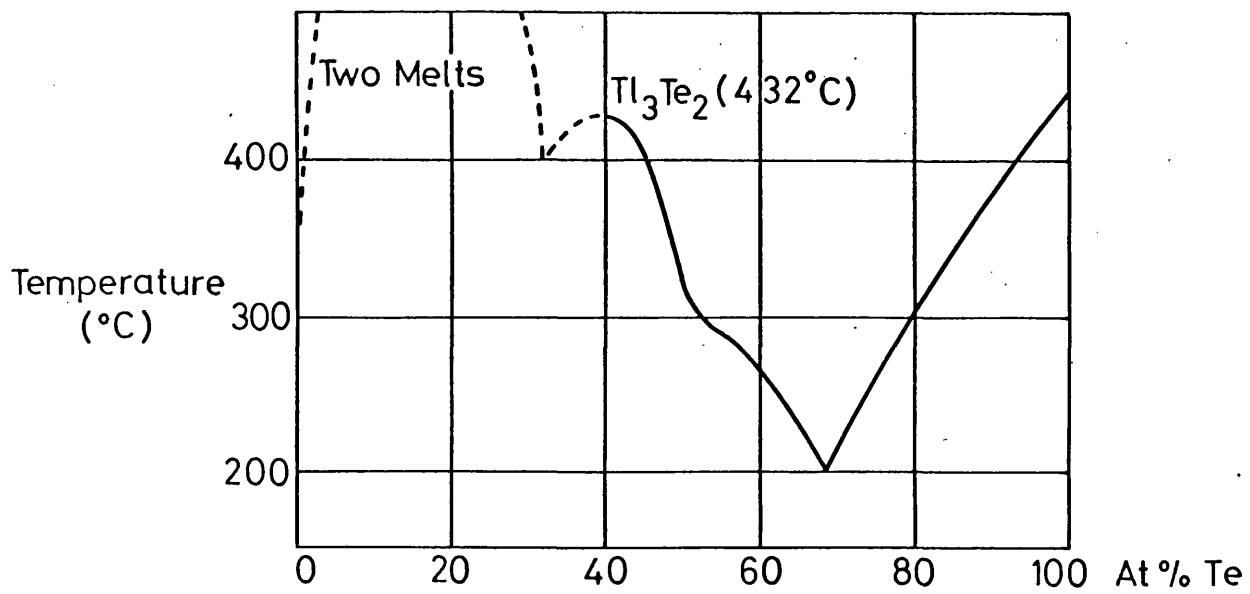


Fig.1.3.6a Phase boundary for Tl-Te

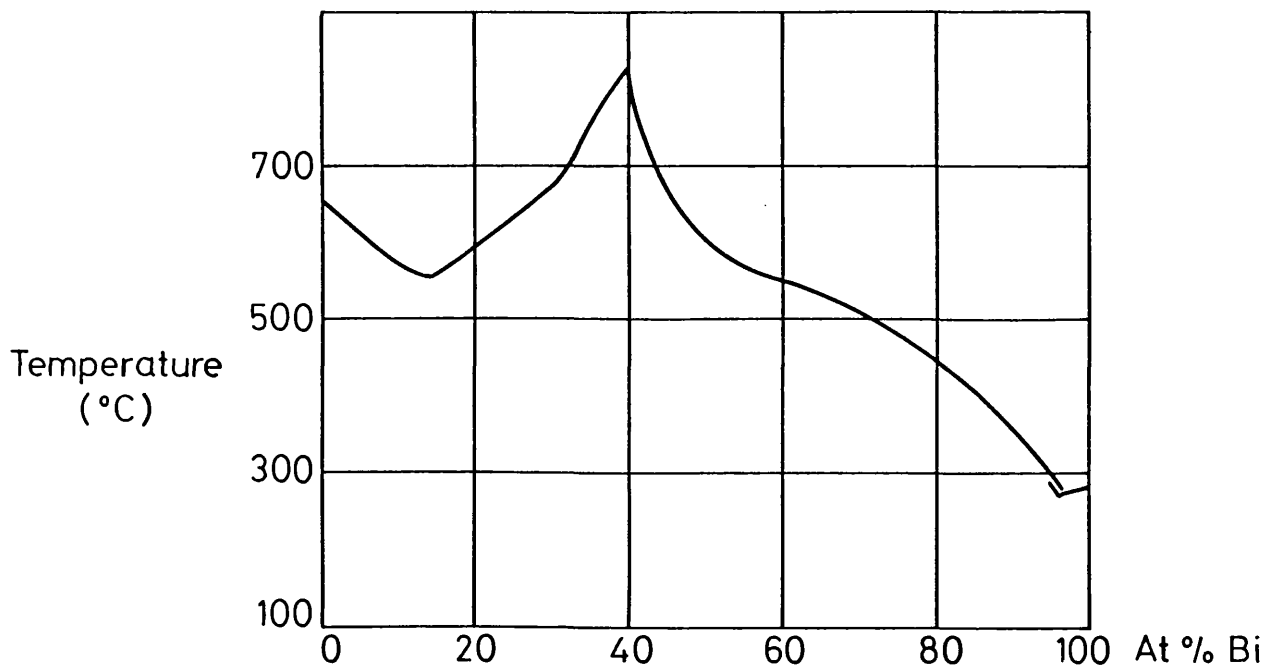


Fig.1.3.6b Phase boundary for Mg-Bi

(3) the thermopower varies rapidly close to the critical composition.

Cutler and Peterson (1970) have measured the transport coefficients of liquid $Tl_x Te_{1-x}$ above $600^{\circ}C$. They observe that their results within the $0.7 < x < 1$ range can be accounted for by assuming that the alloy consists of a solution of semi-conducting Tl_2Te molecules and Tl atoms. This model has been extended (Cutler, 1971) to the $0 < x < \frac{2}{3}$ region where molecules of the form $Tl Te_n Tl$, with $n \geq 1$, are presumed to form.

Enderby and Hawker (1972) have carried out detailed structural studies on liquid $Cu_2 Te$ using neutron diffraction techniques in which the partial structure factors a_{CuCu} , a_{TeTe} , a_{CuTe} have been isolated within experimental error. One of the features noted is the similarity between a_{CuCu} and the structure factor for pure liquid copper which would suggest that the packing of the copper ions in liquid $Cu_2 Te$ is a highly disordered one, dominated by a hard-core interaction similar to that for copper ions in pure liquid copper. A significant difference between a_{TeTe} and the structure factor for pure liquid tellurium is also observed which would indicate that the covalent character of pure liquid tellurium disappears as copper is added. These observations indicate that models involving copper substitution into covalent tellurium chains are unlikely to prove a starting point for explaining the properties of liquid Cu-Te alloys. One further significant conclusion from their study is that the cluster models of Cohen and Sak (1972) and Hodgkinson (1974) for Cu-Te type

semiconducting alloys - islands of semiconducting liquid (10-100 Å across) dispersed in a metallic matrix - are inapplicable. No evidence of long range is found in any of the partial radial functions.

1.3.4 Metal-Semiconductor Systems

Ni-S, Co-S, Tl-Se, In-Se, Bi-Se are some of the alloys which belong to this group. Their electrical properties closely resemble those of the metal-semimetal systems.

1.3.5 Semimetal-Semiconductor Systems

Liquid Te-Se, a member of this group, has been extensively studied by Cutler and Mallon (1962) and Perron (1967). The electrical conductivity of liquid $\text{Te}_{1-x}\text{Se}_x$ alloys taken from Perron are shown in figure 1.3.7. The electrical properties vary smoothly from those typical of pure selenium to those of pure tellurium.

1.3.6 Semiconductor-Semiconductor Systems

This group includes liquid As-Se (Te). It appears as though a change in the sign of the thermopower does not occur around the stoichiometric compound As_2Se_3 .

1.4 THE LIQUID SEMICONDUCTOR PROBLEM

If an understanding of the very remarkable electronic properties of the liquid semiconductors is to be realised, it is necessary to know something of the structure which exists in these systems. It will subsequently be seen that there is a dispute as to whether an ionic or a covalent model is the most appropriate starting point, if, indeed, such suppositions are

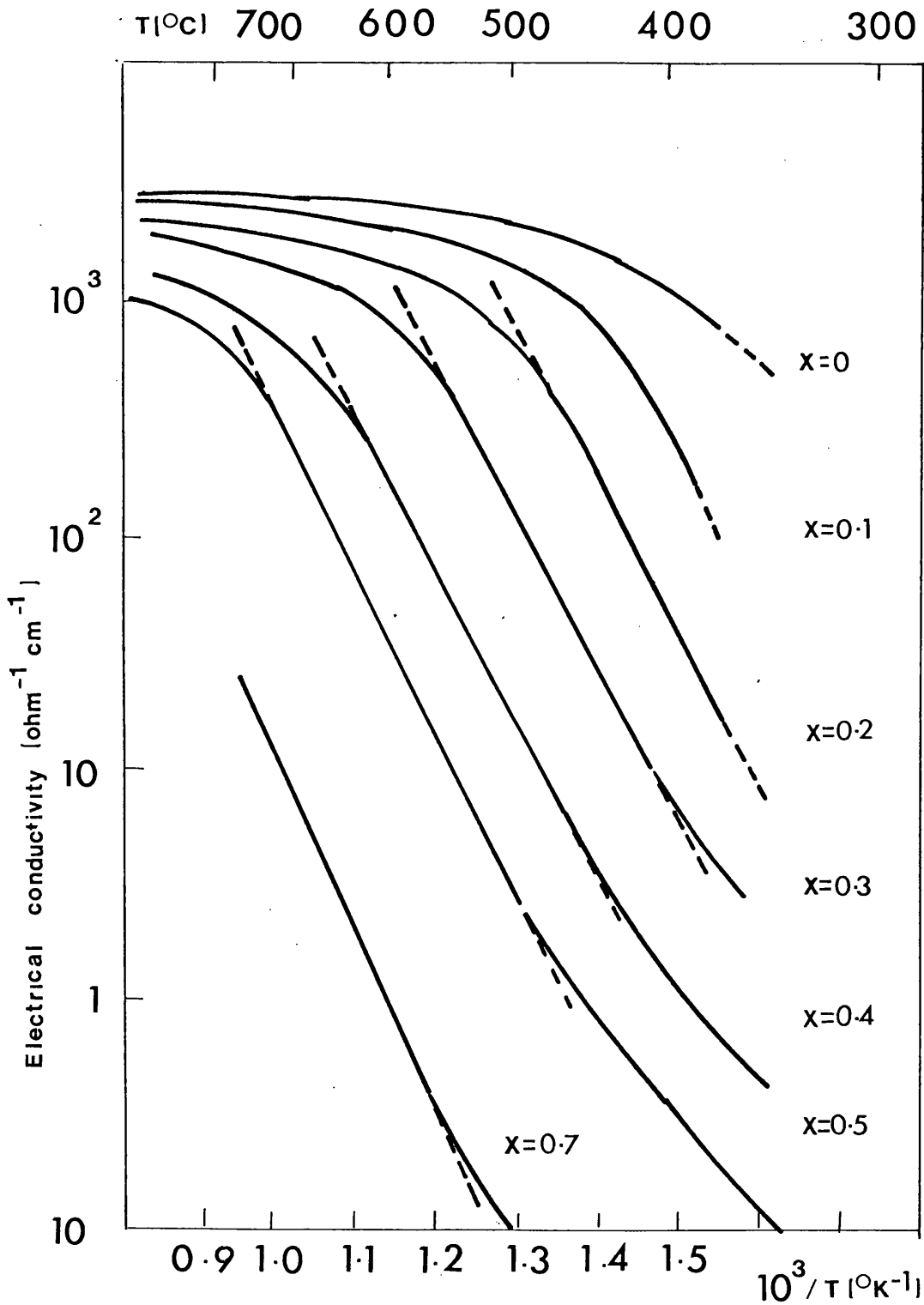


Fig. 1.3.7

Electrical conductivity of $\text{Te}_{1-x}\text{Se}_x$ liquid alloys

reasonable! The metal-metal liquid semiconductors are the obvious systems to look at first since they are metallic, except at compositions close to a critical composition, when they become semiconducting. Hence it may be possible to get a clearer picture of the behaviour of the liquid semiconductors by examining the metal to semiconductor transition. Liquid Mg-Bi is the semiconductor to which reference will frequently be made. It should, however, be pointed out that a common explanation of these systems need not apply. Indeed, in view of the different chemical natures of the wide variety of elements which occur in such alloys, it appears unlikely that a single explanation can explain all the liquid semiconductors.

CHAPTER II

CHARGE TRANSFER IN ORDERED AND DISORDERED ALLOYS

2.1 CHARGE TRANSFER, IONICITY AND COVALENCY

The type of bond which exists between atoms in a crystal depends upon the electron charge distribution about each atom. The covalent and ionic bonds are two extremes which characterize two different types of electron charge distributions which may be found to exist in certain crystals. Covalent crystals such as silicon and germanium have bonds characterized by electron sharing, the covalent bond. This involves sharing between atoms of an even number of valence electrons, two per single bond. The result of this sharing is that the electron charge distribution is high in the region between the atoms. Each atom is limited in the number of covalent bonds it can make, and there is a marked directionality in bonding. The ionic bond is that which results from the electrostatic interaction of oppositely charged ions, the crystal being made up of ions so arranged that the attraction between ions of opposite sign is stronger than the Coulomb repulsion between ions of the same sign. In an ionic solid such as sodium chloride, there is electron transfer from the sodium to the chlorine, leading to an inert gas structure about each ion. Associated with the closed shell structure about each ion, an approximately spherically symmetric charge distribution exists which is high about the negatively charged ion. The distinction between covalent and ionic bonds is then,

in principle, quite clear: the former leads to a piling up of charge between atoms, the latter to complete charge transfer from one atom to another.

For certain liquid semiconductors, one author (Enderby, 1974B), has suggested that the striking electron transport features observed near the critical composition are a direct result of total ionic bonding within the system, charge being localized about ionic sites. It is generally accepted that the transfer of charge from one constituent element in a binary alloy to the other is one of the principal mechanisms in the formation of the alloy. Interatomic forces are thought to be partly ionic in nature. The type of bond which exists between atoms and the amount of charge transfer are therefore very important features which characterize electron behaviour within alloy systems. A knowledge of both will lead to a fuller description of electron transport properties.

The concept of partial ionicity within binary alloy systems is a crucial one and may be understood more precisely by considering atomic levels within the fully ionic sodium chloride crystal. If the level on the sodium atom lies a few electron volts below the chlorine levels, one would expect the extra sodium electron to remain on the sodium atom. This is not observed in sodium chloride. The level on the sodium atom is therefore higher than that on the chlorine atom, but lower than the first excited chlorine state. The extra sodium electron goes to the chlorine, causing a lowering of the unfilled levels of the chlorine to the extent where they are lower than the level on the sodium ion.

The electron wavefunction then contains an admixture of states associated with the chlorine ion. There is still, however, a contribution from the state about the sodium site which will mean that although the electron is more likely to be localized about the chlorine site, there is a finite probability of it remaining on the sodium, or between the two atoms. Hence, although classically a model in which the electron is bound to one atom electrostatically gives sound agreement with experimental data on cohesive energy, quantum mechanically there is always a finite probability that it may remain on the parent atom, or between the two atoms. It is unlikely that the bonds between atoms can either be fully ionic or covalent in character. Indeed, in most bonds, some electronic charge is transferred from one atom to another, in which case the bond is said to be partly ionic and partly covalent. The situation is described as one of resonance between the covalent and ionic extreme.

The degree of ionicity in the bonds between atoms is considered to be an important feature in the formation of an alloy. It is a problem, however, to derive the amount of charge transfer since quantitative estimates depend upon the atomic cell size prescribed. In an ionic crystal, sensible radii for the constituent atoms can be obtained by considering the position of the minimum charge density. However, the values derived will not be independent of the crystal under consideration, and hence ionic radii of the type defined by Pauling and Goldschmidt may be of more value, even though they have no definite meaning in terms of the charge distribution within the crystal. In an obviously non-ionic crystal of an element, such as a metal, or a crystal like

silicon or germanium, the minimum of density will fall midway between the atoms, by symmetry. Since a different atomic cell size will lead to a different derived amount of charge transfer for a disordered alloy, the problem must be faced as to whether a meaningful definition for the atomic cell size in an alloy can be found.

2.2 THE IMPORTANCE OF CHARGE TRANSFER IN DISORDERED ALLOYS

Several attempts have been made to relate charge transfer to the alloy heat of formation. Empirical observations of Miedema, de Boer and de Chatel (1973) and Miedema (1973A) on the metallic alloy heat of formation emphasise the role of charge transfer in alloys. Hume Rothery was the first to point out that when two alloy constituents differ considerably in electrochemical properties, the interatomic forces are often partly ionic in nature. Band structure calculations indicate non-uniform electron charge density distributions. Electronegativity difference is one of the most common parameters used to estimate the ionic contribution to the alloy formation energy. The approach contrasts that of Varley (1954), whose two band model for the concentrated disordered alloy, one for each element, determines charge transfer by the relative positions of the Fermi levels in the pure metals. Efforts have been made to relate electronegativity and Fermi level differences since both are measures of the charge transfer. The work of Miedema and co-workers, in particular, illustrates very well the basic physical principles which have been employed to tackle the

problem of determining the heats of formation of 50-50 concentrated disordered alloys.

Miedema et al propose a scheme to estimate the formation energy of metallic binary alloys in which only two energy contributions are considered. Alloys are regarded as being made up of atomic cells (different cells for different kinds of atoms), which in a first order approximation are similar to the atomic cells of the atoms in the pure metallic state. As a correction to this first order approximation they suggest that there are two main effects. First, the chemical potential, ϕ , for electrons at the two types of cells should be equal, leading to a negative energy contribution proportional to $(\Delta\phi)^2$. Second, the discontinuity in the electron density present at the boundary between dissimilar cells has to be smooth, leading to a positive energy contribution proportional to $(\Delta n)^2$, where n is the electron density at the cell boundary. When charge is transferred from the more electropositive to the more electronegative element, the charged atomic cell will differ from that of the neutral ones. The model results in a simple expression for the alloy heat of formation:

$$\Delta H = f(c)\{-Pe(\Delta\phi)^2 + Q(\Delta n)^2\} \quad (2.2.1)$$

where $f(c)$ is a symmetrical function of concentration, P and Q are approximately constant, e is the electronic charge. (2.2.1) is derived purely on the basis of empirical observations on the heats of formation of a number of metallic transition and non-transition alloy systems. In the analysis of the heat of formation data,

the cross term $\Delta\phi\Delta n$ might also have been present but was not found and, hence, assumed small. Δn is derived empirically from the bulk modulus, B , and the molar volume V_m , for the pure metallic element; it is found to be proportional to $(B/V_m)^{\frac{1}{2}}$ for non-transition elements. $\Delta\phi$, approximately equal to the experimental work function of pure metals, is judged to be a good description for the stability of alloys in terms of (2.2.1). In a subsequent examination the experimental work function is found to vary linearly with the Pauling electronegativity so that ϕ is interpreted as an electronegativity parameter. The charge transfer, Δz , of electrons from the more electropositive to the more electronegative element is proportional to the electronegativity difference, $\Delta\phi$:

$$\Delta z = 2R \Delta\phi (1-c) \quad (2.2.2)$$

where R is an empirical proportionality constant.

From equations (2.2.1) and (2.2.2) it can be seen that the electron transfer plays a very important role in the alloy heat of formation. The relationship between charge transfer and electronegativity difference has, however, been established on an empirical, not a quantitative basis, and is in need of justification. Chapter III investigates the relationship between the formally derived amount of charge transfer within concentrated disordered alloys and electronegativity difference to determine whether or not the latter is a meaningful parameter in estimating the amount of charge transfer. The problem still remains as to a definition for the atomic cell size in the alloy. This is dealt with in detail in chapter IV.

2.3 COHERENT POTENTIAL APPROXIMATION AND BINARY DISORDERED ALLOYS

2.3.1 Coherent Potential Approximation

The coherent potential approximation (CPA) has been introduced as a reasonable approach to the problem of calculating the electronic density of states in a disordered substitutional $A_x B_{1-x}$ alloy within the framework of multiple scattering theory (Soven, 1967). It is a single-site description in which electrons are described in the single-particle approximation, single-particle properties being derived from the one-particle Green function

$$G(z) = (z - H)^{-1} \quad (2.3.1)$$

where H denotes the one-electron Hamiltonian. The coherent potential replaces the random potential by an ordered lattice with the same effective potential. The true potentials at the site, either $v_1(\underline{r} - \underline{\ell})$ or $v_2(\underline{r} - \underline{\ell})$, are replaced by an, as yet, unknown potential, $v_0(\underline{r} - \underline{\ell})$, the formal Green function for the lattice of potentials v_0 being defined by

$$G_M = G_0 + G_0 \sum_{\underline{\ell}} v_0(\underline{r} - \underline{\ell}) G_M \quad (2.3.2)$$

where G_0 is the free space Green function. G_M determines the propagation through the, as yet undetermined medium. Relative to the medium, the actual system consists of perturbing potentials $(v_1 - v_0)$ and $(v_2 - v_0)$. The t-matrix describes the scattering of an electron which is propagating according to G_M when it encounters the perturbing potential $(v_i - v_0)$ defined by

$$t_i = (v_i - v_0) + (v_i - v_0) G_M t_i \quad (2.3.3)$$

These quantities combine to yield an expression for the actual Green function

$$G = G_M + \sum_{\alpha} G_M t_{\alpha} G_M + \sum_{\alpha} \sum_{\beta \neq \alpha} G_M t_{\alpha} G_M t_{\beta} G_M + \dots \quad (2.3.4)$$

The effective medium is chosen self-consistently by requiring that on average there is no scattering from any site - that is,

$$x t_1 + (1-x) t_2 = 0 \quad (2.3.5)$$

with this definition, the average of (2.3.4) is

$$\langle G \rangle = G_M + \sum_{\alpha} \sum_{\beta \neq \alpha} \sum_{\gamma \neq \beta} \sum_{\delta \neq \gamma} \langle G_M t_{\alpha} G_M t_{\beta} G_M t_{\gamma} G_M t_{\delta} G_M \rangle + \dots \quad (2.3.6)$$

and the approximation is made

$$\langle G \rangle \approx G_M \quad (2.3.7)$$

The electronic density of states is then given by

$$\rho(E) = -\frac{1}{\pi} \text{Im Tr } \langle G \rangle \quad (2.3.8)$$

The average component density of states are given by

$$\rho^{A,B}(E) = -\frac{1}{\pi} \text{Im } \langle 0 | \langle (E + i0 - H^{A,B})^{-1} \rangle | 0 \rangle \quad (2.3.9)$$

2.3.2 Single Band Model For The Alloy

A great deal of effort has been put into the study of the binary substitutional alloy $A_x B_{1-x}$ of increasing complexity, the simplest model for which is that developed by Velicky, Kirkpatrick, Ehrenreich (1968). The model assumes a single band for the alloy.

A single orbital, $|n\rangle$, is associated with each site, n . A single band would result in the case of the pure crystal, but two sub-bands may occur in the alloy under certain conditions.

The one-electron Hamiltonian is taken to be

$$H = \sum_n |n\rangle \epsilon_n \langle n| + \sum_{n \neq m} |n\rangle t_{mn} \langle m| \equiv D + W \quad (2.3.10)$$

The second line represents the decomposition of the model Hamiltonian, H , into a diagonal part, D , and an off-diagonal, W , with respect to the Wannier representation. The matrix elements of H depend upon the configuration of A and B atom in the crystal. The assumptions on which the model is based, which are physically realizable when the orbitals are sufficiently localized and the atomic potentials are not too different are:

- (1) the diagonal elements, ϵ_n , can be considered to be atomic levels which assume one or two possible values ϵ^A and ϵ^B depending on whether an atom A or B occupies n ;
- (2) the hopping integrals, t_{mn} , which describe the transfer of electrons between sites, are completely independent of alloy composition.

W may therefore be interpreted as the Hamiltonian of a pure crystal for which $\epsilon^A = \epsilon^B = 0$, $\epsilon^A + W$ and $\epsilon^B + W$, respectively, are the Hamiltonians for the pure A and B crystal. The disorder is reflected in D and is cell localized. The elements of D are diagonal but random, those of W off-diagonal but translationally invariant. The operator W is diagonal in the Bloch representation:

$$\langle k|W|k'\rangle = \delta_{kk'} \sum_n t_{on} e^{i \vec{k} \cdot \vec{a}_n} \equiv \delta_{kk'} w s(k) \quad (2.3.11)$$

where

$$|k\rangle = N^{-\frac{1}{2}} \sum_n e^{i \vec{k} \cdot \vec{a}_n} |n\rangle \quad (2.3.12)$$

relates the Bloch and Wannier bases and w is one-half the bandwidth. $s(k)$ is the dispersion relation describing the k -dependence of the band energy and is dimensionless. It is also convenient to use the same energy units to express ϵ^A and ϵ^B , and to define the zero energy such that

$$\epsilon^A = \frac{1}{2}w\delta, \quad \epsilon^B = -\frac{1}{2}w\delta \quad (2.3.13)$$

(2.3.13) defines the dimensionless parameter

$$\delta = (\epsilon^A - \epsilon^B)/w \quad (2.3.14)$$

Significantly the entire behaviour of the Hamiltonian can be specified in terms of the two parameters x and δ . The bandwidth, which is determined by the hopping integrals, simply scales the energy. It is convenient to choose units such that $w = 1$.

In the single site description, the medium Hamiltonian, H_m , is diagonal in the k -representation:

$$\langle k|H_m(z)|k'\rangle = [s(k) + \Sigma(k,z)]\delta_{kk'} \quad (2.3.15)$$

(2.3.15) defines the quantity $\Sigma(k,z)$ which contains full information about the scattering corrections to the medium Hamiltonian, H_m . It is the self-energy with respect to the perfect crystal having Hamiltonian W . The (average) density of states per atom,

$$\rho(E) = N^{-1} \text{Tr} \langle \delta(E-H) \rangle \quad (2.3.16)$$

may be expressed in terms of the Green function.

$$\rho(E) = - (\pi N)^{-1} \text{Im Tr } \langle G(E+io) \rangle \quad (2.3.17)$$

(2.3.16) may be expressed in the Wannier and Bloch representations:

$$\rho(E) = - \pi^{-1} \text{Im} \langle n=0 | \langle G(E+io) \rangle | n=0 \rangle \quad (2.3.18)$$

Introducing the auxiliary quantity

$$F(z) = N^{-1} \text{Tr } \langle G(z) \rangle = \langle 0 | \langle G(z) \rangle | 0 \rangle \quad (2.3.19)$$

which in view of (2.3.18) has the property

$$\rho(E) = - \pi^{-1} \text{Im} F(E+io) \quad (2.3.20)$$

so that

$$F(z) = \int_{-\infty}^{\infty} \frac{dE}{z-E} \rho(E) \quad (2.3.21)$$

Explicit calculation of the average component density of states $\rho^{A,B}$ is possible since

$$\langle 0 | \langle (z-H^{A,B})^{-1} \rangle | 0 \rangle = \langle 0 | [z-H_m(z) - |0\rangle \langle 0| \epsilon^{A,B}(z)]^{-1} | 0 \rangle \quad (2.3.22)$$

where ϵ_n is replaced by $\epsilon(z)$ everywhere except at the zeroth site

where $\epsilon_0 = \epsilon^{A,B}$, and, therefore,

$$\rho^{A,B}(E) = - \pi^{-1} \text{Im} \{ F [1 - (\epsilon^{A,B}(z)) F]^{-1} \}_{z=E+io} \quad (2.3.23)$$

$\rho^{A,B}$ satisfy

$$\rho(E) = x \rho^A(E) + y \rho^B(E) \quad (2.3.24)$$

where $y = (1-x)$

2.3.3 Single Band Model: CPA

Section 2.3.1 has demonstrated that the CPA can be used to define a medium Hamiltonian, H_m , from the average Green function $\langle G \rangle$

$$G_m = (z - H_m)^{-1} \quad (2.3.25)$$

where $G_m = \langle G \rangle$. In terms of the original Hamiltonian (2.3.10), Velicky et al define a function $u(z)$ via the equation

$$H_m = W + \sum_n |n\rangle u(z) \langle n| = W + u(z) \underline{1} \quad (2.3.26)$$

The self-energy required is related to u and is k -independent. It is useful to define solutions for the pure crystal with Hamiltonian W :

$$G^0(z) = (z-W)^{-1}, \quad G^0(k,z) = [z-s(k)]^{-1} \quad (2.3.27)$$

$$F^0(z) = \int_{-\infty}^{\infty} dz (z-E)^{-1} \rho^0(E) \quad (2.3.28)$$

where $\rho^0(E)$ is the density of states. For H_m defined by (2.3.25) the unperturbed Green function is

$$\begin{aligned} G_m &= [z-u(z)-W]^{-1} \\ &= G^0[z-u(z)] \end{aligned} \quad (2.3.29)$$

The function corresponding to (2.3.19) is then

$$\langle 0 | G_m(z) | 0 \rangle = F^0[z-u(z)] \equiv F(z) \quad (2.3.30)$$

Equations (2.3.29) and (2.3.30) express results for the medium in terms of the pure crystal Hamiltonian W . It is this feature which makes the model tractable.

With H_m defined as above,

$$H - H_m = \sum_n |n\rangle [\epsilon_n - u(z)] \langle n| \quad (2.3.31)$$

To express $H-H_m$ as a sum of single scatterers

$$H - H_m = \sum_n V_n \quad (2.3.32)$$

so that

$$V_n = |n\rangle [\epsilon_n - u(z)] \langle n| = |n\rangle v_n \langle n| \quad (2.3.33)$$

From (2.3.3) and (2.3.30) it can be shown that

$$t_n(z) = |n\rangle v_n [1 - v_n F(z)]^{-1} \langle n| \quad (2.3.34)$$

where $t_n(z)$ represents the scattering off a single site n in the medium. The configurational average of (2.3.34) is

$$\langle t_n(z) \rangle = |n\rangle \left[\frac{x[\epsilon^A - u]}{1 - [\epsilon^A - u]F} + \frac{y[\epsilon^B - u]}{1 - [\epsilon^B - u]F} \right] \langle n| \quad (2.3.35)$$

The self-consistency condition determining $u(z) = \Sigma(z)$ is according to (2.3.5), $\langle t_n(z) \rangle = 0$, so that from (2.3.35),

$$\Sigma(z) = \frac{(2x-1)\delta}{2} - \left[\epsilon_A - \Sigma(z) \right] F(z) \left[\epsilon_B - \Sigma(z) \right] \quad (2.3.36)$$

(2.3.26) is thus the self-consistent condition for the effective medium in the coherent potential approximation.

2.3.4 Model Density Of States

For computational purposes, Velicky et al assume a model density of states to exist of the form first suggested by Hubbard (1964):

$$\begin{aligned} \rho^0(E) &= \frac{2}{\pi w^2} (w^2 - E^2)^{\frac{1}{2}}, & |E| < w \\ \rho^0(E) &= 0, & |E| > w \end{aligned} \quad (2.3.37)$$

which is such that

$$\rho^0(E) = \rho^0(-E)$$

and has a simple shape against which all distortions due to alloying

are clearly revealed. The function $F(z)$ yielding the form (2.3.37) for $\rho^0(E)$ is

$$F(z) = \frac{2}{w^2} \left[z - (z^2 - w^2)^{\frac{1}{2}} \right] \quad (2.3.38)$$

Substitution of (2.3.38) into the coherent potential criterion results in the cubic equation for $F(z)$:

$$\frac{1}{16} F^3 - \frac{1}{2} z F^2 + \left(z^2 - \frac{1}{4} - \epsilon^2 - xy\delta^2 \right) F - (z + \epsilon) = 0 \quad (2.3.39)$$

with
$$\epsilon = x \epsilon^A + y \epsilon^B \quad (2.3.40)$$

Equation (2.3.39) may be solved for real z . From (2.3.20) it can be seen that the density of states, ρ , is obtained from the complex root in the lower half plane. The component densities of state, $\rho^{A,B}$, are given by (2.3.23). Units are taken such that $w = 1$.

The CPA is found to yield correct results for the density of states in the appropriate limits. In the weak scattering limit ($\delta \ll 1$), the common band characteristic of the virtual crystal is reproduced. In the strong scattering limit, for sufficiently large δ (≈ 1), the band splits into the component sub-bands. Further, it interpolates correctly over the entire concentration range.

2.3.5 A Calculation On Binary Disordered Alloys

At 50-50 concentration set $\frac{1}{2}$ electron on each site. There are two quantities of interest:

- (1) the number of electrons at any one site at a fixed concentration; and,
- (2) the density of states at the Fermi level, $\rho(E_F)$, as a function of concentration, x .

The former is calculated to find out if, at a particular energy level separation, δ , a polarization of electrons onto one of the sites occurs corresponding to ionic behaviour. The latter uses $\rho(E_F)$ as a measure of the conductivity of the alloy to see if a significant drop in the density of states at the Fermi level occurs, explaining the behaviour of the liquid semiconductors at the critical concentration. The density of states, $\rho(E)$, is calculated in the CPA for binary disordered alloys in the single band model proposed by Velicky et al using the model density of states of section 2.3.4. $\rho(E)$ is thus obtained by solving equations (2.3.30) and (2.3.39). The Fermi energy is obtained using

$$\int_{-\infty}^{E_F} \rho(E, x) dE = n = \frac{1}{2} \quad (2.3.41)$$

The number of electrons on each site, $n^{A,B}$, are obtained from the local densities of state, $\rho^{A,B}$, using

$$n^{A,B} = \int_{-\infty}^{E_F} \rho^{A,B}(E, x) dE \quad (2.3.42)$$

where $\rho^{A,B}$ are given by (2.3.23). Tables 2.3.1 and 2.3.2 refer specifically to points (1) and (2) respectively

Table 2.3.1

The variation of the number of electrons on one atomic site, n^A , with the energy level separation, δ , in a 50-50 binary disordered alloy

δ	0.25	0.50	0.75	0.80	0.85	0.90	0.95	1.00	1.05	1.10	1.15	1.20	1.25
n^A	0.395	0.294	0.201	0.184	0.168	0.153	0.138	0.125	0.113	0.103	0.095	0.087	0.080

Table 2.3.1 shows the change in the number of electrons on one atomic site, n^A , with increasing energy level separation, δ . It can be seen quite clearly that despite a large separation of the bands, there remains a considerable fraction of an electron on the atomic sites. Complete polarization is not possible with sensible energy level separations.

Table 2.3.2

The density of states at the Fermi energy, $\rho(E_F)$, and the number of electrons on one atomic site, n^A , across the concentration range and with increasing energy level separation, δ .

δ	$\frac{\rho(E_F)}{n^A}$	x=0.20	x=0.35	x=0.50	x=0.65	x=0.80
0.25	$\rho(E_F)$	1.963	1.944	1.936	1.944	1.963
	n^A	0.337	0.365	0.395	0.427	0.459
0.50	$\rho(E_F)$	1.888	1.791	1.732	1.791	1.888
	n^A	0.210	0.243	0.294	0.362	0.428
0.75	$\rho(E_F)$	1.831	1.632	1.323	1.633	1.831
	n^A	0.131	0.152	0.201	0.313	0.408
1.00	$\rho(E_F)$	1.800	1.547	0.218	1.548	1.801
	n^A	0.086	0.098	0.125	0.284	0.397
1.25	$\rho(E_F)$	1.784	1.508	0.097	1.509	1.784
	n^A	0.060	0.067	0.080	0.268	0.391

Table 2.3.2. shows the variation in the density of states at the Fermi energy, $\rho(E_F)$, and the number of electrons on one atomic site, n^A , across the concentration range and with increasing energy level separation, δ . Once more it can be seen that complete polarization of an electron to any one site is not possible for sensible δ . The density of states at the Fermi energy does drop as the critical composition is approached, and as the energy level separation is increased, but not as dramatically as explained in the liquid semiconductor systems.

A very important point to come out of this study of the electronic properties of substitutional binary disordered alloys in the CPA is that no bonding can be completely ionic if only one-electron effects are important.

2.4 CHARGE TRANSFER IN LIQUID SEMICONDUCTORS

Liquid semiconducting systems such as Cu-Te, Ag-Te, Tl-Te, Mg-Bi, Li-Bi are characterized by phase diagrams which show a peak at a critical composition, and which are also known to possess marked heats of formation at the same composition. For the Mg-Bi system, for which detailed measurements of the heats of mixing are available, careful comparisons can be made with the phase diagrams (figure 2.4.1). This indicates the strength of bonding which must exist at the critical composition.

It has been argued, (Enderby and Collings, 1970; Enderby, 1974; Faber, 1972), that the chemical bond must have a significant effect on the density of states at the critical compositions since electron states may become localized as a result of bonding. One model for

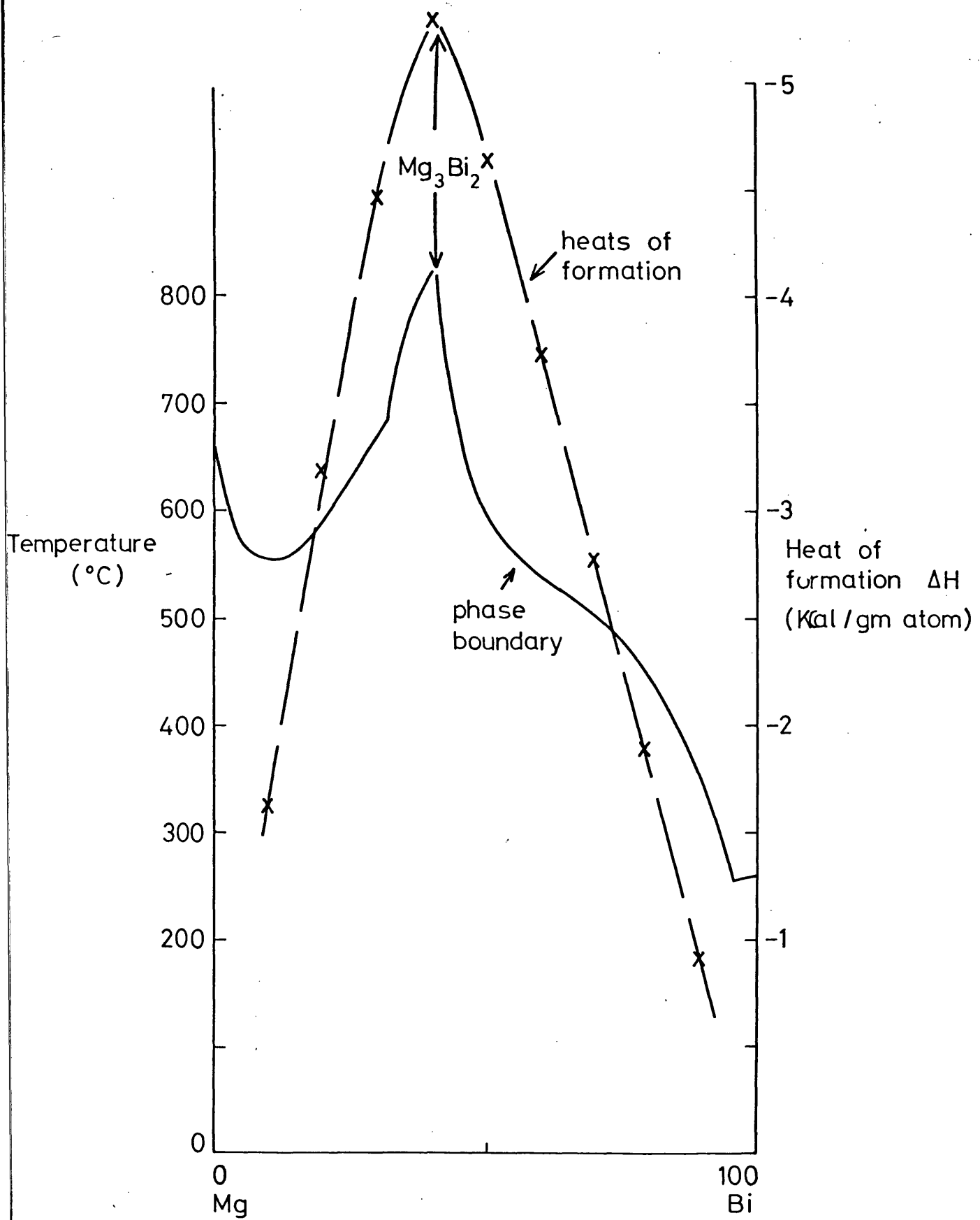


Fig.2.4.1. The phase boundary and heats of formation for the alloy system Mg Bi.

bonding in liquid semiconductor systems is the ionic model of Enderby (1974A). In this Enderby notes that if, at the critical composition a system is completely ionic with electrons localized in ionic sites, then the Stillinger-Lovett (1968) condition for electrical neutrality must be obeyed:

$$a_{11} - a_{22} = \frac{1}{C_1} - \frac{1}{C_2} \quad (2.4.1)$$

where $a_{\alpha\beta}$ is the long wavelength limit of the partial structure factor. A comparison between $(a_{11} - a_{22})$ and $(\frac{1}{C_1} - \frac{1}{C_2})$ is given for liquid Cu-Sn and Mg-Bi in figure 2.4.2. The 'ionic' curve appears to fit the data for the Mg-Bi system about $Mg_3 Bi_2$. This, supported by experimental evidence of electromigration in liquid Mg-Bi (Epstein, 1972), confirmed a notion that liquid Mg-Bi (amongst others) was essentially ionic in character about the critical composition, made up of $Mg_3 Bi_2$ molecules in excess magnesium or bismuth, each molecule being bound together by simple ionic electrostatic interactions. The bismuth atom is regarded as the strongly electronegative component. The electronegativity difference of 0.85 on the revised Pauling scale (Sanderson, 1960) falls within the 0.4 to 0.9 liquid semiconductor range and is considered to be a fair measure of the atomic potential difference.

For the case of a liquid semiconductor system such as Mg-Bi, Enderby's model gives the following pictures of the density of states across the concentration range.

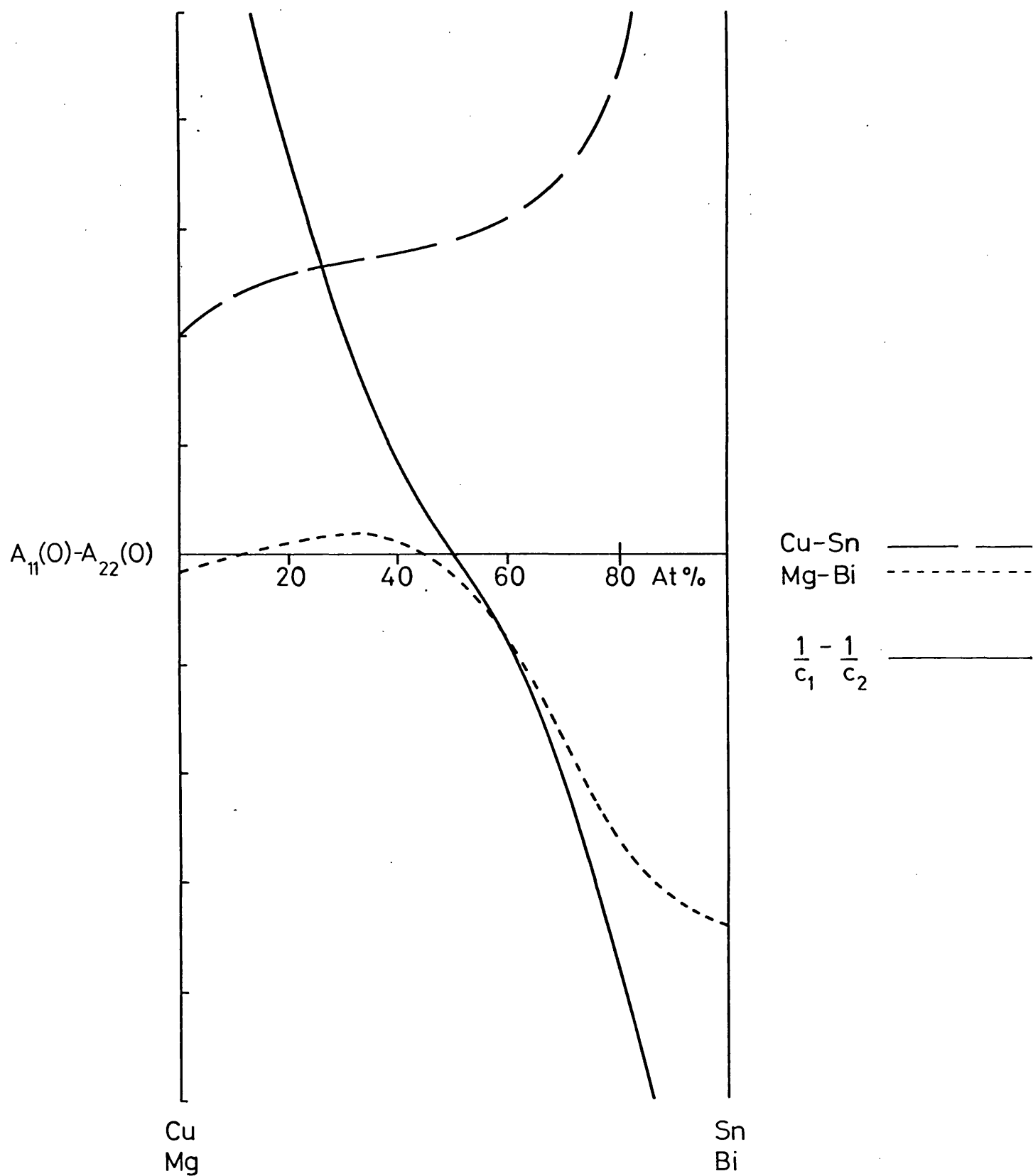
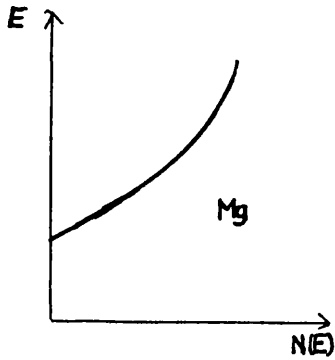
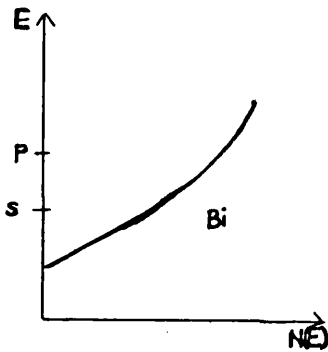


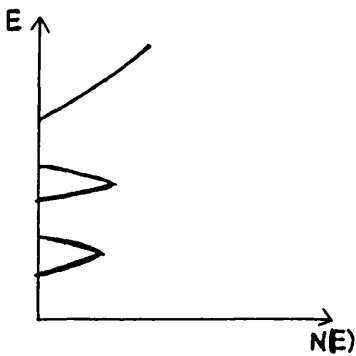
Fig. 2.4.2. Dependence of $A_{11}(O) - A_{22}(O)$ on composition for several alloys.



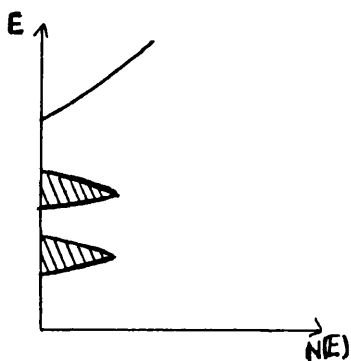
(a) The density of states are free electron-like for the pure elements.

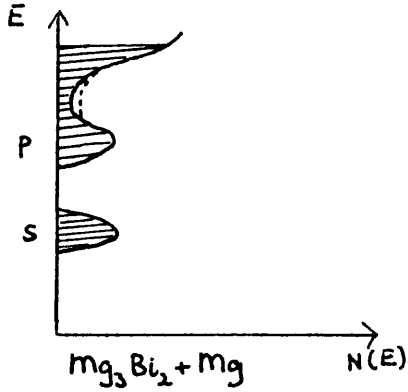


On alloying, bound states may be formed on the bismuth s, p states.



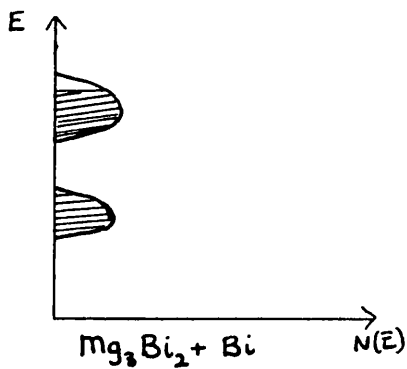
(b) For the $Mg_3 Bi_2$ composition, the bound states will be mostly full with electrons localized about the bismuth atoms. Only a few electrons will be thermally excited into higher states. The result is low conductivity and thermopower.





If excess Mg is added to Mg_3Bi_2 , the density of states is modified as shown. The thermopower will be negative. As more Mg is added the Fermi level may move up but the density of states may change as shown by the dotted line. The rate of change of conductivity with composition may therefore be small.

(c)



The dip in $N(E)$ - the Mott pseudogap - becomes most marked at Mg_3Bi_2 . If excess Bi is added to Mg_3Bi_2 the Fermi level may move back. Because the rate of change of the density of states is high in this region, the thermopower and conductivity will vary rapidly with composition.

The ionic model of Enderby therefore drains electrons out of the conduction band, localizing them about one site at the critical concentration, inferring large transfer. Note that the CPA calculations of the previous section do not substantiate this ionic model.

Faber (1972) has proposed an alternative model which requires more structure in the density of states. The model is illustrated in figure 2.4.1.

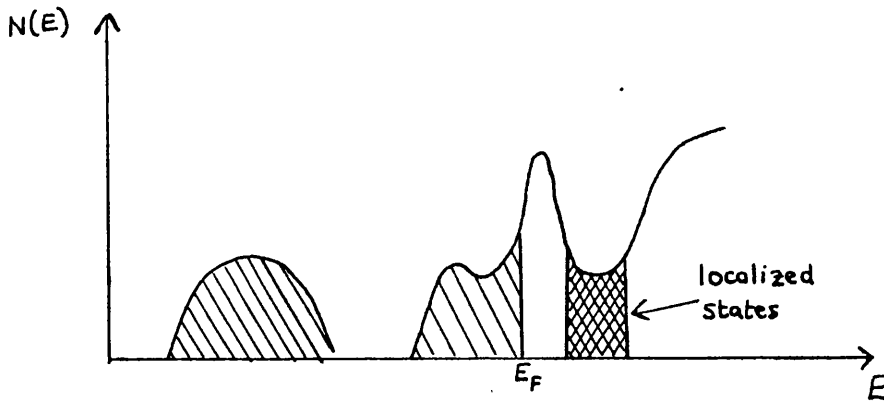


Fig. 2.4.1

The Fermi level position depends upon the nature of the excess element at the critical composition. As this composition is approached, the Fermi level will move to pass through the minimum in the density of states, localizing electron states, giving rise to the observed minimum in conductivity and zero thermopower. The sign of the thermopower will derive from the structure in the density of states.

CHAPTER III

CHARGE TRANSFER AND ELECTRONEGATIVITY DIFFERENCE

3.1 ELECTRONEGATIVITY DIFFERENCE

The electronegativity of an atom has been defined by Pauling (1939) to be the "power of an atom in a molecule to attract electrons to itself". The concept of relative electronegativity arose when it was noted that binary compounds with large electronegativity differences tended to form rocksalt structures, whereas those with smaller electronegativity differences favoured more open covalent structures. When the difference was large the heat of formation of the binary compound was noted to be large, providing a thermochemical use of the concept of electronegativity. The greater the electronegativity difference, the more ionic the bond, and the greater its heat of formation. Hume Rothery was the first to argue that the electronegativity difference might be a useful parameter in determining the charge transfer in a binary alloy since the atom with the greater electronegativity would cause charge to pile up around itself. Indeed, several authors have tried to relate charge transfer and electronegativity difference, but there is some confusion as to which electronegativity scale best describes alloying behaviour. The most commonly used electronegativity scales are those of Pauling and Coulson. Phillips (1970A,B) has argued that both these scales are unsatisfactory since neither can predict crystal structure in chemical compounds. It is not the purpose of this work to argue the merits of using either of these, or any other scale, but to investigate whether or not a crude correlation exists between electronegativity difference and charge transfer. A brief introduction to both these scales will prove helpful.

Pauling (1939) advocates a thermochemical rather than quantum mechanical approach to electronegativity and ionicity, turning from charge distributions to bond energies. When two elements, A and B, differ in electronegativity (X_A and X_B respectively), the heat of formation, D_{AB} , of the AB bond satisfies the relation

$$D_{AB} > (D_{AA} + D_{BB})/2 \quad (3.1.1)$$

where D_{AA} and D_{BB} represent the bond energies of elements A and B, respectively. According to Pauling this extra energy is ionic in origin, arising from charge transfer from the less electronegative (electropositive) to the more electronegative atom. Thus he defines electronegativity by the relation

$$D_{AB} - (D_{AA} + D_{BB})/2 \propto (X_A - X_B)^2 \quad (3.1.2)$$

where the constant of proportionality is chosen to have energy dimensions.

Fractional ionic character is defined by

$$f(A,B) = 1 - \exp \left[-(X_A - X_B)^2/4 \right] \quad (3.1.3)$$

The stability ratio, or Coulson electronegativity, S , of an element is defined as the ratio of the electron density of the element, D , to that of a hypothetical atom of the same atomic number of inert gas configuration. The electron density, D_i , of the hypothetical element is determined by linear interpolation between the higher and lower inert gas density. Thus,

$$S = D/D_i \quad (3.1.4)$$

Sanderson (1960) finds the following empirical relationship relating the Pauling electronegativity, X , and the stability ratio, S :

$$X^{\frac{1}{2}} = 0.21 S + 0.77 \quad (3.1.5)$$

Further, Sanderson states that when the two scales disagree, the physical and chemical evidence invariably favours the stability ratio. Stability ratios will be quoted in accordance with (3.1.5). It is significant to note that Miedema et al (1973) found no correlation between the heats of formation and the stability ratios in their analysis of metallic alloy data.

3.2 ELECTROCHEMICAL EFFECTS IN ALLOYS OF CADMIUM, MAGNESIUM AND MERCURY

3.2.1 Introduction

One of the principal applications of pseudopotential theory to alloy structures has been that of Inglesfield (1969 A,B) to alloys of cadmium, magnesium and mercury. The valuable feature of such systems is that the components have the same valency and roughly the same atomic size so that the electron density will be sufficiently uniform for a nearly free electron theory to work well. The calculations of Inglesfield form a quantitative theory of the effects of electronegativity difference on alloy properties when electronegativity difference is represented by the difference of the two pseudopotentials. In particular the tendency to assume an ionic structure and ordering energy with increase of electronegativity difference is described. It is found that alloys of metals which have a large electronegativity difference form ordered compounds. Enderby extended these conclusions to include the liquid semiconducting alloys by stating that a 0.4 to

0.9 electronegativity difference for such systems was large enough to lead to ionic bonding. It is important to have a closer look at Inglesfield's work.

3.2.2 Pseudopotential Theory of Alloy Structures

Take a crystal of N atoms which contains concentration c of B atoms and (1 - c) of A atoms. This gives a total of cN B atoms and (1 - c)N A atoms. In producing the total pseudopotential for the crystal V(r), add the pseudopotential (v_A) of the A atom at sites r_A and the pseudopotential of the B atom (v_B) at all the sites r_B occupied by B atoms:

$$V(r) = \sum_{r_A} v_A [r - r_A] + \sum_{r_B} v_B [r - r_B] \quad (3.2.1)$$

Fourier transform this to obtain V(q):

$$V(q) = \frac{1}{N} \sum_{r_A} v_A(q) \exp(-iq \cdot r_A) + \frac{1}{N} \sum_{r_B} v_B(q) \exp(-iq \cdot r_B) \quad (3.2.2)$$

where $v_A(q)$ and $v_B(q)$ are the transforms of the two ion pseudopotentials. This can be re-expressed in a more convenient form by writing an average pseudopotential \tilde{v} as the weighted mean of the pseudopotentials:

$$\tilde{v} = (1 - c)v_A + cv_B$$

The crystal can now be built by placing this at all lattice sites and then placing the difference potentials ($v_A - \tilde{v}$) and ($v_B - \tilde{v}$) at A and B sites respectively. There is an average lattice with an average potential \tilde{v} at every site, and a difference lattice with ($v_A - \tilde{v}$) at

all A sites and $(v_B - \tilde{v})$ at all B sites. The difference lattice may be expressed more simply by noting that

$$v_A - \tilde{v} = c(v_A - v_B)$$

and

$$v_B - \tilde{v} = -(1 - c)(v_A - v_B)$$

Accordingly, a single difference potential may be defined:

$$v_d = (v_A - v_B)$$

and $(1 - c)v_d$ may be placed at all B sites and cv_d at all A sites.

The total pseudopotential is then

$$\mathbf{V}(\mathbf{r}) = \sum_{\tilde{\mathbf{r}}_i} \tilde{\mathbf{V}}(\mathbf{r} - \tilde{\mathbf{r}}_i) + \sum_{\tilde{\mathbf{r}}_A} cv_d(\mathbf{r} - \tilde{\mathbf{r}}_A) - \sum_{\tilde{\mathbf{r}}_B} (1 - c)v_d(\mathbf{r} - \tilde{\mathbf{r}}_B) \quad (3.2.3)$$

where the $\tilde{\mathbf{r}}_i$ run over all lattice sites and the $\tilde{\mathbf{r}}_A$ and $\tilde{\mathbf{r}}_B$ only include A and B atoms respectively.

The Fourier transform is now

$$\begin{aligned} \mathbf{V}(\mathbf{q}) &= \frac{1}{N} \sum_{\tilde{\mathbf{r}}_i} \tilde{\mathbf{V}}(\mathbf{q}) \exp(-i\mathbf{q} \cdot \tilde{\mathbf{r}}_i) + \frac{1}{N} \sum_{\tilde{\mathbf{r}}_A} cv_d(\mathbf{q}) \exp(-i\mathbf{q} \cdot \tilde{\mathbf{r}}_A) \\ &\quad - \frac{1}{N} \sum_{\tilde{\mathbf{r}}_B} (1 - c) v_d(\mathbf{q}) \exp(-i\mathbf{q} \cdot \tilde{\mathbf{r}}_B) \end{aligned} \quad (3.2.4)$$

where $\tilde{\mathbf{V}}(\mathbf{q})$ and $v_d(\mathbf{q})$ are the transforms of the average and difference potentials. (3.2.4) may be re-written:

$$\begin{aligned} \mathbf{V}(\mathbf{q}) &= v_d(\mathbf{q}) \left| \frac{c}{N} \sum_{\tilde{\mathbf{r}}_A} \exp(-i\mathbf{q} \cdot \tilde{\mathbf{r}}_A) - \frac{(1 - c)}{N} \sum_{\tilde{\mathbf{r}}_B} \exp(-i\mathbf{q} \cdot \tilde{\mathbf{r}}_B) \right| \\ &= v_d(\mathbf{q}) (cS_A - (1 - c) S_B) \end{aligned} \quad (3.2.5)$$

where the structure factors S_A and S_B are

$$S_A = \frac{1}{N} \sum_{\mathbf{r}_A} \exp(-i\mathbf{q} \cdot \mathbf{r}_A) \quad \text{and} \quad S_B = \frac{1}{N} \sum_{\mathbf{r}_B} \exp(-i\mathbf{q} \cdot \mathbf{r}_B)$$

Treating $V(\mathbf{q})$ as a small perturbation, using perturbation theory, the total energy of the conduction electrons and ions, U , may be written:

$$U = U_0 + U_{BS} + U_E \quad (3.2.6)$$

where U_0 is the structure-independent energy of an atomic sphere, and $(U_{BS} + U_E)$ is structure dependent, being called the structural energy term. Since the mean atomic volume is kept constant, then the structure-independent energy interpolates linearly as a function of concentration:

$$U_0 = (1 - c) U_{0A} + cU_{0B} \quad (3.2.7)$$

U_E is an electrostatic energy term giving the electrostatic energy of the positive ions in a uniform negative background. U_E for the alloy is the same as U_E for A and B. U_{BS} , the 'band structure' energy, is the second order contribution of the matrix element $V(\mathbf{q})$ to the energy of the Fermi sphere of electrons. Heine (1968) has shown that the second-order contribution of $V(\mathbf{q})$ to the Fermi sphere is

$$|V(\mathbf{q})|^2 \epsilon(\mathbf{q}) \chi(\mathbf{q}) \quad (3.2.8)$$

$$\text{where } \epsilon(\mathbf{q}) = 1 + \frac{4}{\pi q^2} \left(\frac{K_F}{2} + \frac{(K_F^2 - q^2/4)}{2q} \ln \left[\frac{q+2K_F}{q-2K_F} \right] \right) \quad (3.2.9)$$

$$\chi(\mathbf{q}) = (1 - \epsilon(\mathbf{q})) \frac{q^2 \Omega}{8\pi}$$

(atomic units $e = \hbar = m = 1$).

The total band structure energy is obtained by substituting (3.2.5) into (3.2.8)

$$\begin{aligned}
 U_{BS} &= \sum_{\substack{q=g \\ \sim \sim}} [S(g)]^2 [\tilde{v}(q)]^2 \chi(q) \epsilon(q) + \sum_{\substack{q \neq g \\ \sim \sim}} [v_d(q)]^2 \chi(q) \epsilon(q) (cS_A - (1-c)S_B)^2 \\
 &= \sum_g [S(g)]^2 \tilde{F}(q) + \sum_{q \neq g} F_d(q) (cS_A - (1-c)S_B)^2 \quad (3.2.10)
 \end{aligned}$$

where the first sum is over all non-zero reciprocal lattice vectors g of the basic lattice, and the second sum is over all wavevectors q . $\tilde{F}(q)$ is the average wavenumber characteristic:

$$\tilde{F}(q) = [\tilde{v}(q)]^2 \epsilon(q) \chi(q)$$

and $F_d(q)$ is the 'alloying energy wavenumber' characteristic:

$$F_d(q) = [v_d(q)]^2 \epsilon(q) \chi(q) \quad (3.2.11)$$

The first term in U_{BS} is the band structure energy of the lattice with the alloy crystal structure and the virtual crystal potential at each site. The second term, called U_a , contains all information regarding the particular arrangement of the A and B atoms on the lattice.

For a random distribution of A and B atoms over atomic sites Inglesfield was able to show that

$$U_a(\text{disordered}) = c(1-c)N^{-1} \sum_q F_d(q) \quad (3.2.12)$$

in the order-disorder transition. When A and B have the same volume and valency the total energy, U , can be expressed in terms of the

energies of pure A and pure B with the same crystal structure as the alloy:

$$\Delta \equiv U - \bar{U} = U_a - C(1-c)N^{-2} \sum_g [S(g)]^2 F_d(g) \quad (3.2.13)$$

where \bar{U} is the means of the energies of A and B with the same crystal structure. (3.2.13) contains only the alloying difference potential v_d .

3.2.3 The Square Well Alloying Potential

To obtain $F_d(q)$, the alloying potential was taken as the difference between the two pseudopotentials calculated by Animalu and Heine (1965). Inglesfield fits the alloying potentials by a spherically symmetric square well described by two parameters - the well depth, A, and radius, R_m . The matrix elements of the square well model are

$$v_o(q) = (4\pi A / \Omega q^3) [\sin(qR_m) - (qR_m) \cos(qR_m)] \quad (3.2.14)$$

Hence,

$$F_d(q) = (4\pi A / \Omega q^3)^2 [\sin(qR_m) - (qR_m) \cos(qR_m)]^2 \chi(q) \epsilon(q) \quad (3.2.15)$$

A^2 is chosen so that $F_d(q)$ is fitted to the same minimum as the computed $F_d(q)$. R_m is the same for the three alloys taken as $R_m = 2.6$ a.u. The volume per ion is 150 a.u.

3.2.4 Ordering and Electronegativity

The values of A used by Inglesfield are shown in table 3.2.1, and in figure 3.2.1 these are plotted against electronegativity

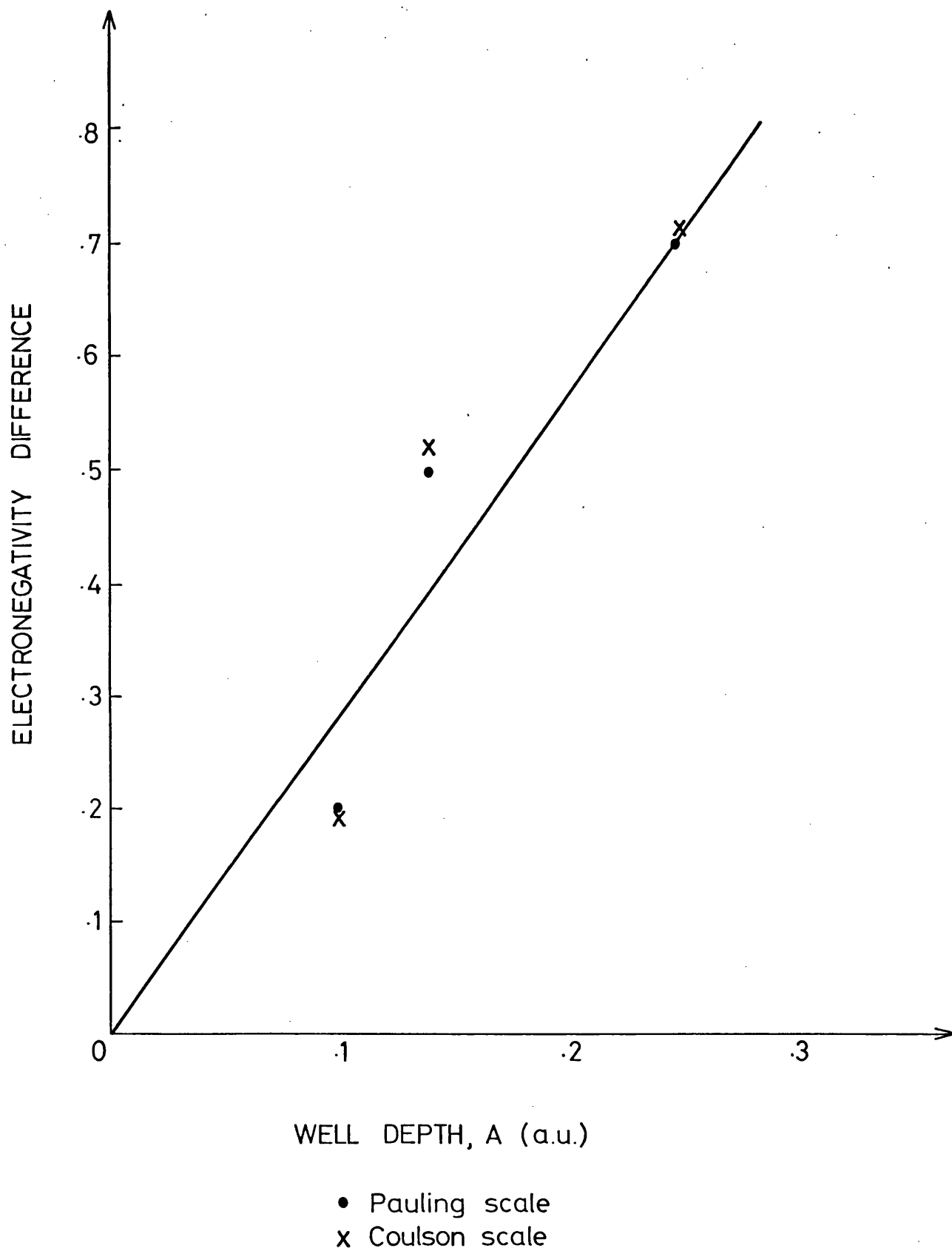


Fig. 3.21. Plot of electronegativity difference against alloying potential square well depth (Inglesfield 1969).

differences for the three systems.

<u>System</u>	<u>Cd-Hg</u>	<u>Cd-Mg</u>	<u>Hg-Mg</u>
A(A.U.)	0.10	0.14	0.25
Pauling Electronegativity Difference	0.2	0.5	0.7
Coulson Electronegativity Difference	0.19	0.52	0.71

The electronegativity differences and well depths are roughly proportional. Inglesfield claims that since charge transfer is related to the differences in pseudopotentials, it must therefore in turn be related to the electronegativity difference.

The important point about the square well potential is that for any crystal structure the ordering energy is proportional to A^2 (c.f. 3.2.13). The values of the ordering energy calculated for an arbitrary choice of $A = 1$, are shown in table 3.2.2 together with a description of the basic crystal structure and ordered energies calculated for the same choice of A .

<u>Basic Structure Type</u>	<u>Description</u>	<u>U_a(ordered) (A.U. per ion)</u>	<u>Ordering Energy (A.U. per ion)</u>
HgMg	bcc	-0.285	0.060
CdMg	hcp(distorted)	-0.262	0.037
CdHg	bct	-0.270	0.045

U_a disordered is equal to -0.225 a.u. per ion so that in all three cases it is energetically favourable to have ordering. The energy difference between the ordered and disordered structures is similar for the three structures. The effect of increasing the well depth (electronegativity difference) is to increase the order-disorder transition for a given crystal structure.

3.2.5 Basic Structures

For each structure, the value of Δ when $A = 1$, Δ_M , is given in table 3.2.3.

<u>Structures</u>	<u>Δ_M</u> <u>(A.U. per ion)</u>
HgMg	-0.169
CdMg	-0.149
CdHg	-0.157
NaCl	-0.172

The typically ionic structures (NaCl and HgMg) have the largest values of Δ_M . Δ favours structures of the ionic type simply because they give large ordering energies.

Rewriting (3.2.13) in terms of Δ , Inglesfield was able to explain basic structures on the basis of the competition of two effects:

$$U = \bar{U} + \Delta$$

\bar{U} , the mean energy of the two component metals evaluated for the same crystal structure, is found to be the primary determinant of the alloy structures of MgCd and CdHg. It favours structures closely related to the observed structures of the component metals. The remaining term Δ , which is proportional to A^2 , comes into the reckoning when MgHg is considered since A is the largest for this system. It favours ionic type structures. The MgHg structure is one such structure.

3.2.6 Summary

The calculations of Inglesfield form a quantitative theory of the effects of electronegativity difference on the properties of the Cd, Mg, Hg alloy systems. In particular, the increase of charge transfer, tendency to assume an ionic structure, and ordering energy with increase of electronegativity difference are all described.

3.3 ELECTROCHEMICAL EFFECT IN SIMPLE METAL ALLOYS

3.3.1 Introduction

The pseudopotential theory techniques used by Inglesfield work well for alloys of magnesium, cadmium and mercury, but the problem for two elements with different valences is not so simple. Consider a substitutional alloy of elements having similar atomic volumes in the pure metal (e.g. LiMg) so that all atoms in the alloy may be thought of as occupying Wigner-Seitz cells of identical shape and size. It then seems natural that the net electric charge in a cell should give a measure of the charge transfer. In pseudopotential theory one starts with the alloy ions immersed in a uniform electron gas, a situation in which charge transfer has already taken place.

Generally the ion of higher valence will have the more attractive pseudopotential. However, as the electrons relax, a large part of the pseudopotential difference will be exhausted in shifting charge from one cell to another in a tendency towards charge neutrality. This means that the difference in pseudopotential well depths is no longer the only factor determining electrochemical effects. Hodges and Stott (1972) recognised this problem and devised a scheme to calculate charge transfer and heats of formation of simple metal alloys based on the theory of the inhomogeneous electron gas proposed by Hohenberg and Kohn (1964). Their approach is similar to that of Varley (1954) and constitutes a justification of his two band model for concentrated disordered alloys.

Consider a metal-metal interface across which no charge transfer has taken place. Electron charge will flow from the metal with the higher Fermi level to that with the lower Fermi level, setting up an electric dipole which produces an additional electrostatic potential which balances the two Fermi levels. Hodges and Stott suggest that the boundary between atomic polyhedra belonging to different elements is similar to such an interface and propose that it may be treated in a similar fashion. They bring the Wigner-Seitz cells of the constituents to the same atomic volume (that appropriate to the alloy), build up the alloy of these cells, and ultimately let the charge distribution relax at the boundaries. The charge transferred they define to be the amount crossing the cell boundary in the relaxation process, and it corresponds to equalisation of the two Fermi levels. The next two sections will put all these ideas on a formal basis with an improvement upon the Hodges and Stott model. The final two

sections will contain results of the charge transfer calculated using this model for some 50-50 simple metal alloys with a discussion of the connection between the amount of charge transferred and electro-negativity differences.

3.3.2 Formalism

The ideas discussed in the introduction may be developed formally using the Hohenberg-Kohn density variational principle for an electron gas. The density-functional formalism is based on the theorem that the ground state energy of a system of electrons moving in a static external potential $v(\mathbf{r})$ is a unique functional $E[n]$ of the density. It follows from the variational principle that for the ground state density distribution $E_V[n]$ is a minimum with respect to other distributions involving the same total number of electrons. The constancy of the number of particles is imposed in the variational problem by means of the Lagrange multiplier μ , and the condition for the correct density is

$$\frac{\delta E[n]}{\delta n(\mathbf{r})} = \mu \quad (3.3.1)$$

where μ is independent of position. The advantage of using this formalism is that it allows determination of the alloy charge distribution and energy starting from a trial density function $n_t(\mathbf{r})$ which, instead of being uniform, may be chosen so that $n_t(\mathbf{r})$ is continuous at the cell boundaries. Suppose the trial functional n_t gives a functional derivative

$$\left[\frac{\delta E[n]}{\delta n} \right]_{n=n_t} = \mu_t(\mathbf{r}) \quad (3.3.2)$$

which instead of being constant has some small r -dependence, one may then expect $n_t(r)$ and the trial functional $E(n_t)$ to be close to the ground state density and energy. $\mu_t(r)$ will be interpreted as a kind of local Fermi level taking on μ_A or μ_B in A or B cells respectively.

A suitable choice for the functional $E[n]$ is that proposed by Hohenberg and Kohn valid for a slowly varying density:

$$E[n] = \int v(r)n(r)dr + \frac{e^2}{2} \iint \frac{n(r)n(r')}{|r-r'|} + \int \epsilon(n)n(r)dr + g'[n] \quad (3.3.3)$$

where $\epsilon(n)$ is the ground state energy per electron of a uniform electron gas generalised to include exchange and correlation, and $g'[n]$ is a functional of the electron density expressed in terms of the derivatives of the density $n(r)$. The variational principle applies to the total electronic density, including the core electrons, which will cause rapid variation of the electronic density in the core region. It is unsure how well the theory will work in such a region, and so it is convenient to regard $v(r)$ as a local energy independent approximation to the valence electron pseudopotential, in which case $n(r)$ represents the more slowly varying pseudo-electron charge density. Since electron redistribution will be considered to take place at the cell boundary, the distinction between the pseudo-electron charge density and the true valence electron density is unimportant. The density gradient term $g'[n]$ which is found to reproduce the wave-number dependent density-density response function is that of Von Weisacker:

$$g' [n] = \lambda \frac{\hbar^2}{8m} \int \frac{(\nabla n)^2}{n} dr \quad (3.3.4)$$

Hodges and Stott have looked at the problem in detail and conclude that the choice $\lambda = 1/9$ ensures the correct response of the electron gas at low q while overestimating the response for $g > 2 k_F$ in the alloy problem, following Jones and Young (1971). The gradient terms represent a contribution to the kinetic energy of the electrons not already included in the local energy $\epsilon(n)$. They are also responsible for eliminating any discontinuities in the distribution $n(r)$.

3.3.3 Gradient Terms - Charge Transfer

$n_o(r)$ is taken to be constant within each cell, $n_c(r)$ is chosen so that the trial density $n_t(r)$ is continuous at the cell boundaries:

$$n_t(r) = n_o(r) + n_c(r) \quad (3.3.5)$$

in which case the gradient terms may be written:

$$g' [n_t] = \lambda \frac{\hbar^2}{8m} \int \frac{[\nabla n_c]^2}{n_t} dr \quad (3.3.6)$$

where the prime denotes exclusion of an infinitesimal region at the boundaries between A and B cells. Expanding $E[n_t]$ to second order in n_c about n_o so that

$$E[n_t] = E_o + E_1 + E_2 \quad (3.3.7)$$

where $E_o = E'[n_o]$ is the sum of the energies of the parent metals after they have been adjusted to the alloy atomic volume and structure.

Thus only E_1 and E_2 contribute to the alloy formation energy. E_1 is linear in n_c and is given by

$$E_1 = \int \left[\frac{\delta E[n]}{\delta n} \right]_{n=n_0} n_c(r) dr$$

$$= \int \mu_0(r) n_c(r) dr \quad (3.3.8)$$

where $\mu_0(r)$ is interpreted to be the local Fermi level of the distribution n_0 , and is equal to μ_A and μ_B according to whether r is in an A or a B cell. The term E_2 which is second order in n_c may be deduced from (3.3.3) and (3.3.6) to be

$$E_2 = \frac{e^2}{2} \iint dr dr' \frac{n_c(r) n_c(r')}{|r-r'|} + \frac{1}{2} \int \left[\frac{d\mu_u}{dn} \right]_{n_0} n_c^2(r) dr$$

$$+ \lambda \frac{\hbar^2}{8m} \int' \frac{|\nabla n_c|^2}{n_0} dr \quad (3.3.9)$$

where μ_u is the chemical potential of an electron gas of uniform density n .

Integrating by parts inside regions A and B,

$$E[n_t] - E[n_0] = \int n_c(r) \left[\mu_0 + \frac{e^2}{2} \int \frac{n_c(r')}{|r-r'|} dr' \right.$$

$$+ \frac{1}{2} \left[\frac{d\mu_u}{dn} \right]_{n_0} n_c(r) - \lambda \frac{\hbar^2}{8m} \frac{\nabla^2 n_c}{n_0} \left. \right] dr + \lambda \frac{\hbar^2}{8m} \int \left[\frac{n_{0+}}{n_{0+}} - \frac{n_{0-}}{n_{0-}} \right] \nabla n_t \cdot ds$$

$$(3.3.10)$$

where the last term is a surface integral taken over the boundary between the A and B cells, and n_{c+} , n_{o+} , n_{c-} , n_{o-} are the values of the discontinuous functions n_c and n_o close to and on either side of this surface. (3.3.10) gives for the functional

$$\frac{\delta E[n]}{\delta n(\mathbf{r})} = \mu_o + e^2 \int \frac{n_c(\mathbf{r}')}{|\mathbf{r}-\mathbf{r}'|} d\mathbf{r}' + \left[\frac{d\mu}{dn} \right]_{n_o} n_c(\mathbf{r}) - \lambda \frac{\hbar^2}{4m} \frac{\nabla^2 n_c}{n_o} \quad (3.3.11)$$

At this stage $\frac{\delta E[n]}{\delta n}$ can be set equal to a constant in which case n_t will be the ground state distribution:

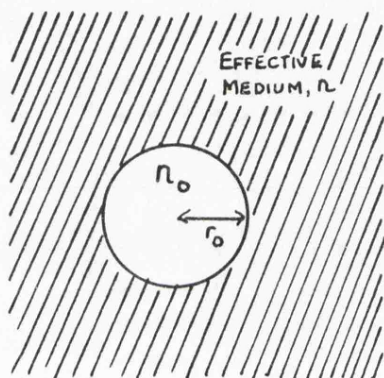
$$\begin{aligned} \left[\frac{\delta E[n]}{\delta n} \right]_{n=n_o} &= \mu_t, \\ &= \mu_A, \text{ a constant inside A cells} \quad (3.3.12) \\ &= \mu_B, \text{ a constant inside B cells} \end{aligned}$$

Equations (3.3.11) and (3.3.12) give an integro-differential equation for n_c which may be converted using Poisson's equation to a linear differential equation with constant coefficients (inside A regions or B regions)

$$4\pi e^2 n_c - \left[\frac{d\mu_u}{dn} \right]_{n_o} \nabla^2 n_c + \lambda \frac{\hbar^2}{4m} \frac{(\nabla^2)^2 n_c}{n_o} = 0 \quad (3.3.13)$$

Equation (3.3.13) may be solved analytically by assuming that n_c is localised near the A-B cell boundary.

Hodges and Stott treat the alloy problem as that similar to an infinite, plane A-B interface. They construct a solution n_c which gives n_t and its first derivative continuous across the interface as well as giving zero charge transfer. A second correcting distribution $n'_c(r)$ is then constructed which governs the amount of charge transferred in the alloying process. This model can be improved upon by considering the three-dimensional case of the 50-50 alloy with A and B atoms in an effective medium chosen such that the charge lost by one atom is



gained exactly the other. $n_c(r)$ is chosen as in (3.3.5) so that $n_t(r)$ and its first derivative are continuous across the respective cell-effective medium boundary, as well as giving the charge transfer across the boundary. Solving (3.3.13) then in this three dimensional situation gives the correcting distributions:

$$\begin{aligned} n_c^0(r) &= A \sinh \alpha_0 r \frac{\sinh \beta_0 r}{r} \quad \text{in } n_0 \\ n_c(r) &= B e^{-\alpha r} \frac{\sinh (\beta r + \eta)}{r} \quad \text{in } n \end{aligned} \tag{3.3.14}$$

with α_0, β_0 given by

$$\alpha_0 = K_0 + \lambda_0$$

$$\beta_0 = K_0 - \lambda_0$$

where

$$K_0 = \left\{ \frac{2mn_0}{\lambda\hbar^2} \left[\left(\frac{d\mu}{dn} \right)_{n_0} + \left[\left(\frac{d\mu}{dn} \right)_{n_0}^2 - \frac{4\pi\lambda e^2 \hbar^2}{mn_0} \right]^{1/2} \right] \right\}^{1/2} \quad (3.3.15)$$

$$\lambda_0 = \left\{ \frac{2mn_0}{\lambda\hbar^2} \left[\left(\frac{d\mu}{dn} \right)_{n_0} - \left[\left(\frac{d\mu}{dn} \right)_{n_0}^2 - \frac{4\pi\lambda e^2 \hbar^2}{mn_0} \right]^{1/2} \right] \right\}^{1/2}$$

The subscripts 0 refer to either an A or a B atom, expressions being evaluated at n_A or n_B respectively. α, β correspond to the above expressions evaluated at n , the density of the effective medium.

The boundary conditions that n_t and its derivative be continuous at the cell boundary, r_0 , enables one to evaluate the constants A and B in terms of η . η may be evaluated from the condition that the total charge throughout the system is constant:

$$\int_0^\infty 4\pi r^2 n_c(r) dr = 0 \quad (3.3.16)$$

These conditions result in the values for A and B given by

$$A = \frac{(n-n_0)r_0 [\beta r_0 - (\alpha r_0 + 1) \tanh(\beta r_0 + \eta)]}{\sinh\alpha_0 r_0 \sinh\beta_0 r_0 [\beta r_0 - \alpha r_0 \tanh(\beta r_0 + \eta)] - X \tanh(\beta r_0 + \eta)}$$

where

$$X = \alpha_0 r_0 \cosh\alpha_0 r_0 \sinh\beta_0 r_0 + \beta_0 r_0 \cosh\beta_0 r_0 \sinh\alpha_0 r_0$$

$$\tanh(\beta r_0 + \eta) = \frac{Y\beta r_0 + X'Z [(\alpha^2 - \beta^2)\beta r_0 - 2\alpha\beta]}{Y(\alpha r_0 + 1) - X'Z [(\alpha^2 - \beta^2)(\alpha r_0 - 1) + 2\alpha^2]} \quad (3.3.17)$$

where

$$X' = X - \sinh\alpha_0 r_0 \sinh\beta_0 r_0$$

$$Y = (\alpha_0^2 - \beta_0^2) (\alpha_0 r_0 \sinh \beta_0 r_0 \cosh \alpha_0 r_0 - \beta_0 r_0 \cosh \beta_0 r_0 \sinh \alpha_0 r_0) \\ - (\alpha_0^2 + \beta_0^2) \sinh \alpha_0 r_0 \sinh \beta_0 r_0 + 2\alpha_0 \beta_0 (\cosh \beta_0 r_0 \cosh \alpha_0 r_0 - 1)$$

$$Z = \frac{n_0}{n}$$

The charge transfer is then given by

$$q = \frac{4\pi AY}{(\alpha_0^2 - \beta_0^2)^2} \quad (3.3.18)$$

The charge transfer in the alloying process is that derived when n is chosen in a self-consistent manner such that the charge flow from one atom into the medium exactly equals the charge flow from the medium into the other atom.

3.3.4 Charge Transfer Calculations

Hodges and Stott estimate the value of the alloy cell radius, R_a , of a series of binary 50-50 simple metal alloys by minimising the elastic energy necessary to compress or dilate the parent metal cells. Their values for R_a and their charge transfer across the infinite, plane interface are given in table 3.3.1 together with the charge transfer calculated with the aid of (3.3.18). Electronegativity differences on both the Pauling and Coulson scales are also given. Plots of charge transfer at the alloy cell radius against electronegativity difference are given in figures 3.3.1a (Pauling) and 3.3.1b (Coulson).

Alloy		Ra (a.u.)	Pauling Electronegativity Difference	Coulson Electronegativity Difference	Charge Transfer (Hodges & Stott)	Charge Transfer (3.3.18)
A	B					
Na	Hg	3.46	1.0	1.07	0.18	0.163
Li	Hg	3.32	0.9	1.0	0.04	0.091
Na	Cd	3.34	0.8	0.88	0.04	0.167
Mg	Cd	3.29	0.5	0.52	0.08	0.014
Cd	Hg	3.29	0.2	0.19	0.08	0.016
Mg	Hg	3.34	0.7	0.51	0.17	0.002
Al	Zn	2.94	0.1	0.47	0.15	0.069
Mg	Al	3.09	0.3	0.18	0.01	0.15
Cd	Ga	3.21	0.7	0.37	0.01	0.101
In	Cd	3.35	0	0.15	0.14	0.042
Cd	Zn	3.05	0.1	0.02	0.07	0.078
In	Hg	3.01	0.2	0.04	0.12	0.050
Zn	Hg	3.42	0.3	0.06	0.23	0.098
Mg	Zn	3.04	0.4	0.65	0.01	0.077

Charge transfer calculated with the aid of (3.3.18) disagrees substantially with that calculated by Hodges and Stott. A revision of the problem along the lines suggested may give the better agreement with experiment on heats of formation data which the Hodges and Stott calculation lacks. The important point to note is the total lack of correlation between charge transfer and electronegativity difference on both scales (figure 3.3.1). Charge transfer calculated with unchanged Wigner-Seitz cell radii for the alloy constituents gives slightly better correlation with electronegativity difference (in particular on the Pauling scale), but it is still poor. One is led to conclude that electronegativity difference is not as meaningful a parameter for determining the amount of charge transfer in solid disordered alloys as it is in ionic solids. Indeed, it is not clear that a simple empirical relationship can exist between charge transfer and electronegativity can exist when electronegativity differences are so small. Further, the formally derived amount of charge transfer for the alloy systems considered is much smaller than one would expect if the solids were ionically bonded.

The theory of the previous section assumes that core levels are localized within the boundaries of the Wigner-Seitz cell and that there is no contribution to charge transfer across cell boundaries. The assumption is not strictly valid for alloy systems involving transition or noble metals, which have therefore been excluded. The validity of the assumption is questionable for elements Hg and Cd included in the alloy systems since it is not certain that a clear distinction exists between core and valence electrons.

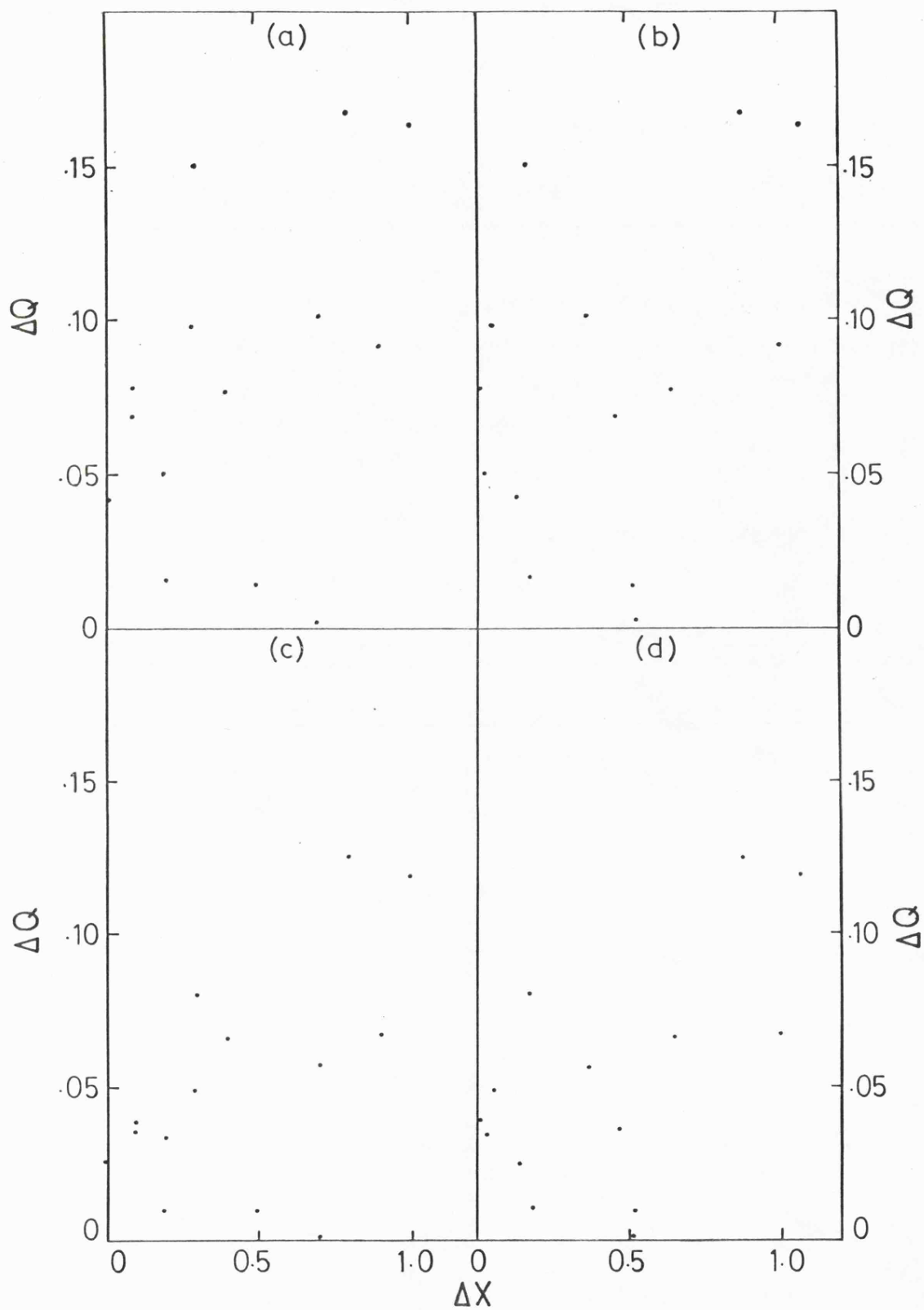


Fig.3.3.1 Comparison of charge transfer, ΔQ , and electronegativity difference, ΔX .

- (a) Plot of ΔQ against ΔX (Pauling) at alloy cell radius
- (b) Plot of ΔQ against ΔX (Stability Ratio) at alloy cell radius
- (c) Plot of ΔQ against ΔX (Pauling) at Wigner-Seitz cell radii
- (d) Plot of ΔQ against ΔX (Stability Ratio) at Wigner-Seitz cell radii

3.3.5 Conclusion

The work presented in this chapter does not support the view that electronegativity difference is a significant parameter in estimating electrochemical effects in solid binary disordered alloys. The ability to determine the degree of ionicity appears to be lost when electronegativity differences are small. Electronegativity differences for liquid semiconductors fall within the range 0.4 to 0.9 on both the Pauling and Coulson scale, which is within the range looked at. This implies that total ionic bonding is improbable within liquid semiconductor systems. Indeed, the amount of charge transfer is likely to be small.

CHAPTER IV

CHARGE TRANSFER AND ATOMIC CELL SIZE

4.1 THE PROBLEM

It is not clear which is the physically most meaningful definition for the charge transfer in ordered and disordered alloys since quantitative estimates of the quantity depend upon the atomic cell size prescribed. Hodges and Stott (1972) adopt a purely geometric definition by bringing the Wigner-Seitz cells of the constituents to the alloy atomic volume, building up the alloy of such cells, and letting the charge distribution relax at the cell boundaries. The charge transfer is that which crosses the cell boundaries in the relaxation process. Miedema et al (1973) view alloys as being constructed from atomic cells (different cells for different atoms) which in the first order approximation are similar to the atomic cells of the atoms in the pure metallic elements. As a result of charge transfer, the atomic cell sizes may change. Their approach is similar to that of Varley (1954) which mathematically relates the charge transfer with the change in atomic cell size (see section 4.2). In chapter II it was seen that the charge density in an alloy must extend continually from one atom to the next. In the region between atoms, the tails of the wavefunction overlap, with a resulting charge density which does not go to zero. It is obvious that the charge density goes to a minimum value between atoms and it seems natural to construct spheres about each atomic site touching each other at the point of minimum density between them, defining the charge about each atom as that within the sphere so constructed.

Different definitions for the atomic cell size clearly will result in the amount of charge taken up, and therefore the meaning of the formally derived amount of charge is not obvious. It is the purpose of this chapter to investigate many of the points raised here, and, in particular, to look at atomic cell size description within ordered and disordered solid alloys. If a suitable definition for the atomic cell size can be found, fuller descriptions for liquid alloy and semiconductor systems may be at hand.

4.2 THE CHANGE IN ATOMIC CELL SIZE WITH CHARGE TRANSFER

4.2.1 Introduction

In an attempt to calculate the heat of formation of binary alloys Varley proposes a two band model for electron states in concentrated disordered alloys, assuming that free electrons exist in two sets of energy levels associated with the two elements in the alloy which are superposed to give a non-uniform electron density. This is a commonly accepted model. With such a description for the electron states, Varley determines not only heats of formation but also charge transfer by allowing the atoms to grow as they take up charge. The change in atomic cell size, which Varley envisages as charge is transferred, is a reasonable and interesting proposition worthy of close examination in the form presented. Suggestions will be made as to possible improvements on the calculation.

4.2.2 General Considerations

Consider the disordered alloy containing $N(1-c)$ A atoms and Nc B atoms. With the nearly free electron two band description, electrons

in A cells have an average energy given by

$$E_A = E_{OA} + \frac{3}{5} k \frac{Z_A^{2/3}}{r_A^2} ; \quad k = \frac{\hbar^2}{8m} \left(\frac{9}{4\pi^2} \right)^{2/3} \quad (4.2.1)$$

while those in B cells have a corresponding energy E_B , provided there is no charge transfer from A cells (say) to B cells. Z_A and Z_B are the numbers of free electrons per atom cell of pure A and pure B; r_A and r_B are the corresponding equilibrium cell radii in the pure states; E_{OA} and E_{OB} are the pure state bottoms of the band. The total energy, NE , of the system is then

$$NE = N(1-c)Z_A E_A + NcZ_B E_B \quad (4.2.2)$$

Suppose that on average a charge n leaves each A cell and is uniformly distributed over Nc B cells. The number of electrons within each cell is changed so that the average energy of an electron in an A cell will change from E_A to E'_A and similarly E_B will change to E'_B . The total energy, NE' , of the disordered alloy will be

$$NE' = N(1-c)(Z_A - n)E'_A + Nc(Z_B + n(1-c)/c)E'_B \quad (4.2.3)$$

The alloy will form only if the resultant energy of the system is lowered as a consequence, hence $E' - E \leq 0$. The charge transfer will give a negative contribution to the alloy heat of formation. The donor cells (A) will become smaller when they lose charge and the cells which accept charge, (B), will expand. The minimum electron energies, E_0 , in the A and B cells will change as will also the

additional kinetic energy per electron. The change in the relative cell sizes when charge is transferred results in a strain energy being present.

4.2.3 Variation in E_0 and Atomic Cell Radius With Charge Transfer

In a pure metal, the equilibrium radius, r_0 , of the atomic cell is approximately determined by

$$\left[\frac{\partial E_0}{\partial r} \right]_{r_0} = - \left[\frac{\partial [E_F(Z)]}{\partial r} \right]_{r_0} \quad (4.2.4)$$

where the atomic volume $\Omega = \frac{4}{3} \pi r_0^3$, and (4.2.4) neglects the effect of closed shell interactions upon r_0 . If on average, there is a change n in the amount of charge in a cell, the new equilibrium radius is determined from

$$\left[\frac{\partial E_0}{\partial r} \right]_{r_0} = - \left[\frac{\partial [E_F(Z+n)]}{\partial r} \right]_{r_0} \quad (4.2.5)$$

Assuming that $\frac{\partial E_0}{\partial r}$ is constant in the region $r = r_0$, neglecting the direct dependence of E_0 upon n (assumed to be small), then

$$\left[\frac{\partial E_0}{\partial r} \right]_{r_0} = \left[\frac{\partial E_0}{\partial r} \right]_r \quad (4.2.6)$$

so that

$$\left[\frac{\partial [E_F(Z+n)]}{\partial r} \right]_r = \left[\frac{\partial [E_F(Z)]}{\partial r} \right]_{r_0} \quad (4.2.7)$$

Since

$$E_F(Z) = \frac{3k}{5} \frac{Z^{2/3}}{r_0^2} ; \quad [E_F(Z+n)] = \frac{3k}{5} \frac{(Z+n)^{2/3}}{r^2}$$

it follows from equation (4.2.7) that

$$r = r_0 \left(1 + \frac{n}{Z}\right)^{2/9} \quad (4.2.8)$$

which is an approximate relationship between the cell size and the charge transfer n . E_0 may now be expressed as a function of r and n as

$$E_0(r) = E_0(r_0) + (r-r_0) \left(\frac{\partial E_0}{\partial r}\right)_{r_0} \quad (4.2.9)$$

When, using (4.2.8) and (4.2.9),

$$E_0(r) = E_0(r_0) - \frac{6kZ^{2/3}}{5r_0^2} \left\{1 - \left(1 + \frac{n}{Z}\right)^{2/9}\right\} \quad (4.2.10)$$

4.2.4 Change in Interaction Energy, and the Strain Energy, with Charge Transfer

If a charge n' enters a cell already containing Z_B electrons, $Z_B n'$ interactions of average energy (q_{OB}/r_B) are produced. Varley follows the Wigner-Seitz cellular construction to get this average interaction energy. The Coulomb interaction energy of $1.2 e^2/r$ per electron pair in an atomic cell r is offset by $0.916 e^2/r$ per electron pair from exchange interactions and $-be^2/r$ per electron pair from correlation interactions between electrons of opposite spin. The

total interaction energy charge is thus,

$$\frac{q_{OB} Z_B n'}{r_B} = \frac{Z_B n' e^2 (0.284 - b(r_{OB}))}{r_{OB} (1 + n'/Z)^{2/9}} \quad (4.2.11)$$

Varley was able to make a rough estimate of the strain energy to be

$$E_S = N(r_A - r_B)^2 c(1-c) Kr_A \quad (4.2.12)$$

where K is the bulk modulus for a particular atom, and Kr_A is taken as an average over the two pure components.

4.2.5 Formation Energy and Charge Transfer

The average energy per atom, E, at absolute zero of an alloy containing NcB atoms and N(1-c) A atoms is

$$\begin{aligned} E = & E_{OA} (Z_A - n) (1-c) + E_{OB} \left[Z_B + \frac{n(1-c)}{c} \right] c - \frac{q_{OA}}{r_A} n(1-c) (Z_A - 1) \\ & + Z_B \frac{q_{OB}}{r_B} \frac{n(1-c)}{c} c + \frac{3}{5} \frac{k}{r_A^2} (Z_A - n)^{5/3} (1-c) \quad (4.2.13) \\ & + \frac{3}{5} \frac{k}{r_B^2} \left(Z_B + \frac{n(1-c)}{c} \right)^{5/3} c + P c(1-c) (r_A - r_B)^2 \end{aligned}$$

where $P = Kr_A$

where an amount of charge n has, on average, left each A cell and distributed itself uniformly over Nc B cells. The sizes of A and B cells have changed so that

$$r_A = r_{OA} \left(1 - \frac{n}{Z_A}\right)^{2/9}; \quad r_B = r_{OB} \left(1 + \frac{n(1-c)}{Z_B^c}\right)^{2/9} \quad (4.2.14)$$

where r_{OA} , r_{OB} are the atomic radii in pure A and B.

The ground state energies $[E_0]$ are also n dependent:

$$[E_{OA}] = E_{OA} - \frac{6kZ_A^{2/3}}{5r_{OA}^2} \left\{1 - \left(1 - \frac{n}{Z_A}\right)^{2/9}\right\} \quad (4.2.15)$$

$$[E_{OB}] = E_{OB} - \frac{6kZ_B^{2/3}}{5r_{OB}^2} \left\{1 - \left(1 + \frac{n(1-c)}{Z_B^c}\right)^{2/9}\right\}$$

Substitution of equations (4.2.14) and (4.2.15) into (4.2.13) gives

$$E = Z_A E_{OA} (1-c) + Z_B E_{OB}^c + \frac{3}{5} \frac{kZ_A^{5/3}}{r_{OA}^2} (1-c) + \frac{3}{5} \frac{kZ_B^{5/3}}{r_{OB}^2} c$$

$$+ Pc(1-c) (r_{OA} - r_{OB})^2 + n(1-c)X + \frac{n^2(1-c)}{c} Y \quad (4.2.16)$$

where

$$X = \left\{ E_{OB} - E_{OA} + \frac{kZ_B^{2/3}}{r_{OB}^2} - \frac{kZ_A^{2/3}}{r_{OA}^2} + \frac{q_{OB}Z_B}{r_{OB}} - \frac{q_{OA}(Z_A-1)}{r_{OA}} \right.$$

$$\left. + \frac{4P}{9} (r_{OB} - r_{OA}) \left(\frac{r_{OB}(1-c)}{Z_B} + \frac{r_{OA}^c}{Z_A} \right) \right\}$$

and

$$\begin{aligned}
 Y = & \left\{ \frac{11kz_A^{-1/3}}{45r_{OA}^2} c + \frac{11kz_B^{-1/3}}{45r_{OB}^2} (1-c) - \frac{2q_{OB}(1-c)}{9r_{OB}} - \frac{2q_{OA}(z_A-1)c}{9r_{OA}z_A} \right. \\
 & + \frac{2P}{8I} \left[\frac{7c^2}{z_A^2} + \frac{7(1-c)^2}{z_B^2} + \frac{4c(1-c)}{z_A z_B} \right] r_{OA} r_{OB} \\
 & \left. - \frac{10P}{8I} \left[\frac{r_{OA}^2 c^2}{z_A^2} + \frac{r_{OB}^2 (1-c)^2}{z_B^2} \right] \right\} \quad (4.2.17)
 \end{aligned}$$

Since the first four terms for E in equation (4.2.16) represent the energy of phase mixture of pure A and pure B, the alloy heat of formation is

$$\Delta E = Pc(1-c)(r_{OA} - r_{OB})^2 + n(1-c)X + \frac{n^2(1-c)Y}{c} \quad (4.2.18)$$

where n must satisfy $\frac{\partial(\Delta E)}{\partial n} = 0$. This gives a value for the charge transfer

$$n = -Xc/2Y \quad (4.2.19)$$

Hence the alloy heat of formation is given by

$$\Delta E = c(1-c) \{ P(r_{OA} - r_{OB})^2 - X^2/4Y \} \quad (4.2.20)$$

4.2.6 Possible Improvements

Two quantities which Varley has difficulty in estimating are the pure metal Fermi level difference and bottom of the band difference for various alloy systems. It is now possible to determine these very accurately using band structure calculations. In his calculations

Varley includes alloys with noble metal constituents without taking account of d-bands; band structure calculations will give a far more accurate determination of the nearly free electron bandwidths. It will not prove fruitful to examine Varley's approach to this problem in detail, but a comparison of these difference parameters is of interest. The results for the Fermi level difference and difference in bottoms of the band for the pure noble metals Cu, Ag and Au, listed in tables 4.2.1 and 4.2.2, respectively, come from the band structure calculations of O'Sullivan, Switendick, Schirber (1970).

TABLE 4.2.1						
System		Varley	Band	Band	Band	Band
B	A	$E_{OA}^B - E_{OB}^A$	Structure	Structure	Structure	Structure
Acceptor	Donor	(eV)	E_{OA}	E_{OB}	$E_{OA}^B - E_{OB}^A$	$E_{OA}^B - E_{OB}^A$
			(Ryd.)	(Ryd.)	(Ryd.)	(eV)
Ag	Cu	1.63	-0.02112	-0.0142	-0.093	-0.17
Au	Cu	0.99	-0.02112	-0.0325	0.0114	0.16
Au	Ag	2.62	-0.0142	-0.0325	0.0183	0.15

TABLE 4.2.2						
System		Varley	Band	Band	Band	Band
B	A	$E_F^B - E_F^A$	Structure	Structure	Structure	Structure
Acceptor	Donor	(eV)	E_F^B	E_F^A	$E_F^B - E_F^A$	$E_F^B - E_F^A$
			(Ryd.)	(Ryd.)	(Ryd.)	(eV)
Ag	Cu	.05	.5003	.6303	-0.13	-1.77
Au	Cu	2.63	.289	.6303	-0.34	-4.63
Au	Ag	2.68	.289	.5003	-0.31	-4.22

The acceptor-donor classification is that of Varley.

Not only does Varley get the ground state energy difference and the Fermi level difference wrong in magnitude, the prediction for the direction of charge flow is also incorrect. This must lead to poor descriptions for the charge transfer and heats of formation.

Varley also deliberately omits to include core exchanges and van der Waal's interactions for noble metals. Once charge transfer has taken place the resultant electrostatic interaction is deemed to be small, and then ignored:

$$E_e \sim \frac{e^2 n^2 p(1-c)}{2} \left\{ \frac{1}{r_{AA}} + \frac{1}{r_{BB}} - \frac{2}{r_{AB}} \right\} \quad (4.2.21)$$

where r_{AA} , r_{BB} , r_{AB} are the nearest neighbour bond lengths, and p is the lattice coordination number. Such an n^2 variation may be an important factor in determining the charge transfer in equation (4.2.18) and the heat of formation, and should be included.

4.2.7 Summary

Varley's attempt to calculate the charge transfer and heats of formation for alloys rely upon the concept of change in atomic cell size with charge transfer. Improvements upon his theoretical treatment have been offered, but the important point to note is the view that charge transfer and atomic cell size are closely related.

4.3 THE ONE-DIMENSIONAL BINARY ALLOY

4.3.1 Introduction

The calculations of section 2.3 demonstrated that in a 50-50 substitutional binary disordered alloy whose potentials are known to differ, electrons will not totally polarize about one of the atomic sites no

matter how different the potentials are made. This effect may be demonstrated in one dimension using the Kronig-Penney model for an ordered binary alloy. Two atoms, whose potentials are modelled by delta-functions of different strengths, are placed in an ordered array throughout the crystal with two atoms per unit cell, the crystal being made up of N such cells. The electron number density across the unit cell is the physical quantity which will give information about polarization effects in the alloy. The problem in ordered and disordered binary alloys is in defining the atomic cell size. For the one-dimensional model, one possible definition for the cell size is half the unit cell, another is the minimum in the electron density, in which case charge transfer has already taken place. Comparisons of electron number densities about each atomic site within the cells so defined in one dimension will advance our understanding of the three-dimensional problem.

4.3.2 Theoretical Treatment

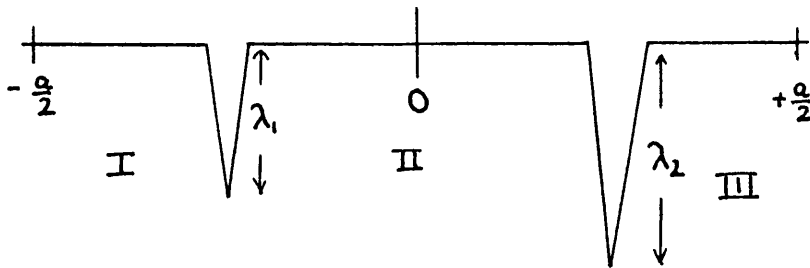


Figure 4.3.0

Consider a one-dimensional ordered binary alloy built up with unit cells of length a such as that illustrated in figure 4.3.0 located $-a/2 < x \leq a/2$. Representing atomic potentials by attractive delta functions of strength λ_1 and λ_2 located at $-a/4$ and $+a/4$, respectively,

the potential within the unit cell is thus

$$v(x) = -\lambda_1 \delta(x + a/4) - \lambda_2 \delta(x - a/4) \quad (4.3.1)$$

in atomic units ($\hbar^2/2m = 1$, $e^2 = 2$) where λ has units of L^{-1} .

The solutions between any two delta functions are

$$\psi(x) = Ae^{\mu x} + Be^{-\mu x} \quad (4.3.2)$$

where μ may be real or imaginary ($E = -\mu^2$), and A and B change from region to region within cells.

For this calculation we shall choose μ real. In the three regions marked in figure 4.3.0

$$\begin{aligned} \psi_I(x) &= Ae^{\mu x} + Be^{-\mu x} & -a/2 < x \leq a/4 \\ \psi_{II}(x) &= Ce^{\mu x} + De^{-\mu x} & -a/4 < x \leq a/4 \\ \psi_{III}(x) &= Ee^{\mu x} + Fe^{-\mu x} & a/4 < x \leq a/2 \end{aligned} \quad (4.3.3)$$

It may be shown that delta function potentials introduce a discontinuity in the slope of the wavefunction. The matching through a delta function located at $x = x_0$, say, is

$$\begin{aligned} \psi(x_0^+) &= \psi(x_0^-) \\ \left[\frac{\partial \psi}{\partial x} \Big|_{x_0^+} - \frac{\partial \psi}{\partial x} \Big|_{x_0^-} \right] &= -\lambda \psi(x_0) \end{aligned} \quad (4.3.4)$$

Electron Number Density Across Unit Cell

One Electron Per Unit Cell

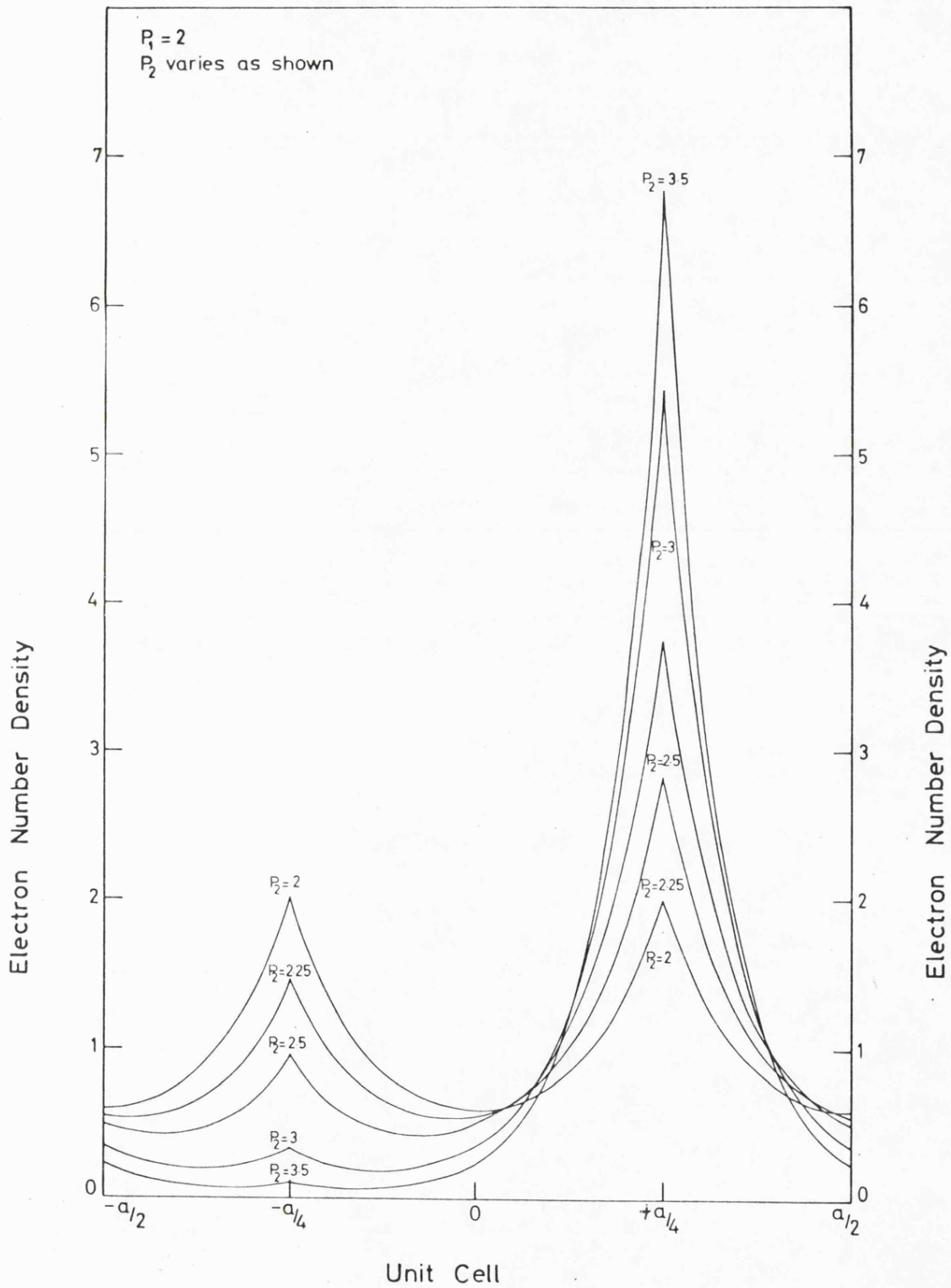


Fig 4.3.1

Electron Number Density Across Unit Cell
Two Electrons Per Unit Cell

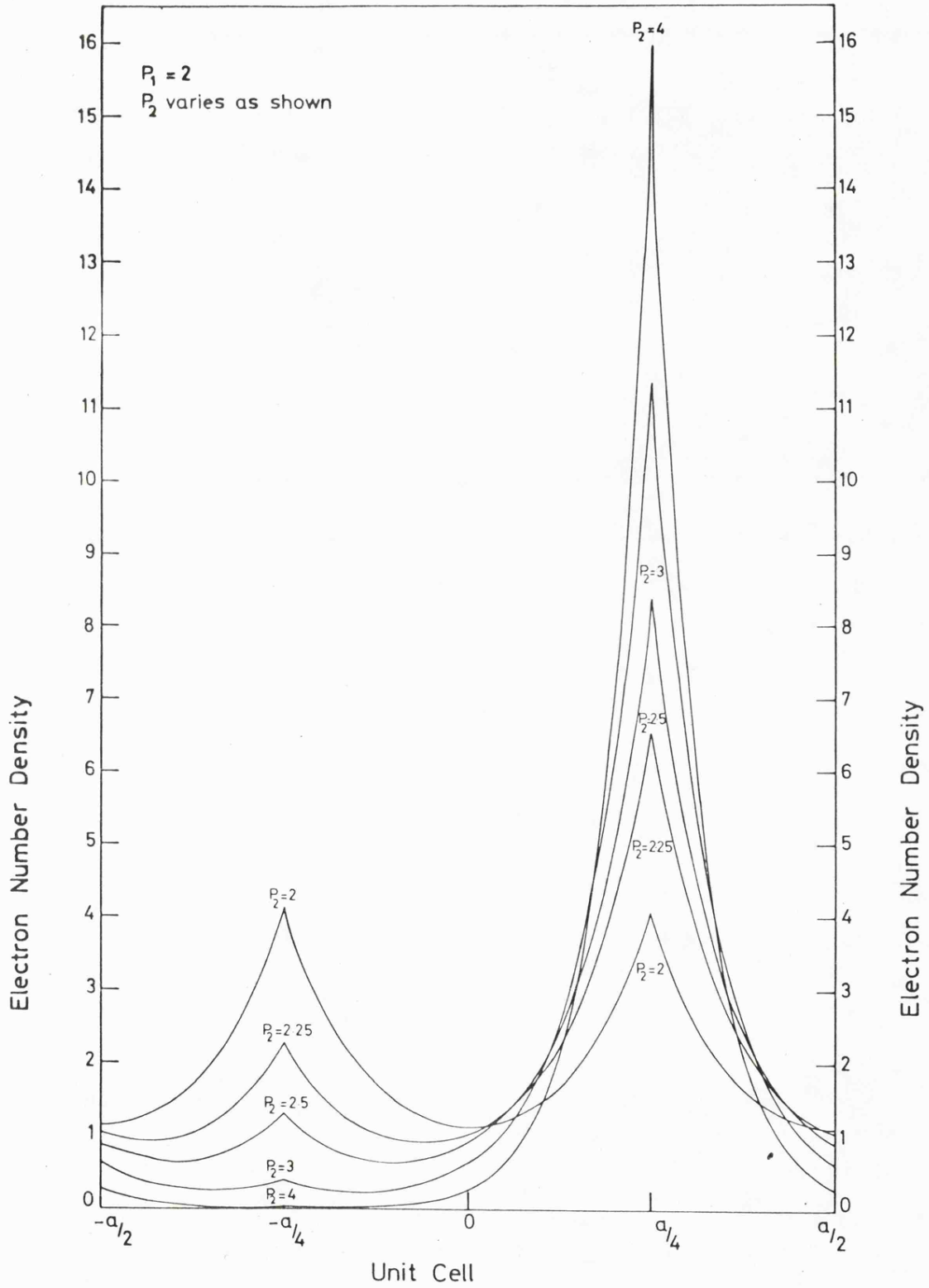


Fig. 4.3.2

where the probability density $\psi_k^*(x)\psi_k(x)$ is given using (4.3.3) in the three separate regions specified. k_F is the Fermi wavevector restricted to positive values. $k_F = \pi/2a$ for one electron per unit cell, $k_F = \pi/a$ for two electrons per unit cell, etc. To find the fractional charge contained within a particular region of the cell, integrate (4.3.10) over x :

$$n(\text{region}) = \int_{\text{region}} n(x) dx \quad (4.3.10)$$

4.3.3 Results and Conclusion

Figures (4.3.1) and (4.3.2) show the variation in the electron number density across a unit cell containing one electron and two electrons respectively. P_1 is fixed at two units, P_2 is varied as shown. The figures clearly show that as λ_2 is increased with respect to λ_1 , electrons tend to pile up about the more attractive atom. However, no matter how large the attractive power of λ_2 is made, there is always a finite probability of the electron remaining on the weaker atom. This reinforces our ideas that no bond in such a system can be fully ionic in nature. Since the attracting power of atoms in alloys is generally agreed not to be as strong as it is in ionic compounds, it is improbable that solid, or liquid, ordered or disordered, alloys will be ionic in the sense that sodium chloride is.

Table 4.3.1 gives the charge enclosed about the less attractive atom site for atomic cell sizes described by

- (i) half the unit cell size, and
- (ii) from minimum to minimum in the electron density.

P_2 is again fixed at two units.

<u>TABLE 4.3.1</u>					
One Electron Per Unit Cell			Two Electrons Per Unit Cell		
P_2	Charge in at. cell size (i)	Charge in at cell size (ii)	P_2	Charge in at. cell size (i)	Charge in at. cell size (ii)
2	0.5	0.5	2	1.0	1.0
2.25	0.384	0.343	2.25	0.622	0.501
3.5	0.257	0.202	2.5	0.409	0.260
3	0.119	0.054	3	0.167	0.063
3.5	0.053	0.014	4	0.044	0.004

The different definitions for the atomic cell size give enclosed charges which do not substantially disagree for relative electron attracting powers likely to be found in the majority of ordered binary alloy systems. It is expected that for the three-dimensional alloy situation, a definition for the cell size to be that from minimum to minimum in the electron density, will give quantitative estimates of the charge transfer not too different from that using the pure metal Wigner-Seitz radius.

4.4 THREE-DIMENSIONS

This section is an extension of the revised Hodges and Stott calculation of section 3.3. The aim is to compare the amount of charge transferred when a different definition for the cell size is used. Charge transfer is calculated self-consistently for a 50-50 disordered alloy with the help of equation (3.3.18). Table 4.4.1 gives the results

of the charge transfer calculated:

(i) at the alloy cell radius, as estimated by Hodges and Stott,

and

(ii) at the pure element Wigner-Seitz cell radii.

<u>TABLE 4.4.1</u>			
Alloy		Charge Transfer at 'Alloy' Cell Radius (i) (fraction of electron)	Charge Transfer at Wigner-Seitz Radius (ii) (fraction of electron)
α	β		
Hg	Na	0.163	0.119
Hg	Li	0.091	0.067
Cd	Na	0.167	0.125
Cd	Mg	0.014	0.009
Cd	Hg	0.016	0.010
Mg	Hg	0.002	0.001
Al	Zn	0.069	0.036
Ga	Cd	0.101	0.056
In	Cd	0.042	0.025
Zn	Cd	0.078	0.039
Ga	Zn	0.034	0.018
In	Hg	0.050	0.034
Zn	Hg	0.098	0.049
Al	Mg	0.150	0.08
Zn	Mg	0.077	0.066

Table 4.4.1 demonstrates that although the different atomic cell size does alter the amount of charge transfer, it does not do so by a great amount. Charge transfer calculated at the Wigner-Seitz radii is smaller than that calculated at the alloy cell radius - that is, different cell size leads to different amount of charge transfer. Hence it may well be reasonable to retain the Wigner-Seitz radius as a definition for the atomic cell size in disordered systems, recognising that the cell size will change the charge transfer.

CONCLUSION: PART I

It has become clear over the last three chapters that it is improbable that concentrated disordered alloys and liquid semiconductors are ionic in the sense that the alkali halides are ionic. This is in disagreement with the proposal of Enderby that it is the existence of ionically bonded molecules which account for the remarkable electronic properties of metal-metal liquid semiconductors at the critical composition. Arguments based on the premise that electronegativity difference is a useful measure of the relative attracting power of atoms for electrons within these systems are not substantiated, since the differences are too small for it to be clear that a correlation does exist between charge transfer and electronegativity difference. The problem of atomic cell size within alloys has been raised. A cell size definition using the minimum in the electron density around each atom site in an ordered alloy is prescribed. It is unlikely, however, that the values derived will practically prove useful since they will not be independent of the systems under consideration. Instead, the Wigner-Seitz cell radii for the pure metal may be used as a first approximation with charge transfer altering cell sizes. It is also clear how difficult it is to determine the degree of ionicity for various systems just by inspection of the charge density. The question as to whether a system is ionic or not is unanswerable, or meaningless, when considered from the operational point of view of starting with the charge density.

CHAPTER V

THE HYDROGEN MOLECULE IN AN ELECTRON GAS

5.1 INTRODUCTION

Enderby's model for the liquid semiconducting metal-metal systems has assumed the formation of chemical complexes at or near the critical concentration which are ionically bonded. The discussions of the previous chapters have effectively ruled out this as a possibility. If these complexes do exist, however, then the bonding may well be covalent. Away from the critical composition the covalent complexes will be present in a sea of electrons provided by the constituent ions. The effect of the free electrons will be to screen potentials within each chemical complex so that the molecular binding will be weakened and internuclear separations lengthened, even to the extent that the molecule may be broken up. Thus the molecular binding energy will vary in a changing free electron environment. It is the purpose of this chapter to demonstrate this point for the case of a single hydrogen molecule located in an electron gas.

Experimental observations have found the binding energy of the hydrogen molecule in free space to be 4.75 eV, with an internuclear separation of 0.74^oA. Two methods for calculating the change in the binding energy of the hydrogen molecule have been adopted. The first is based upon the original Heitler-London calculation, but with all Coulomb potentials screened, falling off exponentially with distance (section 5.2). The second uses the density functional formalism of Hohenberg-Kohn-Sham, and is discussed in detail in section 5.3. Both will be seen to confirm the notion of the change in molecular binding energy with electron density for the hydrogen molecule, even though

binding energies calculated at particular electron densities using both models will not agree. In such a situation, binding energies calculated using the density functional formalism are considered to be the more realistic, particularly near to electron densities in the metallic regime.

5.2 HYDROGEN MOLECULE IN AN ELECTRON GAS I

5.2.1 Treatment

The method of calculation to be employed is a simple one based upon the Heitler-London calculation for the hydrogen molecule in free space (see, for example, Margenau and Murphy (1955)). The coordinate system to be used will be clear from figure 5.2.1. Particles 1 and 2 are electrons; A and B are the protons whose positions are regarded as fixed.

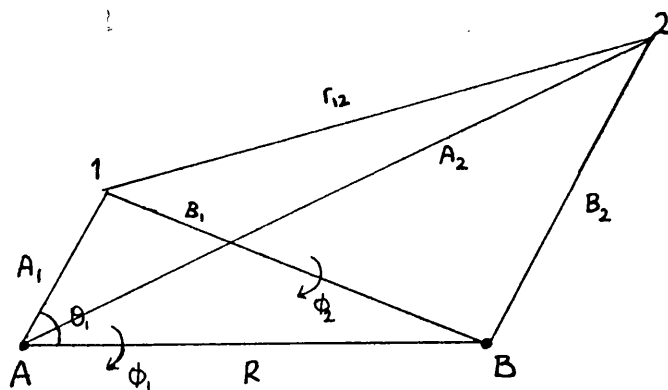


Figure 5.2.1

A convenient coordinate system for the two electrons will contain the six variables $A_1, B_1, B_2, r_{12}, \phi_1, \phi_2,$

$$|B_2 - B_1| \leq r_{12} \leq B_1 + B_2 \quad 0 < B_2 < \infty$$

$$|B_1 - R| \leq A_1 \leq B_1 + R \quad 0 < B_1 < \infty$$

The volume element $d\tau = d\tau_1 d\tau_2$, where

$$d\tau_1 = A_1^2 dA_1 \sin\theta_1 d\theta_1 d\phi_1$$

Now,

$$B_1^2 = A_1^2 + R^2 - 2A_1 R \cos\theta_1$$

i.e. $2B_1 dB_1 = 2A_1 R \sin\theta_1 d\theta_1$

$$d\tau_1 = \frac{1}{R} A_1 dA_1 B_1 dB_1 d\phi_1$$

Similarly, using B_1 as a base line,

$$d\tau_2 = \frac{1}{B_1} r_{12} dr_{12} B_2 dB_2 d\phi_2$$

Hence,

$$d\tau = \frac{1}{R} A_1 dA_1 B_2 dB_2 r_{12} dr_{12} dB_1 d\phi_1 d\phi_2 \quad (5.2.1)$$

Equation (5.2.1) gives a volume element which is very convenient in the numerical work involved in this problem. Several similar volume elements may be constructed by the same method.

The Schrodinger equation for the hydrogen molecule in the electron gas is taken to be given by

$$\begin{aligned}
 H\psi = & \left\{ -\frac{\hbar^2}{2m} (\nabla_1^2 + \nabla_2^2) - e^2 \left(\frac{1}{A_1} e^{-\lambda A_1} + \frac{1}{B_2} e^{-\lambda B_2} + \frac{1}{A_2} e^{-\lambda A_2} \right. \right. \\
 & \left. \left. + \frac{1}{B_1} e^{-\lambda B_1} - \frac{1}{r_{12}} e^{-\lambda r_{12}} - \frac{1}{R} e^{-\lambda R} \right) \right\} \psi \quad (5.2.2)
 \end{aligned}$$

$$= E\psi$$

where the Coulomb potentials, screened by the electron gas, fall off exponentially with distance with a screening radius, $\frac{1}{\lambda}$. λ is given by (Kittel, 1966)

$$\lambda^2 = \frac{6\pi n_0 e^2}{\epsilon_F}, \quad \text{with } \epsilon_F = \frac{\hbar^2}{2m} (3\pi^2 n_0)^{2/3} \quad (5.2.3)$$

where n_0 is the electron number density for the electron gas.

If H did not contain the last four terms in parenthesis multiplying e^2 , it would simply be the sum of two hydrogen atom Hamiltonians, and

$$\psi = U_A(1) U_B(2) \quad (5.2.4)$$

where

$$U_A(1) = (\pi a_0^3)^{-1/2} e^{-A_1/a_0}, \quad U_B(2) = (\pi a_0^3)^{-1/2} e^{-B_2/a_0}$$

are hydrogen 1s orbital functions centred about A and B respectively. The same is also true if one considers the trial function $U_B(1)U_A(2)$. Both of these solutions are equally good approximations to the state

wavefunction and must be included in the trial function. They differ with respect to an exchange of electrons, hence the normalised wavefunction

$$\psi = \frac{1}{\sqrt{1+\Delta}} [U_A(1)U_B(2) \pm U_B(1)U_A(2)] \quad (5.2.5)$$

is adopted, where Δ is the overlap integral given by

$$\Delta = \int U_A(1)U_B(1)d\tau_1 = (1 + \rho + \frac{1}{3} \rho^2)e^{-\rho} \quad (5.2.6)$$

where $\rho = R/a_0$.

The total energy is found by minimising $\int \psi H \psi d\tau$ using (5.2.5) as the trial function. This energy may be written in the form

$$E_{\pm} = 2W_H + \frac{H_0 \pm H_1}{1 + \Delta^2} \quad (5.2.7)$$

where

$$\begin{aligned} H_0 &= e^2 \int U_A^2(1)U_B^2(2) \left(-\frac{1}{B_1} e^{-\lambda B_1} - \frac{1}{A_1} e^{-\lambda A_1} + \frac{1}{r_{12}} e^{-\lambda R} \right) \\ &\quad + \frac{1}{R} e^{-\lambda R} d\tau_1 d\tau_2 \\ &= 2J + J' + \frac{e^2}{R} e^{-\lambda R} \end{aligned} \quad (5.2.8)$$

$$\begin{aligned}
 H_1 &= e^2 \int U_A(1)U_B(1)U_A(2)U_B(2) \left(-\frac{1}{B_1} e^{-\lambda B_1} - \frac{1}{A_1} e^{-\lambda A_1} \right. \\
 &\quad \left. + \frac{1}{r_{12}} e^{-\lambda r_{12}} + \frac{1}{R} e^{-\lambda R} \right) d\tau_1 d\tau_2 \\
 &= 2K\Delta + K' + \frac{e^2 \Delta^2}{R} e^{-\lambda R} \tag{5.2.9}
 \end{aligned}$$

and $W_H = -\frac{me^4}{2h^2}$ is the ground state energy of the hydrogen atom.

J, J', K are λ -dependent integrals given by

$$\begin{aligned}
 J \equiv J(\beta) &= -e^2 \int U_A^2(1)U_B^2(2)B_1^{-1} e^{-\lambda B_1} d\tau_1 d\tau_2 \\
 &= -\frac{e^2}{R} \frac{1}{(1-\beta^2)^2} \{e^{-2\rho\beta} - e^{-2\rho} | (1-\beta^2)^\rho + 1 |\} \tag{5.2.10}
 \end{aligned}$$

$$\begin{aligned}
 J' \equiv J'(\beta) &= e^2 \int U_A^2(1)U_B^2(2)r_{12}^{-1} e^{-\lambda r_{12}} d\tau_1 d\tau_2 \\
 &= \frac{e^2}{R} \frac{1}{(1-\beta^2)^4} \{e^{-2\rho\beta} - e^{-2\rho} | 1 + (1-\beta^2)^\rho \\
 &\quad + \frac{1}{4}(1-\beta^2)^2 (\rho+2\rho^2) + \frac{1}{8}(1-\beta^2)^3 (\rho+2\rho^2 + \frac{4}{3}\rho^3) |\} \\
 &\tag{5.2.11}
 \end{aligned}$$

$$\begin{aligned}
 K \equiv K(\beta) &= -e^2 \int U_A(1)U_B(1) B_1^{-1} e^{-\lambda B_1} d\tau_1 \\
 &= -\frac{e^2}{R} e^{-\rho} \frac{1}{\beta^2(1+\beta)^2} \{ \beta(1+\beta)^\rho + \frac{1}{2}(e^{-2\rho\beta}-1) \} \\
 &\tag{5.2.12}
 \end{aligned}$$

where $\beta = \frac{\lambda a_0}{2}$.

The final integral for K' :

$$K' \equiv K'(\beta) = e^2 \int U_A(1)U_B(1)U_A(2)U_B(2)r_{12}^{-1} e^{-\lambda r_{12}} d\tau_1 d\tau_2 \quad (5.2.13)$$

is a difficult one to evaluate. Interpreting $U_A(1)U_B(2)$ as an exchange point charge, total amount Δ , located on the B nucleus and $U_B(1)U_A(2)$ as an equal exchange point charge located on the A nucleus (Slater, 1963), K' represents the Coulomb repulsion of one exchange charge for another, the repulsion being weakened by the presence of the electron gas. As the distance between the nuclei is increased, the repulsion will decrease. Thus the electron gas and the increase in inter-nuclear separation seek to weaken the exchange point charge repulsion. Near the energy minimum, this behaviour is modelled by writing

$$K'(\beta) = e^{-\lambda \bar{R}} K'(0) \quad (5.2.14)$$

where \bar{R} , a constant, may be determined from

$$J'(\beta) = e^{-\lambda \bar{R}} J'(0) \quad (5.2.15)$$

with

$$J'(0) = \frac{e^2}{R} \left[1 - e^{-2\rho} \left(1 + \frac{11}{8\rho} + \frac{3}{4\rho^2} + \frac{1}{6\rho^3} \right) \right]$$

Sugiura (1927) has evaluated $K'(\beta)$ in the limit β tending to zero (free space), $K'(0)$:

$$K'(0) = \frac{e^2}{5a_0} \left\{ e^{-2\rho} \left(\frac{25}{8} - \frac{23}{4}\rho - 3\rho^2 - \frac{1}{3}\rho^3 \right) + \frac{6}{\rho} [\Delta^2(\gamma + \ln\rho) - 2\Delta\Delta' \text{Ei}(-2\rho) + \Delta'^2 \text{Ei}(-4\rho)] \right\} \quad (5.2.16)$$

where $\gamma = 0.5772157$ (Euler-Mascheroni constant),

$$\Delta' = e^\rho \left(1 - \rho + \frac{1}{3} \rho^2 \right)$$

and $\text{Ei}(x)$ is an abbreviation for the exponential integral

$$\text{Ei}(x) = \int_{-\infty}^x \frac{e^u}{u} du$$

which is tabulated, for instance, in Abramowitz and Stegun (1965).

5.2.2 Results and Conclusions

E_+ in equation (5.2.7) refers to the upper signs in the expressions throughout, and hence is a symmetric function of coordinates, while E_- refers to the lower signs, and is an antisymmetric function of coordinates. Only the symmetric state has a minimum in energy corresponding to binding. Figure 5.2.2 illustrates the change in the length of the covalent bond, and the decrease in the molecular binding energy with increasing electron gas number density. Table 5.2.1 gives the inter-nuclear separation and the energy minimum with increasing β (increasing number density). $\beta = 0.3$ to 0.6 corresponds to the metallic region. Atomic units are taken such that $\hbar^2/2m = 1$, $e^2 = 2$, $a_0 = \hbar^2/me^2$, the Bohr radius, is the unit of length, 1 Rydberg (= 13.6 eV) is the unit of energy.

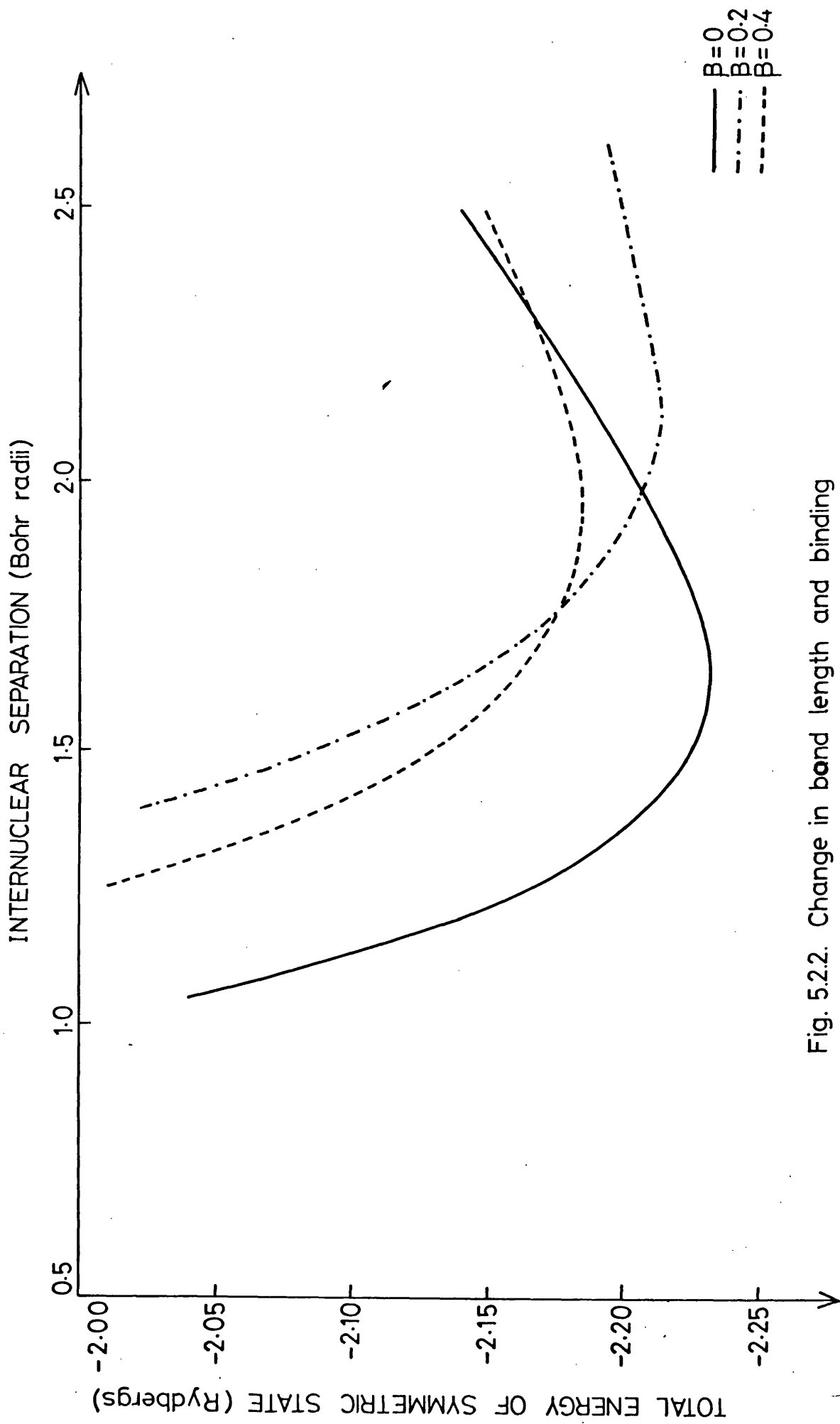


Fig. 5.2.2. Change in bond length and binding energy of H_2 molecule with increasing electron number density.

<u>TABLE 5.2.1</u> <u>Internuclear Separation and Energy Minimum</u> <u>with Increasing β.</u>			
$\beta = \frac{\lambda a_0}{2}$	\bar{R} (Eqn(5.2.15))	R_{\min} (a.u.)	E_{\min} (Ryds.)
0		1.65	-2.2319
0.1	2.01	2.27	-2.2300
0.2	1.90	2.15	-2.2131
0.3	1.81	2.04	-2.1985
0.4	1.72	1.95	-2.1852
0.5	1.65	1.86	-2.1729
0.6	1.58	1.79	-2.1616
0.7	1.51	1.72	-2.1510
0.8	1.45	1.65	-2.1412
0.9	1.40	1.59	-2.1323

It is clear from the table and the figure that, if the approximation (5.2.14) is a reasonable one to the integral for K' near the energy minimum, then the important feature which arises is that the hydrogen molecule persists even at very high electron number densities, but with a lengthened and weakened covalent bond. For larger molecules the closeness of approach of the nuclei is limited by the closed-shell repulsion. This would eliminate the bond length features evident at high number densities in the above results.

5.3 HYDROGEN MOLECULE IN AN ELECTRON GAS II

5.3.1 Introduction

The Hohenberg-Kohn-Sham density functional formalism (Hohenberg and Kohn (1964), Kohn and Sham (1965)) is a theoretical description of many-electron systems in which the mutual Coulomb interaction between the atoms - exchange and correlation effects - which are basically non-local potentials, are treated as a local exchange-correlation potential. For systems which have a net spin, such as the hydrogen atom, the formalism has been extended to include spin. Gunnarsson and Johansson (1975) have applied the spin-density-functional (SDF) formalism with a local-spin-density (LSD) approximation to the study of many small molecules. For the singlet state of the hydrogen molecule, in particular, the experimental energy curve has been reproduced to within an accuracy of 0.25 eV or better. Gunnarsson, Johansson, Lundqvist and Lundqvist (1975) argue that the SDF formalism with the LSD approximation is physically superior to any other method of calculation of the hydrogen molecule energy curves. It has become clear that the density functional formalisms do provide calculated energy curves for small molecules which are faithful to experimental observations. This section calculates the binding energy of the hydrogen molecule in an electron gas using the Hohenberg-Kohn-Sham density functional formalism. The treatment is similar to that offered by Smith, Ying and Kohn (1973) for the calculation of the interaction energy between hydrogen adatoms in chemisorption, the atoms being treated as present in a constant electron density environment.

5.3.2 Theoretical Treatment

The treatment will be developed by considering the hydrogen atom in the electron gas and then by extending the treatment to that of two hydrogen atoms in the electron gas. The theoretical advance offered here for the hydrogen atom in the electron gas stems from the requirement that Poisson's equation be satisfied from point to point in the electron gas - that is to say, there is complete self-consistency between the electrostatic potential used and the charge density obtained.

5.3.2(i) Hydrogen Atom in Electron Gas

The unscreened (or zeroth order) configuration of the hydrogen atom is taken as a proton sitting in the electron gas with the electron joining the conduction band.

Poisson's equation must be satisfied from point to point in the electron gas so that

$$\nabla^2 V = 4\pi [n(\mathbf{r}) - n_0] - 4\pi \delta(\mathbf{r}) \quad (5.3.1)$$

where $\delta(\mathbf{r})$ represents a proton situated at $\mathbf{r} = 0$ and $[n(\mathbf{r}) - n_0]$ is the deviation of the electron density from its constant value n_0 .

The units taken are $\hbar = m = e = 1$ in which case the unit of distance is the Bohr radius, and the unit of energy is the Hartree

(= 2 Rydbergs ≈ 27.2 eV). $n(\mathbf{r})$ may be found self-consistently by minimising the Hohenberg-Kohn-Sham energy functional:

$$E_V[n] = \iint \frac{\left[\frac{1}{2}n(\underline{r}) - \rho^{\text{ex}}(\underline{r}) \right] n(\underline{r}')}{|\underline{r} - \underline{r}'|} d^3_{\underline{r}} d^3_{\underline{r}'} + \frac{3}{10} (3\pi^2)^{2/3} \int n^{5/3} d^3_{\underline{r}} - \frac{3}{4} \left(\frac{3}{\pi}\right)^{1/3} \int n^{4/3} d^3_{\underline{r}} + \frac{1}{72} \int \frac{(\nabla n)^2}{n} d^3_{\underline{r}} \quad (5.3.2)$$

where the integrands of the ~~first~~ second and third terms represent, respectively, kinetic and exchange energy densities. The fourth term is the von Weisacker correction to the kinetic energy (see section 3.3),

$$\rho^{\text{ex}}(\underline{r}) = \rho_0^{\text{ex}}(\underline{r}) + \delta_0(\underline{r})$$

where $\rho_0^{\text{ex}}(\underline{r})$ is the charge density produced by the uniform positive background.

The minimisation proceeds subject to the restriction that

$$\int [n(\underline{r}) - \rho^{\text{ex}}(\underline{r})] d^3_{\underline{r}} = 0$$

$V(\underline{r})$ is the electrostatic potential produced by the proton and its screening charge and is written

$$V(\underline{r}) = - \int \frac{n(\underline{r}') - \rho^{\text{ex}}(\underline{r}')}{|\underline{r} - \underline{r}'|} d^3_{\underline{r}'}$$

On minimising the energy functional, using the Euler equation, one finds that

$$\frac{1}{36} \frac{\nabla^2 n}{n} + V_{\frac{1}{2}}(\underline{r}) - \frac{1}{2} (3\pi^2)^{2/3} n^{2/3} + \left(\frac{3}{\pi}\right)^{1/3} n^{1/3} - \frac{1}{72} \frac{(\nabla n)^2}{n} = 0 \quad (5.3.3)$$

Now writing the electron density $n(r)$ with some correction $n_c(r)$ to the constant electron density n_0 :

$$n(r) = n_0 + n_c(r) \quad (5.3.4)$$

and expanding equation (5.3.3) to the first order in n_c/n_0 gives

$$\begin{aligned} \nabla^2 n_c - \frac{1}{n_0} \nabla n_0 \nabla n_c + n_c \left\{ \left(\frac{1}{n_0} \nabla n_0 \right)^2 - \frac{1}{n_0} \nabla^2 n_0 + 12 \left(\frac{3}{\pi} \right)^{1/3} n_0^{1/3} \right. \\ \left. - 12 (3\pi^2)^{2/3} n_0^{2/3} \right\} + 36 n_0 V = 0 \end{aligned} \quad (5.3.5)$$

Further n_0 constant then implies that equation (5.3.5) reduces to

$$\nabla^2 n_c - \left\{ 12 (3\pi^2 n_0)^{2/3} - 12 \left(\frac{3n_0}{\pi} \right)^{1/3} \right\} n_c + 36 n_0 V = 0 \quad (5.3.6)$$

Equation (5.3.6) must then be solved in conjunction with equation (5.3.1).

5.3.2(ii) Hydrogen Molecule in Electron Gas

So far as all the electrons are concerned the addition of a further electron is not important since there are so many. The Hamiltonian for two protons at r_1 and r_2 is then taken as

$$H = H(\text{all electrons}, n(r)) + \frac{1}{|r_1 - r_2|} + g \left\{ \sum_{\substack{\text{all} \\ \text{electrons} \\ r_i}} \left(- \frac{1}{|r_i - r_1|} - \frac{1}{|r_i - r_2|} \right) \right\}$$

This corresponds to taking

$$\rho = \rho^0 + g \delta(\underline{r} - \underline{r}_1) + g \delta(\underline{r} - \underline{r}_2)$$

which gives the correction to the electron gas density, $n_1(\underline{r})$, to be

$$n_1(\underline{r}) = g n_c(\underline{r} - \underline{r}_1) + g n_c(\underline{r} - \underline{r}_2) \quad (5.3.7)$$

The inclusion of the coupling constant $g(\equiv e^2)$ will now become obvious since the Hellmann-Feynman theorem will be needed to evaluate the total energy, and then the energy of molecular formation (see Appendix 2). The interaction energy, E_{int} , is given by

$$\begin{aligned} E_{\text{int}} &= - \int [n_0(\underline{r}) + n_1(\underline{r})] g \left[\frac{1}{|\underline{r}-\underline{r}_1|} + \frac{1}{|\underline{r}-\underline{r}_2|} \right] d^3 \underline{r} \\ &= - \frac{1}{8\pi^3} \int [n_0(\underline{r}) + n_1(\underline{r})] \frac{4\pi g}{k^2} [e^{i\mathbf{k} \cdot (\underline{r}-\underline{r}_1)} + e^{i\mathbf{k} \cdot (\underline{r}-\underline{r}_2)}] d\underline{r} d\underline{k} \\ &= - \frac{1}{8\pi^3} \int [n_0(\underline{k}) + n_1(\underline{k})] \frac{4\pi g}{k^2} [e^{-i\mathbf{k} \cdot \underline{r}_1} + e^{-i\mathbf{k} \cdot \underline{r}_2}] d\underline{k} \end{aligned}$$

Now,

$$\frac{4\pi}{k^2} n_0(\underline{k}) = -V_0(\underline{k}) \quad \text{since } \nabla^2 V = -4\pi\rho$$

whilst

$$\frac{4\pi}{k^2} n_c(\underline{k}) = -\bar{V}(\underline{k}) \quad \text{since } \bar{V}(\underline{k}) = V(\underline{k}) - \frac{4\pi}{k^2}$$

(5.3.8)

Also, from the definition of $n_1(\underline{r})$,

$$n_1(\underline{k}) = (e^{i\underline{k}\cdot\underline{r}_1} + e^{i\underline{k}\cdot\underline{r}_2}) g n_c(\underline{k})$$

$$E_{\text{int}} = \frac{1}{8\pi^3} \int \{V_o(\underline{k}) + g\bar{V}(\underline{k}) (e^{i\underline{k}\cdot\underline{r}_1} + e^{i\underline{k}\cdot\underline{r}_2})\} \{e^{-i\underline{k}\cdot\underline{r}_1} + e^{-i\underline{k}\cdot\underline{r}_2}\} g d\underline{k}$$

$$\frac{1}{g} E_{\text{int}} = V_o(\underline{r}_1) + V_o(\underline{r}_2) + 2g\bar{V}(0) + g[\bar{V}(\underline{r}_1 - \underline{r}_2) + \bar{V}(\underline{r}_2 - \underline{r}_1)]$$

Since the ground state energy, E_o , is given by

$$\frac{dE_o}{dg} = g^{-1} E_{\text{int}}(g) \quad (5.3.9)$$

$$\int_0^{e^2} g^{-1} E_{\text{int}}(g) dg = e^2 \{V_o(\underline{r}_1) + V_o(\underline{r}_2) + e^2 \bar{V}(0) + \frac{1}{2} e^2 [\bar{V}(\underline{r}_1 - \underline{r}_2) + \bar{V}(\underline{r}_2 - \underline{r}_1)]\} \quad (5.3.10)$$

notice then that $[V_o(\underline{r}_1) + \frac{1}{2} \bar{V}(0)] + [V_o(\underline{r}_2) + \frac{1}{2} \bar{V}(0)]$ is the total energy of the isolated protons. The remainder, $\bar{V}(\underline{r}_1 - \underline{r}_2)$ is the interaction energy between the protons - that is, the energy of molecular formation.

The Fourier transforms of equations (5.3.1), (5.3.6) and (5.3.8) give the Fourier transform of the interaction energy between the protons, now written as $\bar{V}(\underline{k})$:

$$\bar{V}(\underline{k}) = \frac{4\pi\beta}{k^2(k^4 - \mu k^2 + \beta)} \quad (5.3.11)$$

where $\beta = 144 \pi n_o$

$$\mu = 12 \left(\frac{3n_o}{\pi} \right)^{1/3} \{1 - 3\pi^5 n_o\}^{1/3}$$

Writing

$$(k^4 - \mu k^2 + \beta) = (k^2 + a)(k^2 + b) \quad (5.3.12)$$

this leads to

$$V(r) = - \left[\frac{1}{r} + \frac{be^{-r\sqrt{a}} - ae^{-r\sqrt{b}}}{(a-b)r} \right]$$

where a, b must be chosen so that $\text{Re}(\sqrt{a}, \sqrt{b}) > 0$.

To this $\tilde{V}(r)$ must be added the Coulomb repulsion between the protons which gives for the total energy of the molecule

$$E(r) = \frac{ae^{-r\sqrt{b}} - be^{-r\sqrt{a}}}{(a-b)r} \quad (5.3.13)$$

Notice that $E(r)$ has the correct behaviour as r tends to zero and to infinity. $E(r)$ in (5.3.13) will be split into ranges (from (5.3.11) and (5.3.12)). The results are as follows:

$$E(r) = 0 \quad 0 \leq n_0 < \frac{1}{81\pi^5}$$

$$E(r) = \frac{e^{-pr}}{r \sin 2\theta} \sin(2\theta - qr) \quad \frac{1}{81\pi^5} \leq n_0 < \frac{1}{3\pi^5}$$

$$\begin{aligned} \text{with } p &= \lambda \sin \theta & \text{where } \theta &= \frac{1}{2} \tan^{-1} \left[\sqrt{\frac{4\beta}{\mu} - 1} \right] & \frac{\pi}{4} < \theta < 0 \\ q &= \lambda \cos \theta & \lambda &= \beta^{1/4} \end{aligned}$$

...cont.

$$E(r) = \frac{e^{-pr}}{r \sin 2\theta} \sin(2\theta + qr) \quad \frac{1}{3\pi^5} \leq n_0 < \frac{9}{\pi^5}$$

with $p = \lambda \cos \theta$ λ, θ as above

$$q = \lambda \sin \theta$$

$$E(r) > 0, \frac{\partial E}{\partial r} < 0 \rightarrow \text{no binding} \quad n_0 \geq \frac{9}{\pi^5} \quad (5.3.14)$$

The relations (5.3.14) give the energy of molecular formation in an electron gas of number density n_0 .

5.3.3 Results and Conclusions

Table 5.3.1 gives the binding energy of the hydrogen molecule as a function of the electron number density calculated from equations (5.3.14). Figure 5.3.1 illustrates the variation close to the low density limit and the onset of the metallic regime.

TABLE 5.3.1 Variation of Hydrogen Molecule Bond Length and Energy With Increasing Number Density			
n_0 (electrons cm^{-3} $\times 10^{-23}$)	n_0 (electrons a.u. $^{-3}$)	Bond Length (a.u.)	Bond Energy (eV)
.047	6.99	3.412	-6.2828
.082	12.10	3.668	-3.1421
.141	20.96	3.733	-1.8987
.245	36.31	3.725	-1.2134
.424	62.89	3.693	-0.7765
.735	108.93	3.665	-0.3650
1.273	188.66	3.667	-0.2709
2.205	326.77	3.731	-0.1319
3.8197	565.99	3.914	-0.0483
6.615	980.33	4.358	-0.0096

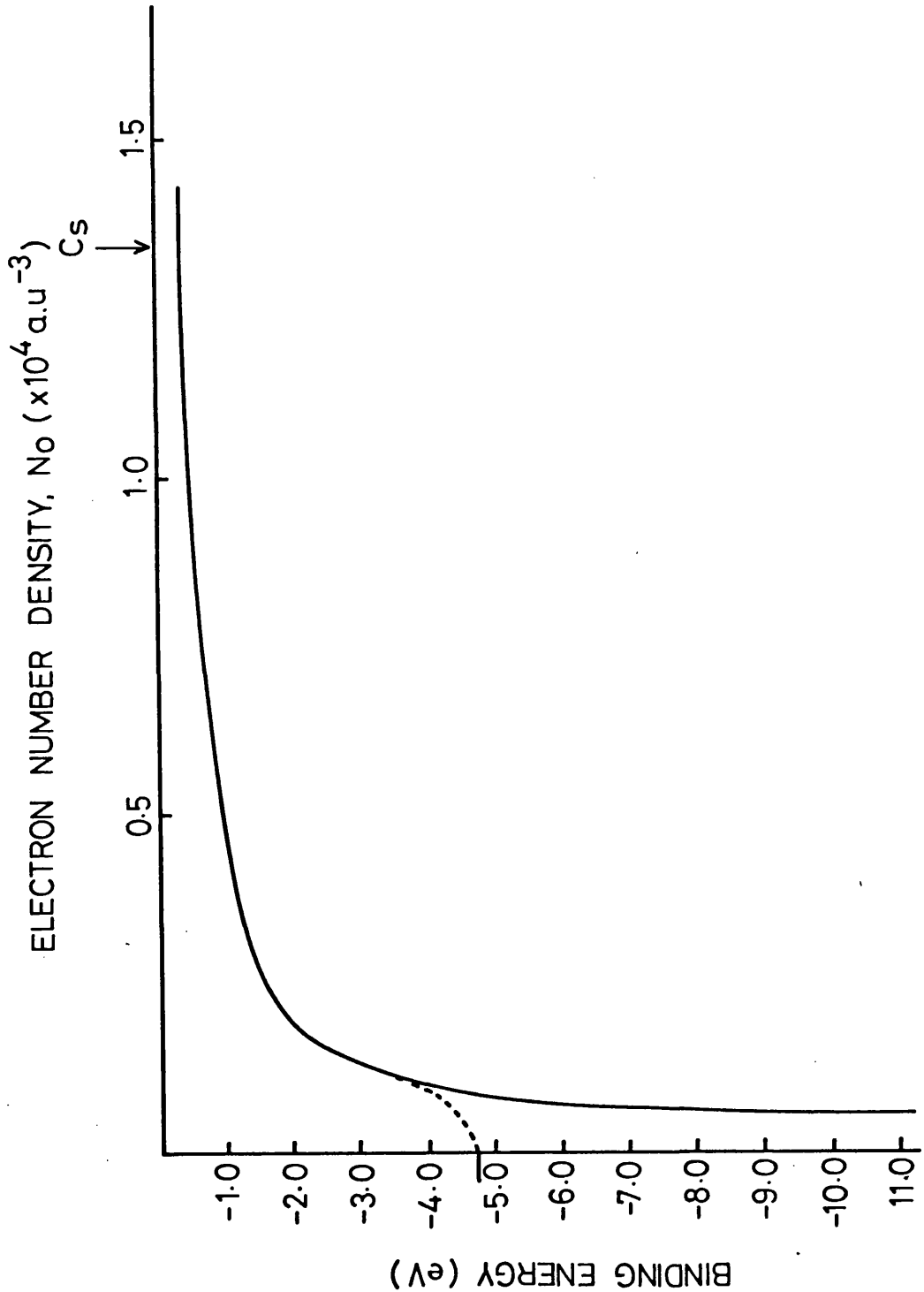


Fig.5.31. Variation in binding energy of H₂ molecule with electron number density

Equations (5.3.14) leads one to conclude that the typical form of interaction energy for a covalent bond will be replaced by a screened oscillatory interaction for electron densities satisfying $\frac{1}{81\pi^5} \leq n_0 < \frac{1}{3\pi^5}$. The bond length is increased compared to that in the free space situation and the bond energy weakened. The greater the electron gas density, the weaker the bond until at large enough densities ($n_0 \geq \frac{9}{\pi}$) the bond cannot form. At very low electron densities Nozière's believes (private communication) that there is a Mott transition which may well explain the curious behaviour in the binding energy over this region.

5.4 CONCLUSION

The two distinct methods set out in the previous sections for investigating what happens to a hydrogen molecule when placed in an electron gas both agree in two qualitative features: one, there is a lengthening of the bond; two, the energy required to separate the protons is reduced from the free space value of 4.7 eV. Further, as the electron density is increased, the binding energy is decreased. It is thought that the approximation made in the Heitler-London calculation with screened potentials make it a cruder model for the change in the molecular binding energy with electron number density than that derived using the density functional formalism. The latter is believed to be exact for reasonably high electron number densities ($\sim 8 \times 10^{20}$ electrons cm^{-3}). A particular feature of the density functional model is that for electron number densities at the 'high' end of the metallic regime ($\sim 20 \times 10^{22}$ electrons cm^{-3}), the molecule will not form.

CHAPTER VI

THE CHEMICAL COMPLEX IN MOLTEN Mg-Bi AND Tl-Te

6.1 INTRODUCTION

Ratti and Bhatia (1975) have examined the electrical properties of the compound forming magnesium-bismuth and tellurium-~~tantalum~~^{thallium} systems, demonstrating that the concentration dependence of the electronic transport coefficients may be understood on the basis of the formation of chemical complexes and the consequent depletion of the free electron density. Following Enderby and Simmons (1969), the formation of the chemical complexes $A_{\mu}B_{\nu}$ with low lying electron states is postulated where μ and ν are small integers specified by the composition at which the system forms in the solid phase. The equilibrium numbers n_1, n_2, n_3 of the separate A and B ions and of A B respectively as a function of the temperature, T, pressure, P, and the concentration, c, of A atoms, or, (1-c), B atoms in the $A_{\mu}B_{\nu}$ binary alloy are determined from the thermodynamic properties of the system. The conduction process is treated in the nearly free electron approximation, except close to the compound concentration, c_0 . Nothing, however, is said about the nature of the bonding which exists in these chemical complexes. It has become clear from previous chapters that the bonding within liquid magnesium-bismuth is unlikely to be totally ionic, leading one to suspect the possibility of the covalently bonded complex. The calculations of Chapter V have shown that the binding energy of a molecule does

vary with a changing electron environment, in which case covalently bonded Mg_3Bi_2 molecule complexes must have binding energies which vary away from the critical concentration. This behaviour has been modelled with the aid of the hydrogen molecule calculations and the Ratti and Bhatia equations reformulated. The final section of this chapter looks at the curious consequences of the assumption of covalency, while the intermediate sections set out the original and revised theory and results of Ratti and Bhatia. Most of the discussions are confined to the liquid magnesium-bismuth system.

6.2 THERMODYNAMIC PROPERTIES

6.2.1 Basic Equations

The treatment is in the nearly free electron approximation so that if Z_A denotes the number of conduction electrons contributed by a separate A atom and Z_B by a B atom, the number of conduction electrons per atom in the mixture is given by $N = Z_A n_1 + Z_B n_2$.

From the conservation of atoms,

$$n_1 = c - \mu n_3 ; \quad n_2 = (1 - c) - \nu n_3$$

hence,

$$N = cZ_A + (1 - c)Z_B - (\mu Z_A + \nu Z_B)n_3 \quad (6.2.1)$$

In the nearly free electron approximation, the Hall coefficient, R , is

$$R^{-1} = - N|e|/\Omega \quad (6.2.2)$$

where Ω is the volume per atom, e the electronic charge. Thus, to determine N and R , it is necessary to know n_3 .

In a series of papers (Bhatia and Thornton, 1973; Bhatia and Hargrove, 1973, 1974) the functional form for the free energy of mixing (per gm mole of binary alloy A-B) for the Mg-Bi and Tl-Te systems in particular was introduced:

$$G_M = -n_3 g + RT \left[\sum_{i=1}^3 n_i \ln n_i + n_3 \ln(\mu + \nu) + \sum_{i < j} (n_i n_j) v_{ij} \right] \quad (6.2.3)$$

g is the (free) energy of formation of the chemical complex per gm mole of $A_\mu B_\nu$, so that $(-n_3 g)$ represents the lowering of the (free) energy due to the formation of the chemical complexes. The second term in (6.2.3) is Flory's approximation for $(-T)$ times the entropy of mixing of the three species. The assumption made is that the volume per atom of A and B atoms is nearly the same, say ν , and the volume of $A_\mu B_\nu$ is $(\mu + \nu)\nu$.

v_{ij} are the pairwise interactions. The equilibrium condition $(\partial G_M / \partial n_3)_{T,c} = 0$ gives

$$n_1^\mu n_2^\nu = n_3 k f(n_3, c) \quad (6.2.4)$$

where $k = \exp(-g/RT)$ and $f(n_3, c)$ involves v_{ij} and is a slowly varying function of n_3 and c . g and v_{ij} in equation (6.2.3) are determined from the thermodynamic data on G_M . From (6.2.3) and (6.2.4) the experimental free energy of mixing, G_M , heat of mixing, H (involving $\partial G_M / \partial T$), and concentration fluctuations, a_{cc} (involving

$\partial^2 G / \partial c^2$), are reproduced well over the concentration range for both Mg-Bi and Tl-Te. The temperature dependence of g and v_{ij} are thought to be small, hence neglected. The success of (6.2.3) and (6.2.4) in studying the thermodynamic properties of the two systems encouraged Ratti and Bhatia to apply it to a study of the electronic transport coefficients. Various thermodynamic parameters for the Mg-Bi and Tl-Te systems are shown in figure 6.2.1.

For Mg-Bi and Tl-Te, $g/R \approx 1.6 \times 10^4$ °K and 9.5×10^3 °K respectively, so that at temperatures of observation (~ 1000 °K) $K \ll 1$. Further $f \sim 1$. Under these conditions, (6.2.4) may be solved to a first approximation ($K \rightarrow 0$),

$$n_3^{(0)} = c/\mu \quad n_1^{(0)} = 0 \quad n_2^{(0)} = 1 - c - \nu n_3^{(0)} \quad (6.2.5)$$

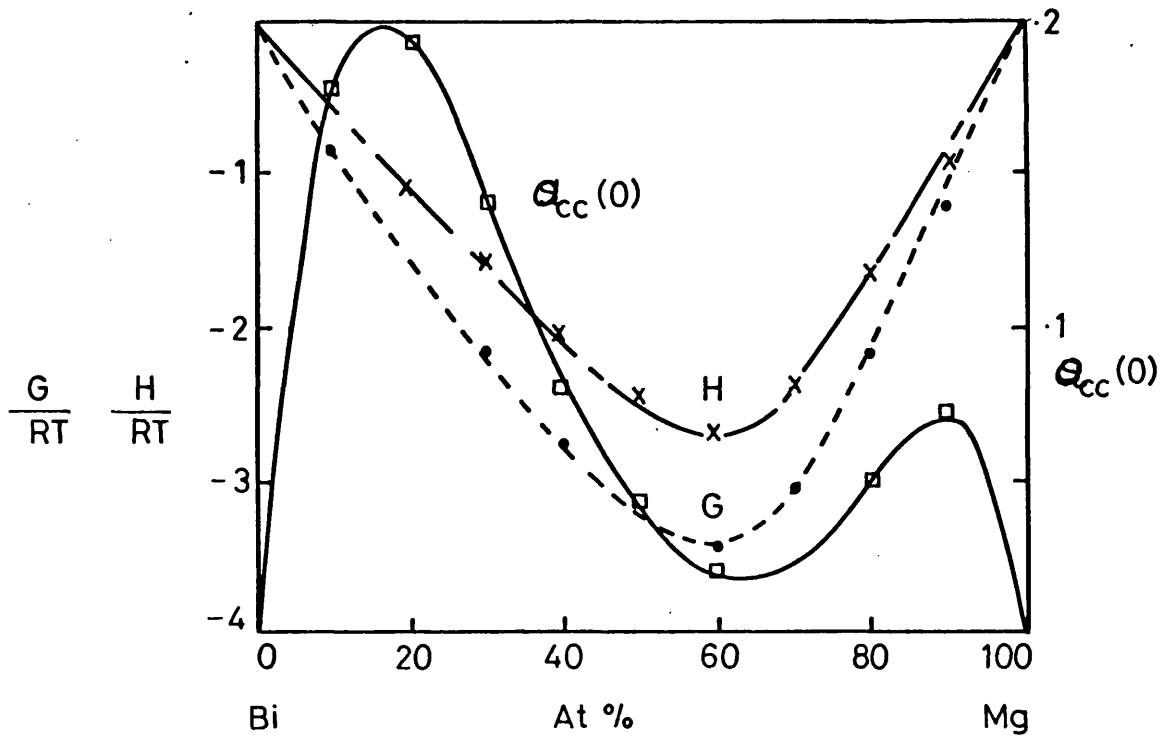
for $0 < c < c_0$, where $c_0 = \mu/(\mu+\nu)$. For $c_0 < c < 1$,

$$n_3^{(0)} = (1 - c)/\nu \quad n_2^{(0)} = 0 \quad n_1^{(0)} = c - \mu n_3^{(0)} \quad (6.2.6)$$

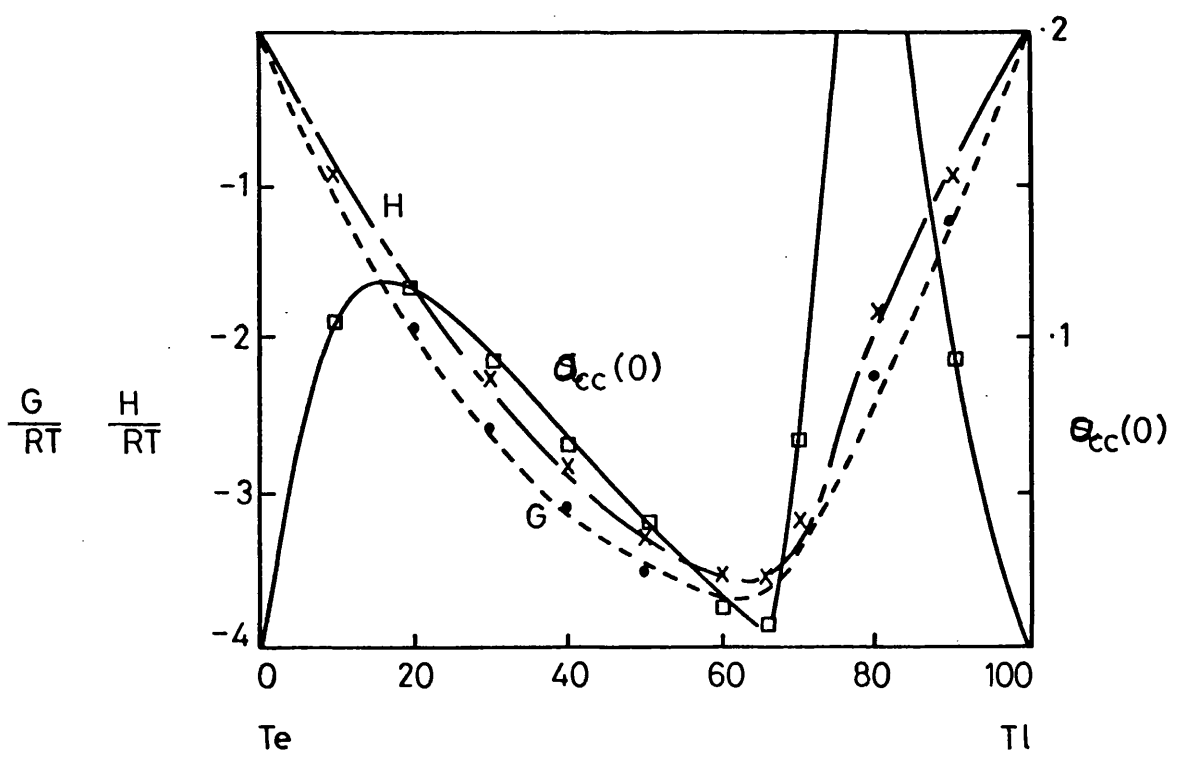
These equations are not valid in the $c \rightarrow 0$ or $(1 - c) \rightarrow 0$ limits, or if μ or $\nu \gg 2$ (Bhatia and Hargrove, 1974). Thus to a first approximation the mixture can be regarded as a pseudobinary mixture of $A + \frac{A}{\mu} B$ in the A rich region and $B + \frac{A}{\mu} A$ in the B rich region.

n_3 may be determined to a higher approximation by writing $n_3 = n_3^{(0)} - \Delta n_3$ in (6.2.4) and keeping only the terms linear in Δn_3 . For $c < c_0$

$$\Delta n_3 \approx [k_0 n_3^{(0)} / \mu^\mu (n_2^{(0)})^\mu]^{1/\mu} \quad (6.2.7)$$



G, H, $a_{cc}(0)$ for Mg - Bi



G, H, $a_{cc}(0)$ for Tl-Te system

Fig. 6.2.1.

Various thermodynamic parameters for Mg-Bi and Tl-Te systems

where $K_0 \equiv K f(n_3^{(0)}, c)$. The solution is valid when $v \Delta n_3 \ll n_2^{(0)}$. For $c > c_0$, the solution corresponding to (6.2.7) is obtained by replacing $n_2^{(0)}$ by $n_1^{(0)}$ and interchanging μ and ν . At $c = c_0$ where both $n_1^{(0)}$ and $n_2^{(0)}$ tend to zero,

$$\Delta n_3 \approx \{K_0 / |(\mu+\nu)\mu^\mu \nu^\nu|\}^{1/(\mu+\nu)} \quad (6.2.8)$$

6.2.2 The Covalent Mg_3Bi_2 Complex in an Electron Sea

The thermodynamic and electronic studies of Bhatia and coworkers accept the possible existence of chemical complexes $A_\mu B_\nu$ but make no statements about the type of bonding which exists within these complexes. It has been argued in previous chapters that the Mg_3Bi_2 complex in molten Mg-Bi is more likely to be covalently rather than ionically bonded. In the covalent extreme the calculations of Chapter V have demonstrated that the binding energy of a molecule in an electron gas must change with varying electron number density, in which case one would expect covalently bonded Mg_3Bi_2 complexes to have binding energies which vary away from the critical concentration. Hence in equation (6.2.3), g must vary with N . It is possible to model this behaviour and reformulate the equations of section 6.2.1 for the liquid Mg-Bi system.

The binding energy of the hydrogen molecule in an electron gas decreases as the electron number density increases. Although the calculation of the preceding chapter is that for the hydrogen molecule, if a Born-Mayer repulsion term of the form $A \exp[-(r-r_0)/\rho]$ is included in the calculation, it is possible to model the closed ion core repulsion effect experienced in larger molecules. A is a constant of value 5.588×10^{-2} Rydbergs appropriate for ions of

unlike sign, and ρ another constant equal to 0.652 atomic units (Mott and Gurney, 1940). r_0 is chosen to be the interionic separation at the energy minimum of the hydrogen molecule without the repulsion term. Figure 6.2.2 gives a plot of the new energy minima obtained (in Rydbergs) against a parameter β related to the conduction electron density, n_0 , through $\beta = (3a_0^3/\pi n_0)^{1/6}$, where a_0 is the atomic unit of distance. The binding energy decreases almost linearly with β passing through energies of 0.1259 and 0.1212 Rydbergs associated with electron densities corresponding to magnesium and bismuth respectively. The variation is not linear very close to the binding energy calculated for this larger molecule (0.1797 Rydbergs). Increasing the free electron number density then leads to a bond weakening for the larger molecule. In order to simulate the variation of the binding of the Mg_3Bi_2 molecule in a sea of electrons provided by excess magnesium or bismuth ions in liquid Mg-Bi one can retain the approximately linear behaviour and write

$$\begin{aligned}
 g(n) &= -g_0 \{1 - \alpha n_2^{1/6}\} & 0 < c < c_0 \\
 &= -g_0 \{1 - \beta n_1^{1/6}\} & c_0 < c < 1
 \end{aligned}
 \tag{6.2.9}$$

with $\alpha = \frac{0.0585}{g_0}$ referring to the Bi end

$\beta = \frac{0.0538}{g_0}$ referring to the Mg end

and g_0 is the free energy of binding of the Mg_3Bi_2 molecule at the

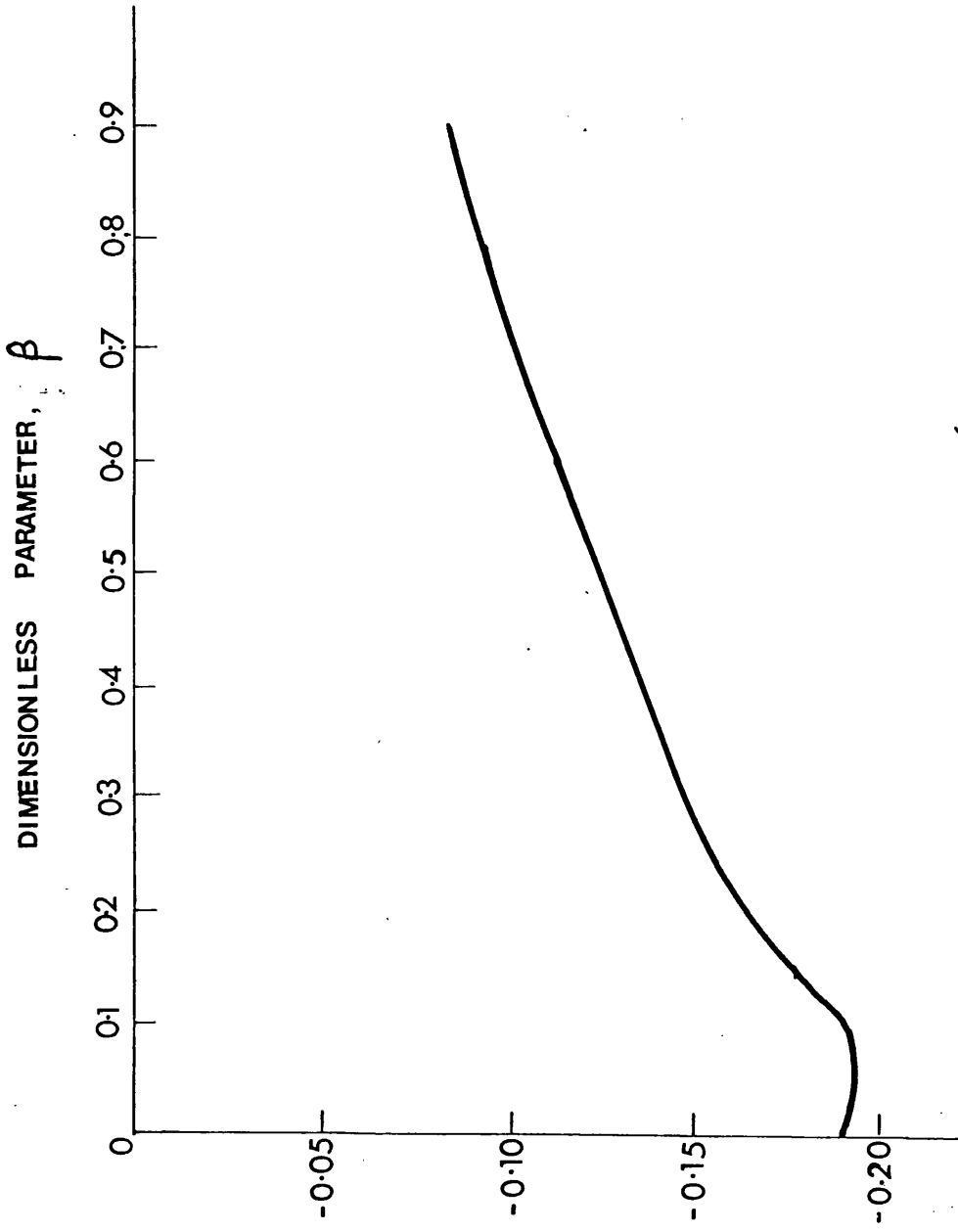


Fig. 6.2.2 Binding energy of large molecule (H₂ molecule + Born-Mayer repulsion term) plotted against $\beta \equiv \left(\frac{3Q_0^2 n_0}{\pi}\right)^{1/6}$, with n_0 the electron number density, a_0 the Bohr radius.

critical concentration (~ 0.1 Rydbergs): It is assumed that the majority of nearly free electrons come from excess ions not trapped in molecular Mg_3Bi_2 . The thermodynamic and electronic properties can now be formally derived.

The functional form for the free energy of mixing per gm mole of the alloy becomes

$$G_M = n_3 g(n) + RT\{n_1 \ln n_1 + n_2 \ln n_2 + n_3 \ln(\mu+\nu)n_3\} + \sum_{i<j} (n_i n_j) V_{ij} \quad (6.2.10)$$

The condition $(\partial G_M / \partial n_3)_{T,c} = 0$ will give the equilibrium value of n_3 determined from

$$n_1^\mu n_2^\nu = n_3 f(n_3, c) \exp\left\{-\frac{g_0}{RT} \left[1 - \alpha n_2^{-5/6} \left(n_2 - \frac{1}{6} \nu n_3\right)\right]\right\} \quad 0 < c < c_0 \quad (6.2.11)$$

$$= n_3 f(n_3, c) \exp\left\{-\frac{g_0}{RT} \left[1 - \beta n_1^{-5/6} \left(n_1 - \frac{1}{6} \mu n_3\right)\right]\right\} \quad c_0 < c < 1$$

$f(n_3, c)$ is the same slowly varying function of n_3 and c given in (6.2.4); its explicit form is omitted for brevity. g_0 and V_{ij} are fixed from the best fit on the observed experimental data of the free energy of mixing G_M . (6.2.11) must be solved numerically for n_3 , enabling one to determine the free energy of mixing from (6.2.10) and the number of conduction electrons in the mixture from (6.2.1).

6.3 HALL EFFECT, CONDUCTIVITY AND ENERGY OF MIXING

For Mg-Bi, $Z_A = Z_{Mg} = 2$ and $Z_B = Z_{Bi} = 5$. Also $\mu = 3$ and $\nu = 2$. The volume per atom, $\Omega = c\Omega_{Mg} + (1 - c)\Omega_{Bi}$, since the departure from linearity is small and produces negligible effect on (N/Ω) . Figure 6.3.1 gives:

(a) The resistivity, ρ , calculated from Faber-Ziman theory assuming no depletion on N - that is, $N = cZ_{Mg} + (1 - c)Z_{Bi}$. The free electron expression used for the resistivity is,

$$\rho = \frac{A}{E_F} \frac{1}{L_{eff}} \quad (6.3.1)$$

where A is the constant $3\pi^2 h/e^2$ and $E_F = (3\pi^2 N/\Omega)^{2/3}$. L_{eff} is a mean free path which is a composite of the mean free path due to scattering by the complexes and a mean free path arising from scattering by excess Bi or Mg ions (following Enderby and Simmons, Schaich and Ashcroft (1970)). $L_{eff} \equiv L_{eff}(c, E_F)$ and will have different values in pure Mg and Bi.

(b) Keeping L_{eff} the same and changing E_F in (6.3.1) according to Ratti and Bhatia solving (6.2.4) for n_3 .

(c) Keeping L_{eff} the same as in Ratti and Bhatia, for the sake of comparison solving (6.2.11) for n_3 .

(d) The experimental curve from Enderby and Collings (1970).

Curve A clearly does not agree with experiment even well away from the compound composition. Curve B indicates the depletion of N as stoichiometry is approached, even though the assumption that

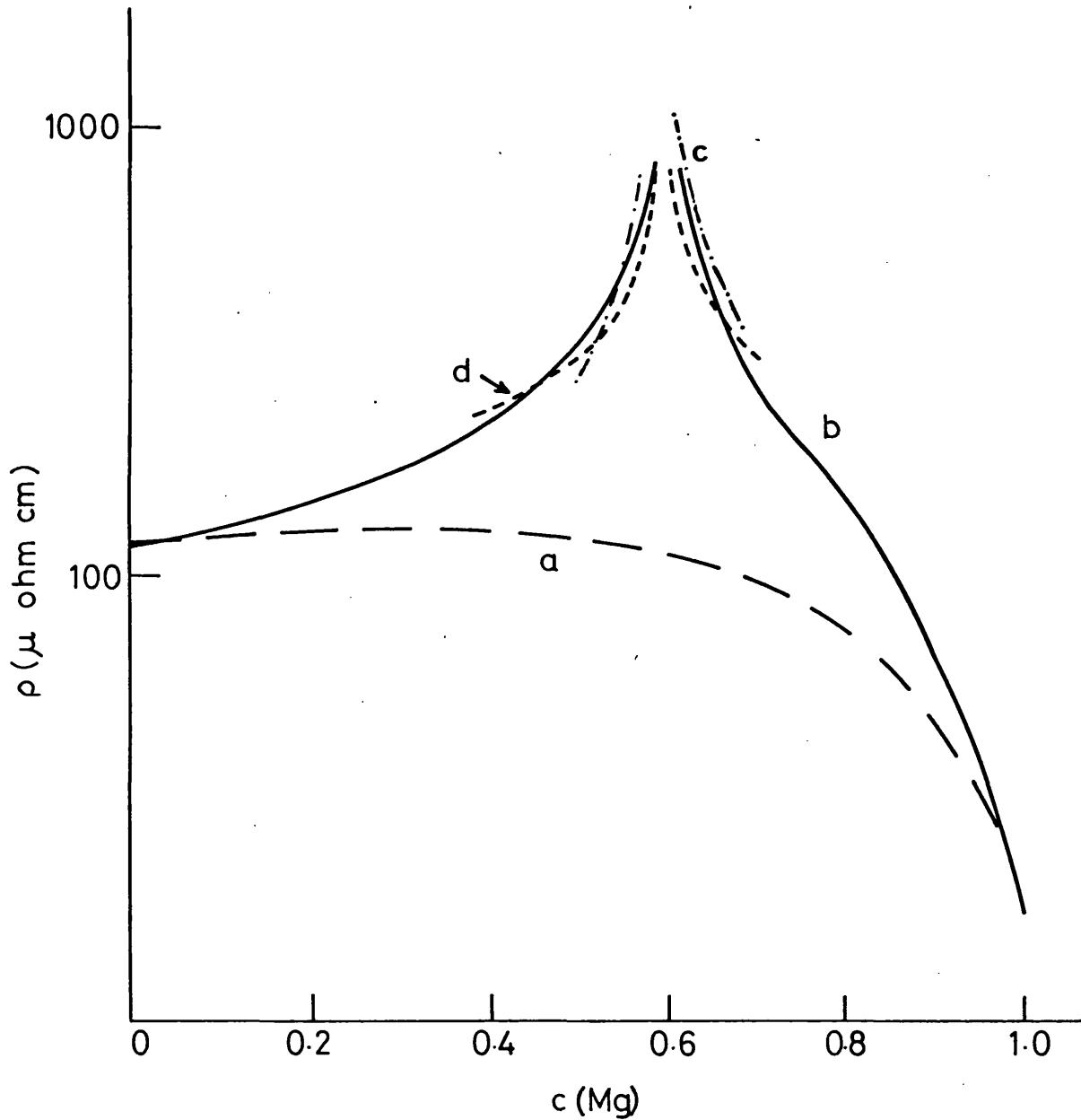


Fig.6.31.

Resistivity of Mg-Bi system as a function of concentration c of Mg. Curves (a) and (b) as explained in the text. Curve d is experimental. Curve c is calculated from (6.2.11)

L_{eff} is the same as in Faber-Ziman theory is unjustified. Curve C shows a sharper peak in the resistivity compared with Curve B, apparently modelling well the dramatic reduction in the free electron number density near the critical concentration. However, whereas detailed calculations of $\frac{1}{N} \frac{dN}{dT}$ (table 6.3.1) using (6.2.4) show a maximum close to c_0 dropping sharply both sides of the maximum, those determined using (6.2.11) do not.

TABLE 6.3.1

Temperature Dependence of the Conduction Electron Density in Mg-Bi. C is the fraction of Mg atoms. The second and third columns refer to n_3 determined by (6.2.4) and (6.2.11) respectively.

c	$\frac{N'}{N} \times 10^4$ (6.2.4)	$\frac{N'}{N} \times 10^4$ (6.2.11)
0.50	2.0	0.82
0.55	5.0	1.31
0.57	6.5	1.41
0.58	13.0	1.14
0.59	20.0	0.33
0.60	25.0	-
0.61	25.0	0.04
0.62	18.0	0.30
0.63	11.0	0.44
0.65	3.8	0.44
0.70	0.8	0.25

Figure 6.3.2 plots $\frac{G_M}{RT}$ and n_3 as functions of concentration for liquid Mg-Bi. The solid curve gives those results calculated using the model of Bhatia and coworkers (equations 6.2.3 and 6.2.4). The broken curve gives those calculated on the assumption of the covalent Mg_3Bi_2 complex (equations 6.2.10 and 6.2.11). The solid circles are data for G_M taken from Hultgren et al (1963) at $T = 973^{\circ}K$. The free energy of mixing curves show quite clearly that a model which assumes covalent bonding within the Mg_3Bi_2 complex and an associated variation in binding energy with changing electron environment cannot reproduce the thermodynamic data, whereas a model in which the binding energy remains constant can. This latter model, however, is unable to show the dramatic reduction in the number of conduction electrons near the critical concentration.

Figure 6.3.3 gives the experimental and theoretical values for the Hall effect as a function of the concentration of Tl. $Z_{Tl} = 3$, and $\mu = 2$, $\nu = 1$ corresponding to the compound value Tl_2Te . The value of Z_{Te} was calculated at $800^{\circ}K$ from matching the Hall coefficient as $Z_{Te} = 1.8$. The agreement between the curves is good, as is the experimental ratios of resistivities $\rho(0.1)/\rho(c)$.

6.4 CONCLUSION

Ratti and Bhatia have demonstrated that the concentration dependence of the Hall coefficient and the resistivity in liquid Mg-Bi and Tl-Te can, at least qualitatively, be understood on the basis of the formation of chemical complexes and the consequent depletion of the free electron density. The work presented in this chapter has attempted to attain a deeper understanding of these

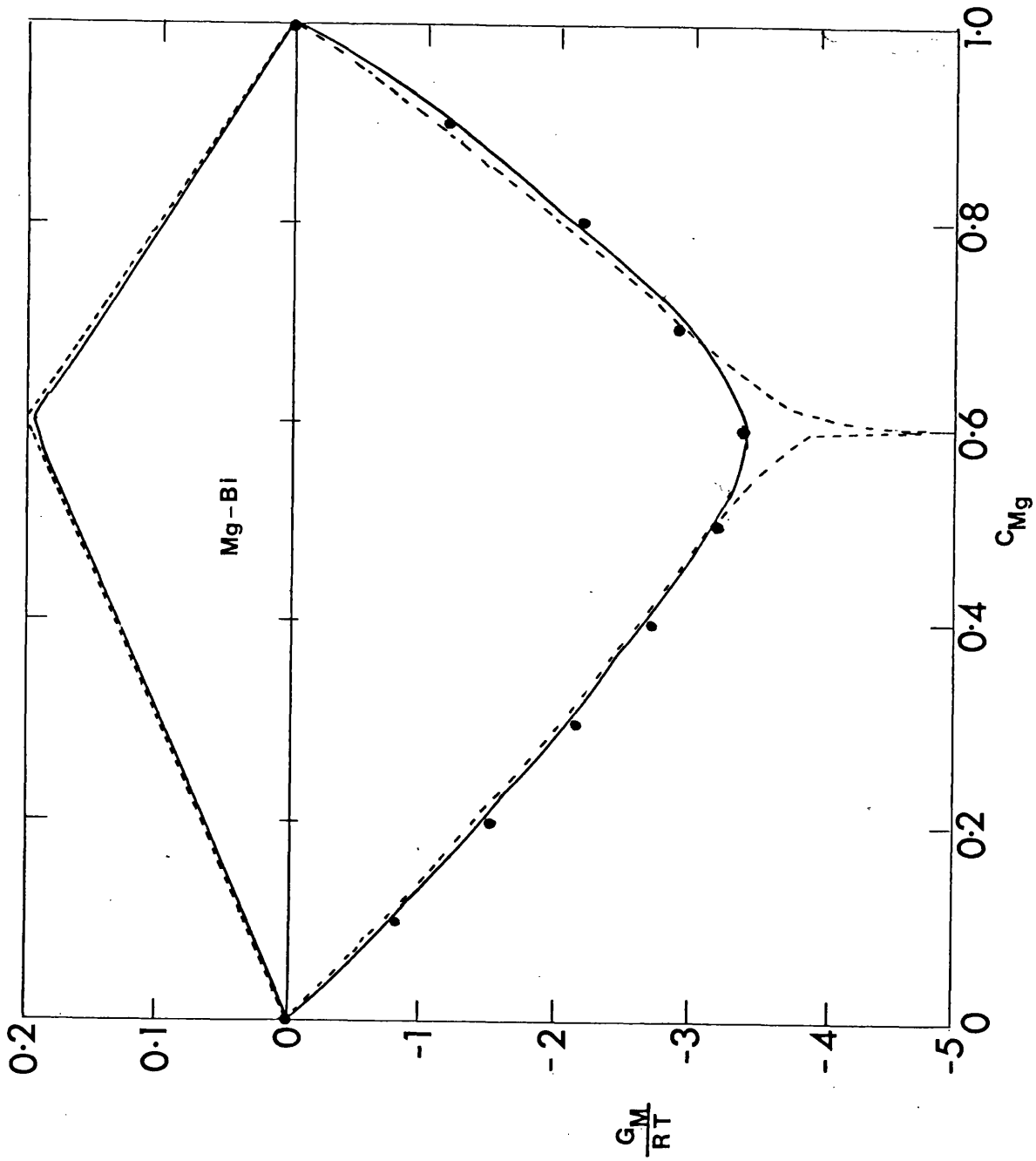


Fig. 6.3.2

G_M and n_3 as a function of concentration

- Rattia and Bhatia, 1975~
- - - determined via 6.2.11
- experimental

= RH x 10 (e.m.u.)

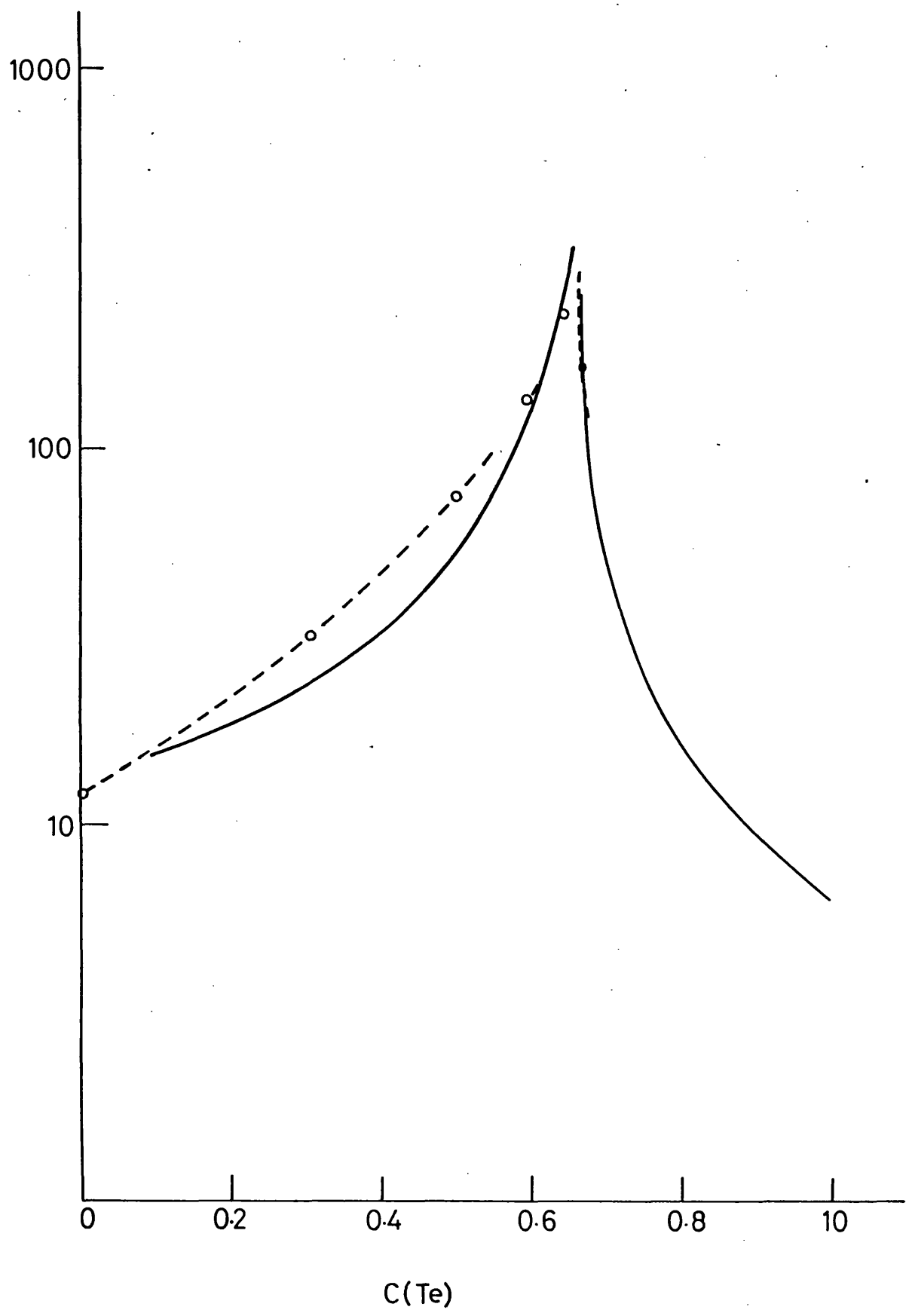


Fig. 6.3.3.

Hall coefficient of Te-Te system as a function of concentration c of Te. Dashed curve is experimental and continuous curve is theoretical.

liquid semiconductors by looking more closely at the nature of the bonding within the chemical complexes formed, and the effect that this has on the thermodynamic and electronic properties of the system. For liquid Mg-Bi, in particular, whose constituents are simple liquid metals and which are considered to have a strong tendency to form chemical complexes, there is a greater likelihood of covalent rather than ionic bonding within each complex. The calculations of the previous chapter would lead one to believe that should such covalently bonded complexes exist, then their binding energy must vary away from the critical concentration. This variation in binding energy has been simulated with the aid of the hydrogen molecule calculations, and the theory of Bhatia and coworkers reformulated for this change. The result is to worsen agreement with experimental data for heats of mixing and the electronic transport coefficients. It would appear as though covalent Mg_3Bi_2 complexes behave as if they do not interact strongly with an electron gas environment provided by excess magnesium or bismuth ions in liquid Mg-Bi. A very curious situation has thus arisen in which the molecular binding energy remains constant across the concentration range. There is, however, enough discrepancy between the experimental heats of mixing data and that calculated in the Bhatia formulation to suggest that this cannot be the case. Indeed, a matching can be obtained if the molecular binding energy is assumed to increase across the concentration range away from the critical concentration.

CHAPTER VII

MUFFIN-TINS : PHASESHIFTS

7.1 INTRODUCTION

This chapter introduces many of the concepts which form the basis of a calculation carried out on the liquid semiconducting magnesium bismuth system, a discussion of which is given in the following chapter. The many-body problem for the system is treated by replacing the electron-electron interactions by a self-consistent potential within which only a one-electron Schrodinger equation need be solved. The single particle potential will be assumed to consist of spherical non-overlapping spheres with a constant interstitial potential, taken as the zero of energy. The construction of such a potential about each site is described in section (7.2). The power of multiple scattering formalism lies in the observation that the wavefunction outside each scattering centre depends only upon the scattering phaseshifts of the potential. Section (7.3) introduces the concept of phaseshifts for a single isolated scattering centre. Particular attention is paid to the interpretation of phaseshifts for different systems. The local electronic density of states for each scattering centre of a system of several non-overlapping potentials is an important concept. Section (7.4) relates this local property for each scatterer to the scattering path operator which itself is related to the total scattering for the entire system.

Atomic units are used throughout this and the next chapter. The

unit of energy is the Rydberg given by $1 \text{ Ryd} = \frac{1}{2} e^2/a_0$, where e is the electronic charge, and the unit of length is the Bohr radius, $a_0 = \frac{\hbar^2}{me^2}$

7.2 CONSTRUCTION OF THE MUFFIN-TIN POTENTIAL

7.2.1 The Muffin-Tin Potential

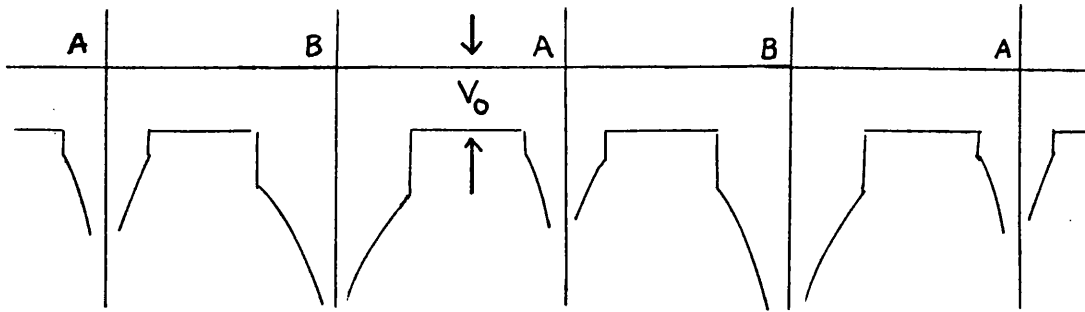


Fig. 7.2.1 The muffin-tin potential with respect to the line ABABA, V_0

The muffin-tin potential is a one-electron potential in which each atom of the crystal is surrounded by a sphere inside of which the potential is approximately spherically symmetric and rather like the potential in a free atom. Between spheres there is a shared influence coming from neighbouring atoms which leads to a flattening of the potential in these regions; hence the potential is assumed to be a constant, V_0 (figure 7.2.1). The spheres are usually chosen to be large enough to touch, so as to minimise the region between them. Thus the sum of muffin-tin potentials in an approximation to the real crystal potential.

7.2.2 Potential Construction: Mattheiss Prescription

Ideally one would like to calculate the potential function $V(r)$

inside each sphere in a self-consistent manner. However, in many cases it is possible to obtain fairly accurate energy-band results by using 'muffin-tin' potentials derived from self-consistent atomic charge densities. Hartree-Fock-Slater charge densities obtained from Herman and Skillman (1963) are usually employed.

Mattheiss (1964) treats Coulomb and exchange contributions to $v(r)$ separately. The Coulomb contribution is given by

$$V_o(r) = V_c(r) + \bar{V}'(r) \quad (7.2.1)$$

$V_o(r)$ is the atomic Coulomb potential for the atom and is obtained from

$$V_o(r) = \frac{Z}{r} - U_o(r) \quad (7.2.2)$$

where Z is the nuclear charge and $U_o(r)$ is the electronic contribution which is determined from a numerical solution of Poisson's equation:

$$\nabla^2 U_o(r) = - 8\pi\rho_o(r) \quad (7.2.3)$$

where

$$\rho_o(r) = \sum_{\text{occupied}} |\psi_{\ell m}|^2 \quad (7.2.4)$$

$\rho_o(r)$ is the atomic electronic density taken from Herman and Skillman $\bar{V}'(r)$ is the spherical average of the contribution to the Coulomb potential about the atom due to neighbouring atoms and is determined using the Löwdin alpha-expansion technique (see Loucks, 1967):

$$\bar{V}'(r) = \sum_m \frac{1}{2a_m r} \int_{|a_m - r|}^{|a_m + r|} r' \bar{V}'_o(r') dr' \quad (7.2.5)$$

Here a_m is the distance between the neighbour m and the point about which V_o is being expanded. Since only the magnitude of a_m enters, the sum over neighbours can be converted to a sum over shells of

neighbours, each shell being weighted by the number of neighbours it contains. The most significant results of adding these contributions to the atomic potential are a lowering and flattening of the potential in the vicinity of the sphere radius.

The exchange potential is treated in an analogous manner. The electronic charge density about a given atom is represented by the appropriate atomic charge density plus the spherical average of overlapping charge densities due to its neighbours:

$$\rho(r) = \rho_0(r) + \sum_m \frac{1}{2a_m r} \int_{|a_m - r|}^{|a_m + r|} r' \rho_0(r') dr' \quad (7.2.6)$$

The exchange potential is then treated according to Slater's free electron exchange approximation:

$$V_x(r) = -6 \left(\frac{3}{8\pi} \rho(r) \right)^{1/3} \quad (7.2.7)$$

The exchange potential is added to the total Coulomb contribution to give the total potential, $V_T(r)$, about the atom:

$$V_T(r) = V_C(r) + V_x(r) \quad (7.2.8)$$

This is a spherically symmetric potential which will be slowly varying in the region between the spheres. The muffin-tin zero is obtained by performing a spherical average of $V_T(r)$ over the region between the sphere radius, A , and the Wigner-Seitz sphere radius, r_s , since $V_T(r)$ will generally be very flat in this region. Thus,

$$V_0 = \frac{3 \int_A^{r_s} V_T(r) r^2 dr}{r_s^3 - A^3} \quad (7.2.9)$$

Hence inside the spheres the muffin-tin potential is taken to be

$$V(r) = V_T(r) - V_0 \quad (7.2.10)$$

7.3 SINGLE SCATTERER: PHASESHIFTS

7.3.1 Introduction

When considering a system of scatterers, at energies above muffin-tin zero, conveniently chosen as energy zero, electrons can be thought of as propagating freely in the interstitial region, and being scattered by the muffin-tin potentials. Scattering from a single site with a potential $V(r)$, where $V(r) = 0$ for $r > A$, the muffin-tin radius, then becomes important.

Consider a single spherically symmetric muffin-tin potential at the origin of position coordinates. The solution of the time-independent Schrödinger equation for the potential $V(r)$ may be expanded in angular momentum eigenstates. Inside the sphere the solution is expanded in terms of products of radial wave functions and spherical harmonics.

$$\phi(\vec{r}) = \sum_L a_L R_L(r) Y_L(\hat{r}) \quad (7.3.1)$$

$Y_L(\hat{r})$ is the real spherical harmonic of angular momentum $L = (\ell, m)$

$$\sum_L = \sum_{\ell=0}^{\infty} \sum_{m=-\ell}^{+\ell} \quad (7.3.2)$$

is the convention used. $R_L(r)$ satisfies the radial wave equation

$$\left\{ -\frac{1}{r} \frac{d^2}{dr^2} r + \frac{\ell(\ell+1)}{r^2} + V(r) \right\} R_L(r) = E R_L(r) \quad (7.3.3)$$

where E is the energy. Outside the sphere the solution of (7.3.3) must be a linear combination of independent free space solutions. A general solution can thus be written, for $r > A$,

$$R_L(r) = 4\pi i^l A_L (\cos \delta_l j_l(\sqrt{Er}) - \sin \delta_l n_l(\sqrt{Er})) \quad (7.3.4)$$

where $j_l(x)$ and $n_l(x)$ are spherical Bessel and Neumann functions respectively (as defined in Abramowitz and Stegun, (1965)). The $4\pi i^l$ factor in (7.3.4) is introduced to correspond with the plane wave expansion,

$$\exp(i \underline{k} \cdot \underline{x}) = 4\pi \sum_L i^l j_l(kx) Y_L(\hat{x}) Y_L^*(\hat{k})$$

The constants $\delta_l(E)$ which appear in (7.3.4) are the phaseshifts. Other conventional forms for the radial wave function given in (7.3.4) can be used depending upon the context in which the scattering is being considered. Two alternative forms which differ only by an amplitude factor are

$$R_L(r) = 4\pi i^l A_L \{ h_l^-(\sqrt{Er}) + \exp(2i\delta_l) h_l^+(\sqrt{Er}) \} \quad (7.3.5a)$$

$$= 4\pi i^l A_L \{ j_l(\sqrt{Er}) - i\sqrt{E} [-\sin \delta_l \exp(i\delta_l)/\sqrt{E}] h_l^+(\sqrt{Er}) \} \quad (7.3.5b)$$

where $h_l^+(x)$ and $h_l^-(x)$ are spherical Hankel functions given by

$$h_l^\pm(x) = j_l(x) \pm i n_l(x) \quad (7.3.6)$$

(7.3.5a) is convenient in the description of the scattering in terms of the true wave packets and defines the scattering factor

$$S_L(E) = \exp(2i\delta_\ell(E)) \quad (7.3.7)$$

(7.3.5b) defines the transition factor

$$t_L(E) = -\sin \delta_\ell \exp(i\delta_\ell)/\sqrt{E} \quad (7.3.8)$$

which gives the rate of scattering from an incident plane wave of electrons into the L th partial wave.

Phaseshifts are determined from matching conditions of the interior and exterior wave functions at the muffin-tin radius. At this radius the radial wave function and its derivative must be continuous so that

$$\left[\frac{1}{R_L} \frac{dR_L}{dr} \right]_{r=A} = \frac{k [\cos \delta_\ell j'_\ell - \sin \delta_\ell n'_\ell]_{r=A}}{[\cos \delta_\ell j_\ell - \sin \delta_\ell n_\ell]_{r=A}} \quad (7.3.9)$$

(7.3.9) may be solved for $\tan \delta_\ell$. Given $V(r)$, the left-hand side of (7.3.9) may be found by numerical integration of the radial Schrödinger equation out from the origin. The scattering properties of the potential are expressed entirely in terms of the phaseshifts δ_ℓ . The "modulo π " ambiguity can be removed by setting $\delta_\ell(E) = 0$ at $E = 0$. The alternative convention is to take $\delta_\ell(\infty) = 0$ (at sufficiently high energies the incident electron will not be affected by the scattering potential), then to make the reduction since Levinson's theorem states that $\delta_\ell(0) - \delta_\ell(\infty) = \rho_\ell \pi$, where ρ_ℓ is the number of bound states of angular momentum ℓ in the potential.

7.3.2 Wigner Delay Time

Consider the scattering of a wave packet of prescribed velocity. For simplicity one may regard the packet as made up of two homogenous beams of nearly equal energies $E \pm \Delta E$ and wave numbers $\underline{k} \pm \Delta \underline{k}$ respectively, so that the wave function describing the incident packet will be asymptotically

$$\psi_{inc} = r^{-1} \{ \exp i [(\underline{k} + \Delta \underline{k}) \cdot \underline{r} - \frac{1}{\hbar} (E + \Delta E) t] + \exp i [(\underline{k} - \Delta \underline{k}) \cdot \underline{r} - \frac{1}{\hbar} (E - \Delta E) t] \}$$

The centre of the wave packet is located at the point where the two waves are in phase so that

$$\Delta \underline{k} \cdot \underline{r} - \frac{1}{\hbar} \Delta E t = 0 \quad \text{i.e. } \underline{v}_G = \frac{1}{\hbar} \nabla_{\underline{k}} E_{\underline{k}}$$

Scattering of the packet by the central potential introduces phaseshifts $\delta \pm \Delta \delta$ in the outgoing waves of wave numbers $\underline{k} \pm \Delta \underline{k}$ respectively, so that, at a great distance from the scatterer, the wave function for the outgoing wave packet will be

$$\begin{aligned} \psi_{out} = r^{-1} \{ & \exp i [(\underline{k} + \Delta \underline{k}) \cdot \underline{r} - \frac{1}{\hbar} (E + \Delta E) t + 2(\delta + \Delta \delta)] \\ & + \exp i [(\underline{k} - \Delta \underline{k}) \cdot \underline{r} - \frac{1}{\hbar} (E - \Delta E) t + 2(\delta - \Delta \delta)] \} \end{aligned}$$

The centre of this wave packet is now located where

$$\Delta \underline{k} \cdot \underline{r} - \frac{1}{\hbar} \Delta E t + 2 \Delta \delta = 0$$

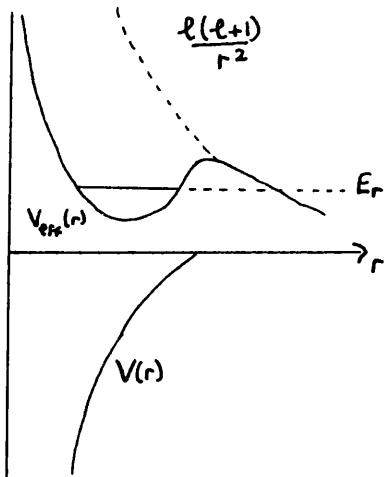
so $\underline{r} = \underline{v}_G (t - 2\hbar \frac{d\delta}{dE})$ since $\nabla_{\underline{k}} \delta = \nabla_{\underline{k}} E \frac{d\delta}{dE}$

Thus the outgoing wavepacket is retarded by a time

$$\tau_W = 2\hbar \frac{d\delta}{dE} \quad (7.3.10)$$

relative to the time in the absence of the scattering potential.

If $\delta(E)$ is a very rapidly varying function of energy, the Wigner delay time can be very long, as in the case of a scattering resonance (Figure 7.3.1)



The attractive potential $V(r)$ combines with the centrifugal potential $\frac{l(l+1)}{r^2}$ to give rise to a metastable state. The phaseshift near a resonance behaves like

$$\delta(E) \sim \tan^{-1} \left| \frac{\Gamma}{(E_r - E)} \right|$$

Fig. 7.3.1 Effective radial potential giving rise to a metastable state and a scattering resonance.

showing that it passes rapidly but continuously through the value $\pi/2$ at $E = E_r$. Thus for a resonant state the delay time becomes extremely large. For a bound state the "delay time" is in fact infinite.

7.3.3. The Friedel Sum Density Of States

Consider the introduction of the single scattering centre into a free electron gas. The presence of the scatterer leads to an accumulation (or deficit) of the electron density in its neighbourhood, since an incoming flux of electrons, of given angular momentum,

is delayed by the Wigner delay time τ_w before being converted into the outgoing flux. Flux is defined by

$$I = \frac{\hbar}{mi} \left[\psi^* \Delta \psi - \psi \Delta \psi^* \right]$$

The basic radial wave is $4\pi i^\ell j_\ell(\sqrt{Er})$ and since $j_\ell = \frac{1}{2} |h_\ell^+ + h_\ell^-|$ the incoming flux through a sphere of radius r is

$$r^2 \frac{\hbar}{8mi} \left[h_\ell^{-*} \frac{d}{dr} h_\ell^- - h_\ell^- \frac{d}{dr} h_\ell^{-*} \right] = \frac{4\pi^2 \hbar}{mk}$$

The accumulation of density is given by the incoming of flux multiplied by the delay time so that the additional number of electrons in the neighbourhood of the scattering centre is given by

$$\begin{aligned} N(E) &= 2 \int_{k=\sqrt{E}} \frac{k^2 dk}{(2\pi)^3} [4\pi^2 \hbar / mk] \left[2\hbar \sum_{\ell=0}^{\infty} (2\ell+1) \frac{d\delta_\ell}{dE} \right] \\ &= \frac{2}{\pi} \sum_{\ell=0}^{\infty} (2\ell+1) \delta_\ell(E) \end{aligned} \quad (7.3.11)$$

This is the well known Friedel sum rule (Friedel, 1953). It can also be derived from the radial wavefunction by taking

$$N(E) = 2 \int_{k=\sqrt{E}} \frac{k^2 dk}{(2\pi)^3} \int_0^\infty r^2 dr \left\{ \sum_{\ell=0}^{\infty} (2\ell+1) \left| |R_\ell(r)|^2 - |4\pi i^\ell j_\ell(kr)|^2 \right| \right\}$$

where the radial function $R_\ell(r)$ is given by equation (7.3.4). It follows that the integrated density of states per atom, $N'(E)$, is given by

$$N'(E) = N_0(E) + \frac{2}{\pi} \sum_{\ell} (2\ell+1) \delta_{\ell}(E)$$

where $N_0(E)$ is the free electron contribution, and

$$g(E) = g_0(E) + \frac{2}{\pi} \sum_{\ell} (2\ell+1) \frac{d\delta}{dE}$$

7.3.4 Interpretation Of Phaseshifts

For the muffin-tin potentials and energies with which one is usually concerned, only the $\ell=0,1,2,3$ phaseshifts are significant. Typical phaseshifts calculated using equation (7.3.9) for a simple free electron metal, transition metal, and a semiconductor are given in figure 7.3.2, taken from Greenwood (1973). Figure 7.3.3 shows the phaseshifts calculated for copper, a typical noble metal. The $\ell=3$ phaseshifts are negligible for these systems.

For sodium, the phaseshifts and their energy derivatives are all small up to the Fermi energy. The Friedel sum will be small, the Wigner delay time short. These are characteristics of a weak scatterer of which sodium must be one. This contrasts the transition metal, iron, in which the d-phaseshift is important. The energy derivative of the d-phaseshift is large near the Fermi energy which implies a d-resonance of long Wigner delay time at this energy. Iron is a strong scatterer. For copper the d-phaseshift is small near to and far away from muffin-tin zero, although its energy derivative is large over an energy range below the Fermi energy. The d-resonance lies below the Fermi energy, electrons are well localised within the muffin-tins, and therefore behave somewhat like core electrons (House and Smith, 1973). All

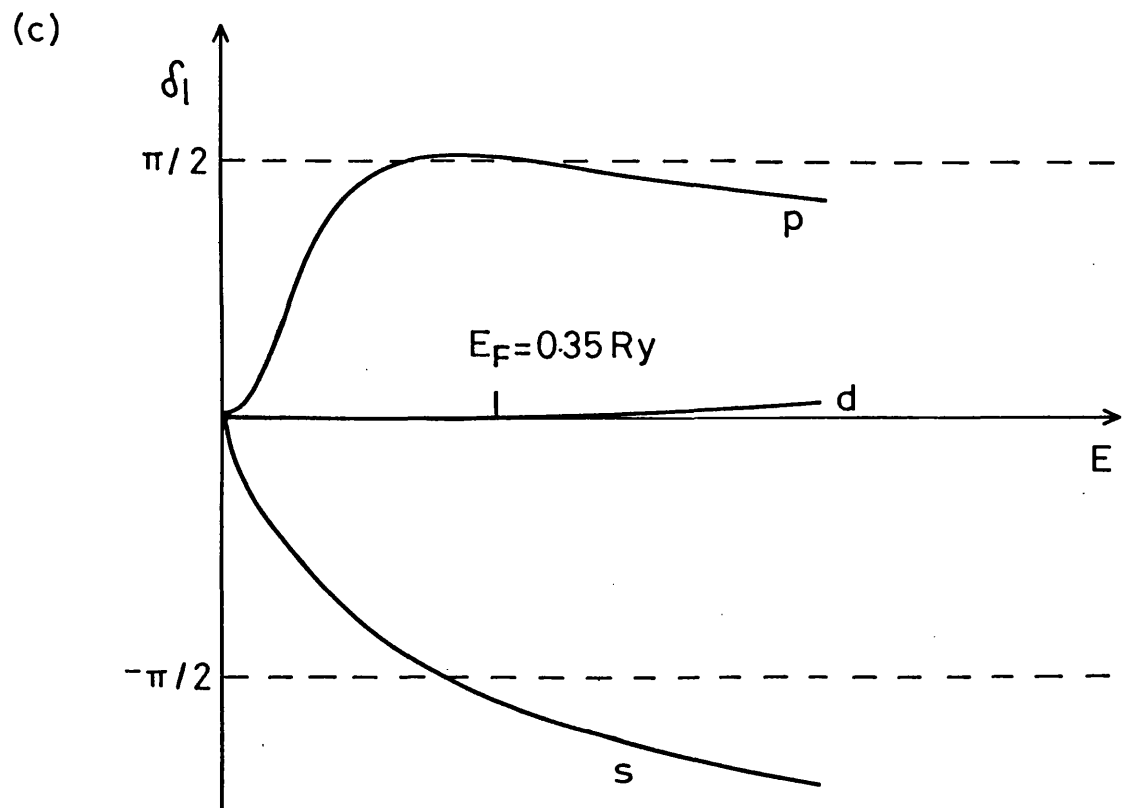
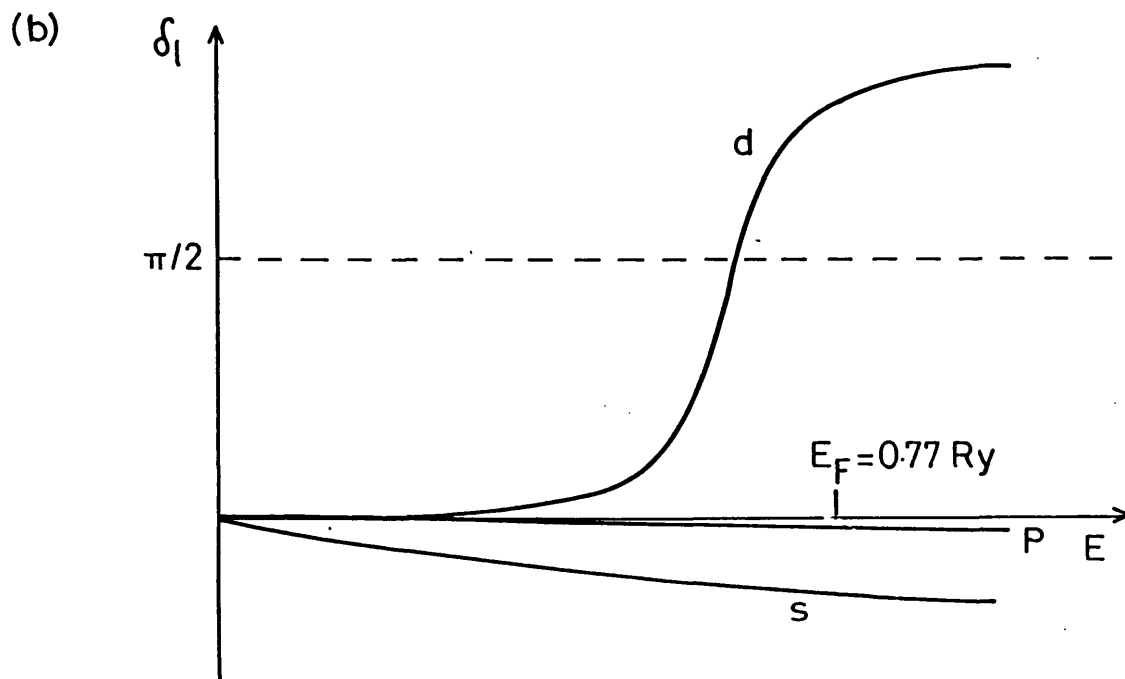
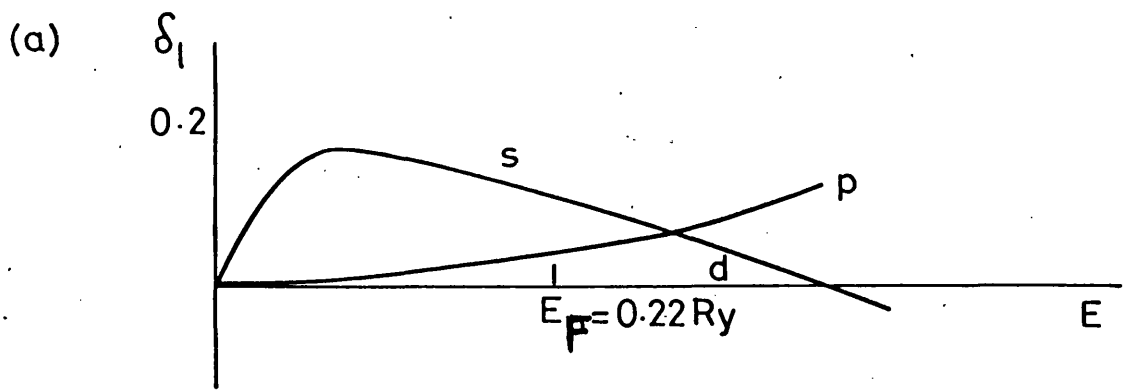


Fig.7.3.2. Typical muffin-tin phaseshifts for
(a) sodium (b) iron (c) germanium.

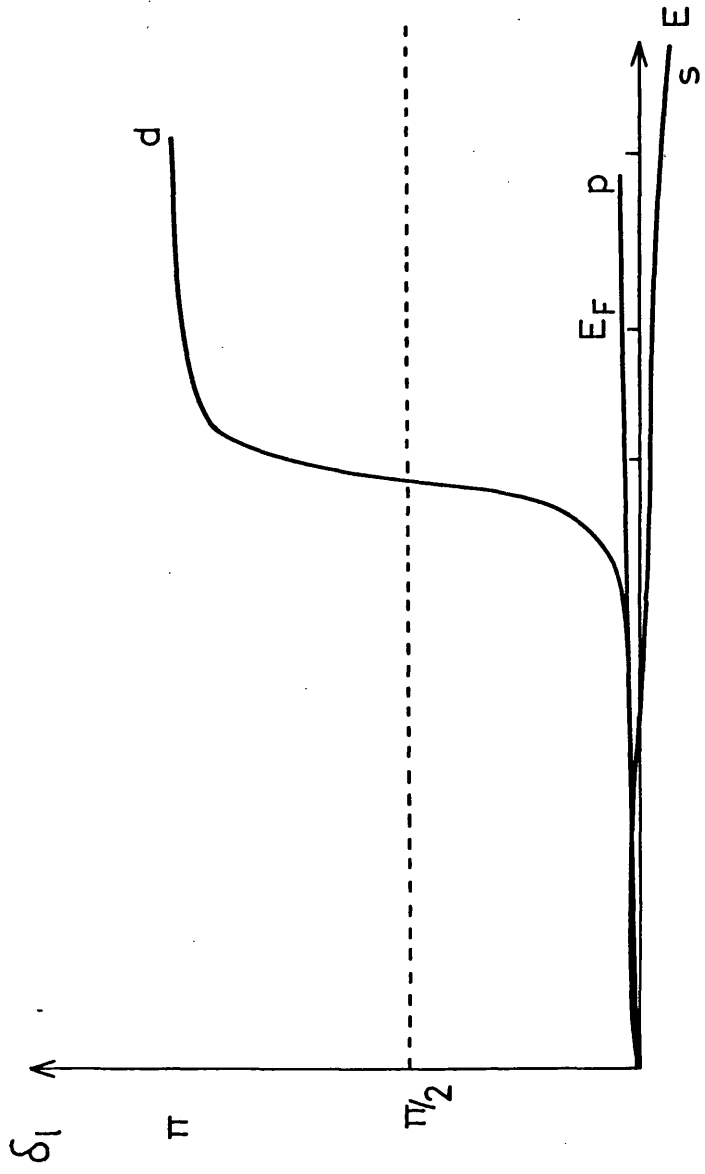


Fig.73.3. Muffin-tin phaseshifts for copper
(House, 1974)

phaseshifts and their energy derivatives are small at the Fermi energy; it is this feature which enables one to treat noble metals as weak scatterers at this energy. For germanium the s- and p-phaseshifts are approximately equal to $-\frac{\pi}{2}$ and $+\frac{\pi}{2}$, respectively, at the Fermi energy. Close to the muffin-tin zero the phaseshifts and their derivatives are large which would imply that germanium is a strong scatterer near this energy; away from muffin-tin zero the phaseshift derivatives are small which suggests some free electron qualities. There is an apparent duality in which nearly free electron theory is acceptable at higher energies, but not near muffin-tin zero. Germanium is an elemental semiconductor whose atoms are characterized by long range order in a crystal array.

In Chapter VIII the electronic properties of the liquid magnesium-bismuth system will be discussed with reference to the phaseshifts characteristic of each constituent atom across the concentration range. The sodium and germanium phaseshifts considered above will serve as a useful introduction to the discussion.

7.4 LOCAL ELECTRONIC DENSITY OF STATES: SCATTERING PATH OPERATOR

The muffin-tin density of states for a single scatterer in a system of several ($\sim 10^{23}$) scatterers, $n_L^\alpha(E)$, is defined as the integral of the particle density over the volume of a spherical scattering centre:

$$n_L^\alpha(E) = \int_{r=0}^A d^3r \int \frac{d^3k}{(2\pi)^3} \psi_{\underline{k}}^*(\underline{r}) \psi_{\underline{k}}(\underline{r}) \delta(E-E_{\underline{k}}) \quad (7.4.1)$$

In a review article, Smith and Lloyd (1972) have related $n_L^\alpha(E)$ to the single site muffin-tin density of states, $n_L^d(E)$, using the scattering path operator $\tau^{\alpha\alpha}$:

$$n_L^\alpha(E) = n_L^d(E) \operatorname{Im} \left[-\sqrt{E} \tau_{LL}^{\alpha\alpha}(E) / \sin^2 \delta_\ell(E) \right] \quad (7.4.2)$$

The scattering path operator $\tau^{\alpha\beta}$ is defined by the relations (Gyorfy, 1973):

$$\tau^{\alpha\beta} = t_{\alpha\beta}^\alpha + \sum_{\gamma \neq \alpha} t^\alpha G t^{\gamma\beta} \quad (7.4.3)$$

$$\tau^{\alpha\beta} = t_{\alpha\beta}^\alpha + \sum_{\gamma \neq \beta} \tau^{\alpha\gamma} G t^\beta$$

where t^α , t^β are the scatterings from an α and a β site respectively (angular momentum components given in (7.3.8)), and $\tau^{\alpha\beta}$ is the scattering from an α to a β site. Summing over all α and β sites, the total scattering for the entire system, T (the total T-matrix), is given by

$$T = \sum_{\alpha, \beta} \tau^{\alpha\beta} \quad (7.4.4)$$

Thus $\tau^{\alpha\beta}$ is the site decomposition of the total T -matrix, relating to the scattered wave from one site to an incident wave and another.

G is a matrix whose angular momentum components are defined by

$$G_{LL'}(r_{\alpha\beta}) = \begin{cases} i\sqrt{E} \sum_{L''} 4\pi i^{\ell-\ell'+\ell''} h_{\ell''}^+ (\sqrt{E} r_{\alpha\beta}) Y_{L''}(\hat{r}_{\alpha\beta}) C_{LL'}^{L''} & |r_{\alpha\beta}| > 0 \\ 0 & |r_{\alpha\beta}| = 0 \end{cases} \quad (7.4.5)$$

It is a propagator which describes the motion of electrons between site α and β at energy E . $h_{l''}^+(x)$ is the spherical Hankel function defined in equation (7.3.7), given in Abramowitz and Stegun (1965), $Y_{L''}(\hat{r}_{\alpha\beta})$ is a real spherical harmonic.

$$C_{LL'}^{L''} = \int Y_L(\Omega) Y_{L'}^*(\Omega) Y_{L''}(\Omega) d\Omega$$

are integrals over spherical harmonics (known as Gaunt numbers).

CHAPTER VIII

A CALCULATION ON THE SEMICONDUCTING MAGNESIUM-BISMUTH SYSTEM

8.1 INTRODUCTION

As far as is known, all liquid semiconductors are also amorphous semiconductors. The electrical behaviour of amorphous materials which are semiconductors or semimetals in the crystalline state is not fully understood. In ordered crystals the periodic lattice has the effect of carving the energy distribution of the conduction electrons into a series of bands. Each band can contain two electrons per unit cell and they are filled up depending upon the number of atoms per unit cell and the number of electrons per atom. The last two bands to be filled are known as the valence and conduction bands and these are sometimes separated from each other by an energy gap where electron states are not allowed. Consider a small amount of disorder introduced into an otherwise ordered crystal by assuming that there are different regions of the crystal with slightly different crystal structure and lattice spacing. There will exist electron states in some of these regions with energies in the gap of the full sample which are not allowed in most regions. In some sense these are localized states which give rise to tails in the valence and conduction bands. Mott (1969) has suggested that there are tails to both the valence and conduction bands in amorphous materials which, depending on the disorder present, can result in a pseudogap corresponding to a minimum in the density of states (figure 8.1.1). In this region electron states may be localized

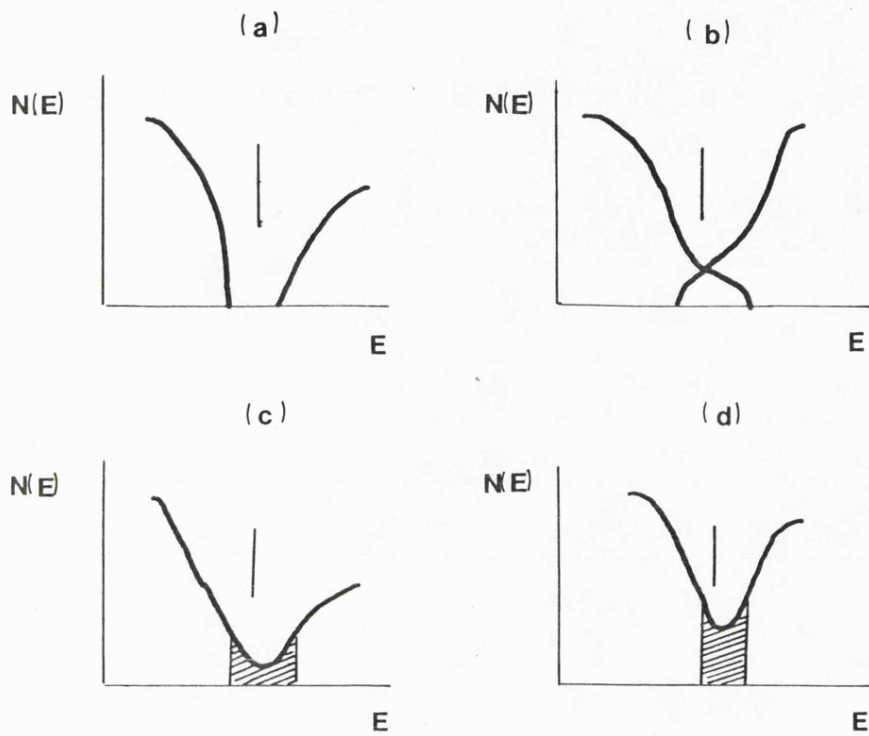


Fig.8.1.1

Suggested density of states in amorphous semiconductors

(c) and semimetals (d) compared with crystalline (a) and (b). The region of localized states is shaded, and the Fermi level is indicated by a vertical line.

with the electrons moving by thermally activated hopping. The conductivity is low ($<200\Omega^{-1}\text{cm}^{-1}$). Moving away from the composition at which the alloy is a semiconductor or semimetal (e.g. Mg_3Bi_2), the Fermi level will move out of the pseudogap and the region of localized states will fall to zero. As localization weakens, each localized wavefunction will overlap a large number of others until the conduction is no longer by hopping but by extended states.

Ferrier and Herrell (1970) have investigated the electrical properties of amorphous Mg-Bi measuring the electrical conductivity and thermoelectric power of the alloy as a function of temperature and composition (figure 8.1.2). At the composition corresponding to Mg_3Bi_2 the thermopower changes sign and the conductivity shows a pronounced minimum, although the drop is not as narrow as in the liquid state. Particular attention is given to the region near the Mg_3Bi_2 composition. Here they find the properties to be in agreement with a model of localized states, with the electrons moving by thermally activated hopping. From their data Ferrier and Herrell (1970a) have deduced the form of the density of states around the gap for amorphous Mg-Bi, estimating a gap width of 0.02 Rydbergs. They propose that the electrical properties of the liquid state may also be understood by assuming the existence of a pseudogap in the density of states. The origin of the gap is not, however, clear.

Keller and Ziman (1970) have looked at the general problem of generating an energy gap in a system without long range order. For amorphous semiconductors it has been shown that short range order

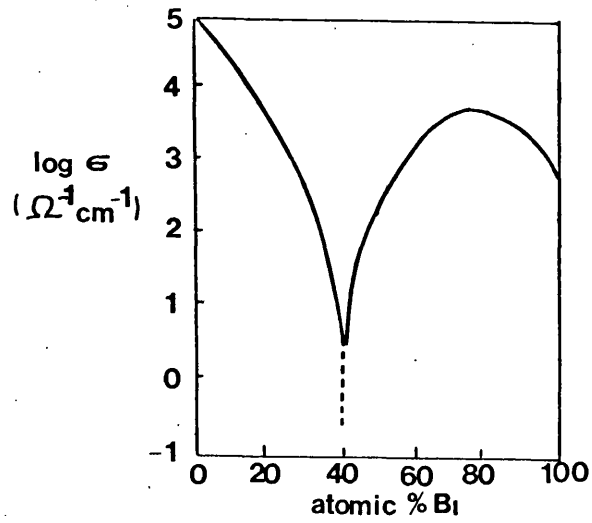


Fig. 8.1.2 a

Variation of log conductivity
for amorphous MgBi alloys
at 80° K.

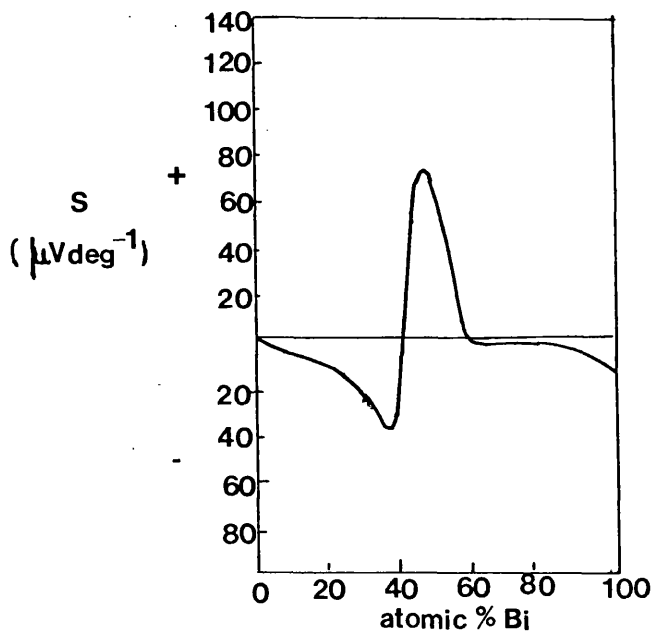


Fig. 8.1.2 b

Thermopower as a function
of composition at 100° K.

tends to produce a low density of states in the gap region. Indeed, the analysis of Ferrier and Herrell (1970b) reveals that the nearest neighbour distance falls to a sharp minimum at the $Mg_3 Bi_2$ composition suggesting that some short range structural changes are taking place. It is the purpose of this chapter to investigate how and why an energy gap is produced. The general theoretical approach adopted is outlined in the following section. Section 8.3 gives the approximate expression for the bottom of the conduction band in a liquid alloy used to facilitate the estimation of the Fermi energy. Section 8.5 suggests a simple interpretation for the origin of the band gap in liquid Mg-Bi based on the calculations and results presented in Section 8.4. The implications of this model for the transport coefficients are given in section 8.6, while section 8.7 is a brief summary of the chapter. The work presented in this chapter follows from an investigation carried out by Jewsbury and Dooley on the liquid semiconducting Mg-Bi system.

8.2 THEORETICAL APPROACH

Ziman (1972) has reviewed a wide variety of theoretical techniques which are available for studying the electronic properties of condensed systems. For a general alloy comprising strong and weak scatterers, the most useful approach to apply to a disordered system is the multiple scattering method as developed by Korringa (1947). The technique relies on being able to subdivide the total potential into non-overlapping parts, centred on the nuclei. It is usual to employ muffin-tin potentials in such calculations, as described in Chapter VII.

The muffin-tin approximation was first applied to metallic crystalline solids assuming the crystal potential to consist of spherical non-overlapping spheres around the nuclei with a constant interstitial potential. Systems which have a spherically symmetric local environment (large co-ordination numbers) and non-directional bonding are most suitable for this approximation. The success of this approximation has led many workers (e.g. Evans et al, 1973) to suggest its use in liquid systems. The basic features of a spherically symmetric central core region and a fairly flat interstitial potential apply equally to a solid or liquid, but it is unlikely that the local environment of a general atom in the liquid will be spherically symmetric. Furthermore, in a practical calculation all the muffin-tin potentials of a species in the liquid are likely to be taken equal. As the potentials are not allowed to overlap this implies that the apparent interstitial volume increases from about 30% in the solid to about 60% in the liquid. Hence although the muffin-tin approximation appears reasonable in a liquid, the error must be greater than in the equivalent solid.

Close to the critical composition the $Mg_3 Bi_2$ alloy is semiconducting, and semiconductors generally have directional bonding. Muffin-tin calculations have been carried out on amorphous elemental semiconductors (eg. Keller and Smith, 1972; Keller and Fritz, 1974) in the multiple scattering cluster approximation (McGill and Klima, 1970) producing satisfactory densities of states including a reasonable energy gap. This is encouraging for a muffin-tin calculation on the $Mg_3 Bi_2$ alloy.

In a phenomenological study of the behaviour of the transport properties of liquid Mg-Bi, as opposed to a detailed calculation of them, it seems reasonable to believe that calculating muffin-tin potentials across the concentration range will provide realistic information on those properties. Calculations of these potentials have been carried out using the Mattheiss prescription, details of which are given in section 8.4 together with the relevant necessary data and results. With such potentials many details of the system may be determined directly. One of the properties which is useful in descriptive accounts is the energy of the bottom of the extended states. A simple expression which may be used to calculate this quantity will be given in section 8.3. Two complications, however, should be considered for a calculation of the type described. If charge transfer takes place it is not clear that the muffin-tin method will be as valid for an alloy as for a pure substance. A calculation on the magnesium-bismuth 50-50 alloy finds a charge transfer of the order of 0.05 electrons from the magnesium to the bismuth atom (c.f. Chapter III). Also, for a heavy element, such as bismuth, spin orbit and relativistic corrections are required for a full description of electronic properties (Herman and Skillman, 1963). Energy level splittings arise because of the large kinetic energies and velocities of the outer electrons of the atom where the potential energy is small. Nevertheless, a non-relativistic description should include the same features, e.g. an energy gap arising from the same mechanism, as a more complete relativistic calculation. The true width of the gap will be reduced by these corrections. Energy level separations can be estimated from atomic spectra to be

of the order of $\frac{2}{3}$ eV.

8.3 THE BOTTOM OF THE BAND IN A LIQUID ALLOY

Several simple approximate expressions exist to calculate the bottom of the band energy, E_B , in single component systems. However, the expression which most accurately evaluates E_B , usually within 2 milli-Rydbergs, is the Ziman (1965) expression. In an ordered solid the energy eigenvalue versus Bloch vector \underline{K} , must have a minimum (or maximum) at $K = 0$ and this generally, but not always, corresponds to the bottom of the band. $K = 0$ is nearly always assumed to be the bottom of the band. When this is true, it is generally believed that, close to the energy E_B , the band structure is free electron like (parabolic) and the electron wavefunction is s-type. This suggests that the non-s phaseshifts should be small at energy E_B and if they are not, then it is likely that $\underline{K} = \underline{0}$ is not the bottom of the band.

The Ziman approximation is to include only the reciprocal lattice vector, $\underline{g} = \underline{0}$, contributions to the KKRZ secular determinant - i.e.

$$\epsilon = E_B - E_{MTZ} = \Gamma_{00} \quad (8.3.1)$$

Here $\Gamma_{\underline{g}\underline{g}}$ are components of an effective pseudopotential given by

$$\Gamma_{\underline{g}\underline{g}'}(K=0) = -\frac{4\pi n}{\sqrt{\epsilon}} \sum_{\ell} \frac{j_{\ell}(gr) j_{\ell}(g'r')}{\left\{ \cot \delta_{\ell} - \frac{n_{\ell}(\sqrt{\epsilon}r)}{j_{\ell}(\sqrt{\epsilon}r')} \right\} j_{\ell}(\sqrt{\epsilon}r) j_{\ell}(\sqrt{\epsilon}r')} P_{\ell} \frac{\underline{g} \cdot \underline{g}'}{|\underline{g}| |\underline{g}'|} \quad (8.3.2)$$

where n is the atom number density, E_{MTZ} the muffin-tin zero energy, $j_\ell(x)$ and $n_\ell(x)$ spherical Bessel and Neuman functions and $P_\ell(x)$ the Legendre polynomial. If no approximations are made \underline{r} and \underline{r}' are arbitrary position vectors within a unit cell subject to $\underline{r}' > \underline{r}$.

The approximation of including the $g = g' = 0$ term only necessarily implies that only s-wave scattering is important since $j_\ell(0) = \delta_{\ell,0}$. If this is adopted as a proposition then the Ziman expression may be derived directly from KKR theory. The KKR determinant (Kohn and Rostoker, 1954) is just

$$\det \left\| \left\| A_{L_1 L_2} k_{L_2} - \delta_{L_1 L_2} \right\| \right\| = 0 \quad (8.3.3)$$

where $k_L(E) = -\frac{1}{\sqrt{E}} \tan \delta_\ell$ is the single site k-matrix. The coefficients $A_{L_1 L_2}$ are given as the sum over lattices sites

$$A_{L_1 L_2} = \frac{1}{N} \sum_{\substack{\alpha, \beta \\ \alpha \neq \beta}} \sum_{L_3} 4\pi C_{L_1 L_2 L_3} i^{\ell_1 - \ell_2 + \ell_3} \sqrt{\epsilon} n_{\ell_3} (\sqrt{\epsilon} R_{\alpha\beta}) Y_{L_3}(\hat{R}_{\alpha\beta}) e^{-i \underline{k} \cdot \underline{R}_{\alpha\beta}}$$

where $C_{L_1 L_2 L_3}$ are Gaunt numbers and $\underline{R}_{\alpha\beta}$ the position vector between sites α and β . Including only the $L=0$ terms in the KKR determinant (8.3.3) taking only the $g = 0$ term in an expression for $A_{L_1 L_2}$ written as a sum over reciprocal lattice vectors, and selecting $\underline{r} = \underline{r}' = A$, the muffin-tin radius, the Ziman condition is obtained:

$$z_f = 1 + \frac{\tan \delta_0}{\sqrt{\epsilon}} \left| \frac{4\pi n A^2}{\sin^2(\sqrt{\epsilon} A)} + \sqrt{\epsilon} \cot(\sqrt{\epsilon} A) \right| = 0 \quad (8.3.4)$$

Hence the Ziman starting energy, E_B , for the band of conduction electrons in a single component system with reference to muffin-tin zero, $E_B - E_{MTZ}$, is obtained as the solution of the implicit equation (8.3.4).

In a general system the equivalent expression to the KKR determinant (Smith and Lloyd, 1974) is

$$\det || G_{L_1 L_2}^{\alpha\beta} k_{L_2}^{\beta} - \delta_{L_1 L_2}^{\alpha\beta} || = 0 \quad (8.3.5)$$

where $G_{L_1 L_2}^{\alpha\beta}$ is given by

$$G_{L_1 L_2}^{\alpha\beta} = (1 - \delta_{\alpha\beta}) \sum_{L_3} 4\pi C_{L_1 L_2 L_3} i^{\ell_1 - \ell_2 + \ell_3} \sqrt{\epsilon} n_{\ell_3} (\sqrt{\epsilon} R_{\alpha\beta}) Y_{L_3}(\hat{R}_{\alpha\beta}) - i \sqrt{\epsilon} \delta_{L_1 L_2} \delta_{\alpha\beta}$$

and the determinant of (8.3.5) is taken over angular momentum and site variables. Including only $g = 0$ contribution is ^{the} zeroth order in the structure and can be generalized in the liquid alloy by assuming that site occupancies are also unimportant. The choice of values for r and r' is not, however, straightforward. It is therefore suggested that it is reasonable to include them with the averaging as appropriate muffin-tin radii. Thus the determinant becomes

$$\det || \langle A_{L_1 L_2} k_{L_2} \rangle - \delta_{L_1 L_2} || = 0 \quad (8.3.6)$$

where $\langle A_{oo} k_o \rangle = C_a A_{oo}^a k_o^a + C_b A_{oo}^b k_o^b$

Here a and b represent the alloy species and the $A_{oo}^{a/b}$ are expressed by the Ziman approximation. Hence the generalization of the Ziman condition for the bottom of the band in a binary liquid alloy yields the condition

$$z_f^{ALLOY} = C_a z_f^a + C_b z_f^b \quad (8.3.7)$$

where C_a and C_b are the concentrations of species a and b, and $z_f^{a/b}$ is defined as in (8.3.4) with the s-phaseshift and muffin-tin radius appropriate to the a/b type muffin-tin.

In the Mg-Bi system, the Bi p-phaseshift is large ($\frac{\pi}{4}$) at the solution of (8.3.4). Thus, although this formula has been employed, it is unlikely to be very accurate, with an error of 0.1 Rydbergs, say.

8.4 CALCULATION AND RESULTS

In order to perform calculations on the liquid semiconducting Mg-Bi system using one electron muffin-tin potentials over a wide range of compositions, it is necessary to have some knowledge of the Mg-Bi structure. The structural studies of Ferrier and Herrell (1970) on amorphous Mg-Bi and Waseda and Suzuki (1972) on liquid bismuth provide the near-neighbour distances and co-ordination numbers which appear in table 8.4.1.

In view of the lack of knowledge of the Mg-Bi structure only the nearest neighbour shell of atomic wavefunctions were overlapped. This is generally found to be as realistic as including contributions from all shells. The atomic wavefunctions for magnesium and bismuth

TABLE 8.4.1

Data relevant to the potential construction

Bismuth Concentration	Nearest Neighbour Distance (Å)	Co-ordination Number	Atomic Volume ($\times 10^{24}$) cm ³
0	3.20	12.2	20.2
0.2	3.08	8.4	24.2
0.4	2.83	5.5	27.6
0.6	3.22	4.2	29.5
0.8	3.37	4.8	32.1
1.0	3.38	8.8	34.6

atoms were taken from Herman and Skillman (1963). Muffin-tin potentials for magnesium and bismuth atoms were calculated across the composition range in the Mattheiss prescription with Slater exchange, a recipe which should ensure realistic potentials to be calculated in a reasonable approximation to self-consistency (equations (7.2.1) to (7.2.8)). The muffin-tin radii were taken to be half the nearest neighbour distance, and the muffin-tin zeros appropriate to the type of centre atom (magnesium or bismuth) were calculated by averaging the potential between the muffin-tin radius, A , and the Wigner-Seitz radius, r_s , according to equation (7.2.9). The alloy muffin-tin zero was taken as a concentration

weighted average of the muffin-tin zeros calculated for the different atoms. The energy of the bottom of the conduction and valence bands arising from the hybridisation between the atomic 3s (on Mg site) and 6s and 6p (on Bi site) states was determined according to equation (8.3.7). Solutions were only found at energies above alloy muffin-tin zero.

Values of the alloy muffin-tin zero energies and bottom of the band energies are given in table 8.4.2.

TABLE 8.4.2

Relevant energies with respect to atomic zero, in Rydberg, for Mg-Bi.

Bismuth Concentration	E_{MTZ} (Rydbergs)	E_B (Rydbergs)	$E_F - E_B$ (Rydbergs)
0	-0.957		
0.2	-0.996	-0.899	0.557
0.4	-1.134	-0.963	0.578
0.6	-0.847	-0.613	0.482
0.8	-0.819	-0.570	0.433
1.0	-0.965	-0.747	0.499

Phaseshifts for these potentials are shown in figures 8.4.1 and 8.4.2. The magnesium phaseshifts are small whereas the bismuth s and p phaseshifts are large. Indeed the difference is sufficiently marked that for many purposes the magnesium phaseshifts may be neglected - that is to say, even in the alloy the magnesium exhibits very free electron behaviour.

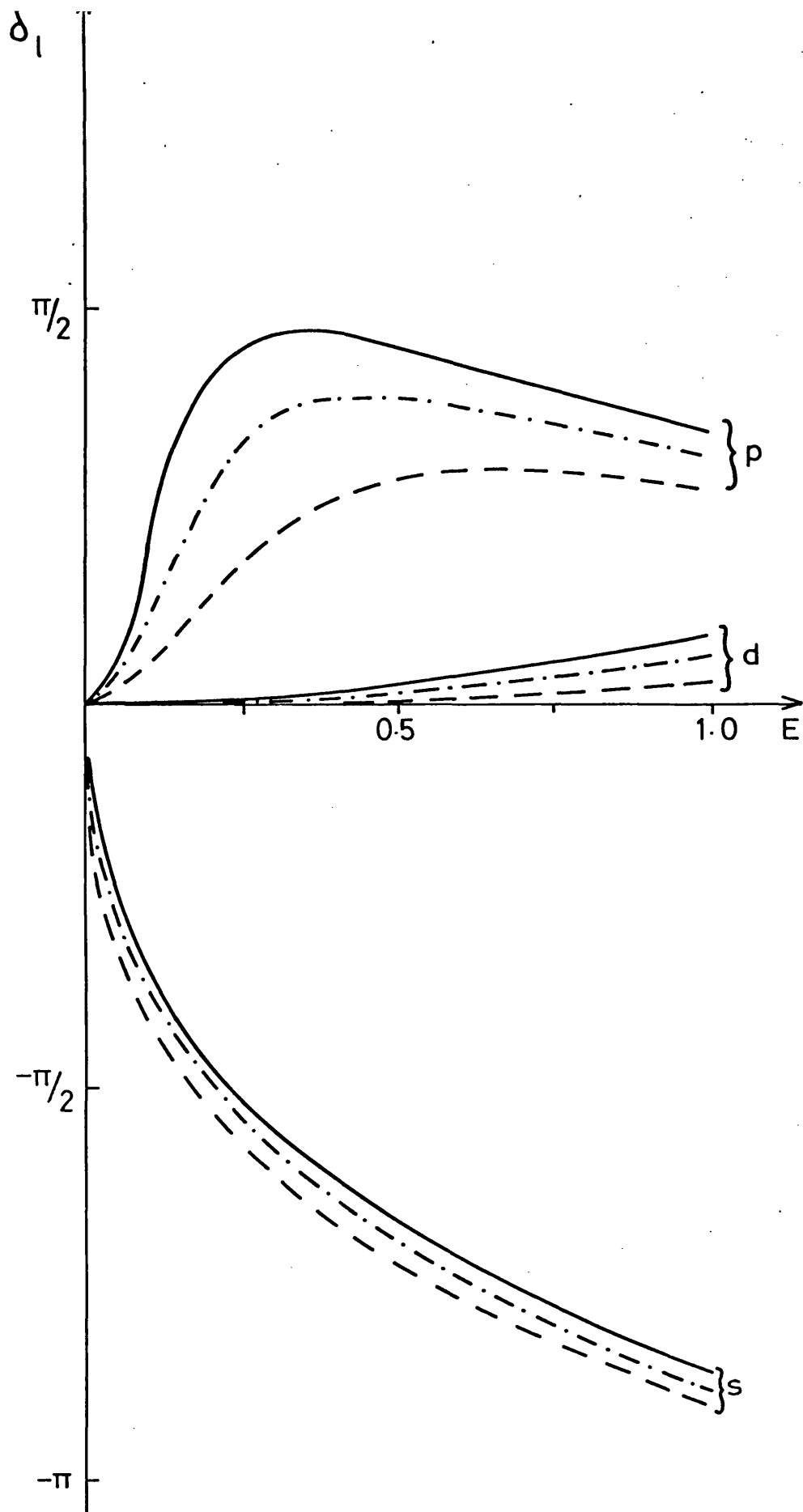


Fig.8.4.1 Calculated phaseshifts for Bi atoms in

$\text{Mg}_x \text{Bi}_{1-x}$
 $x = .4$ (—)
 $x = .6$ (---)
 $x = .8$ (-·-·-)

Energies are measured from alloy muffin-tin zero.

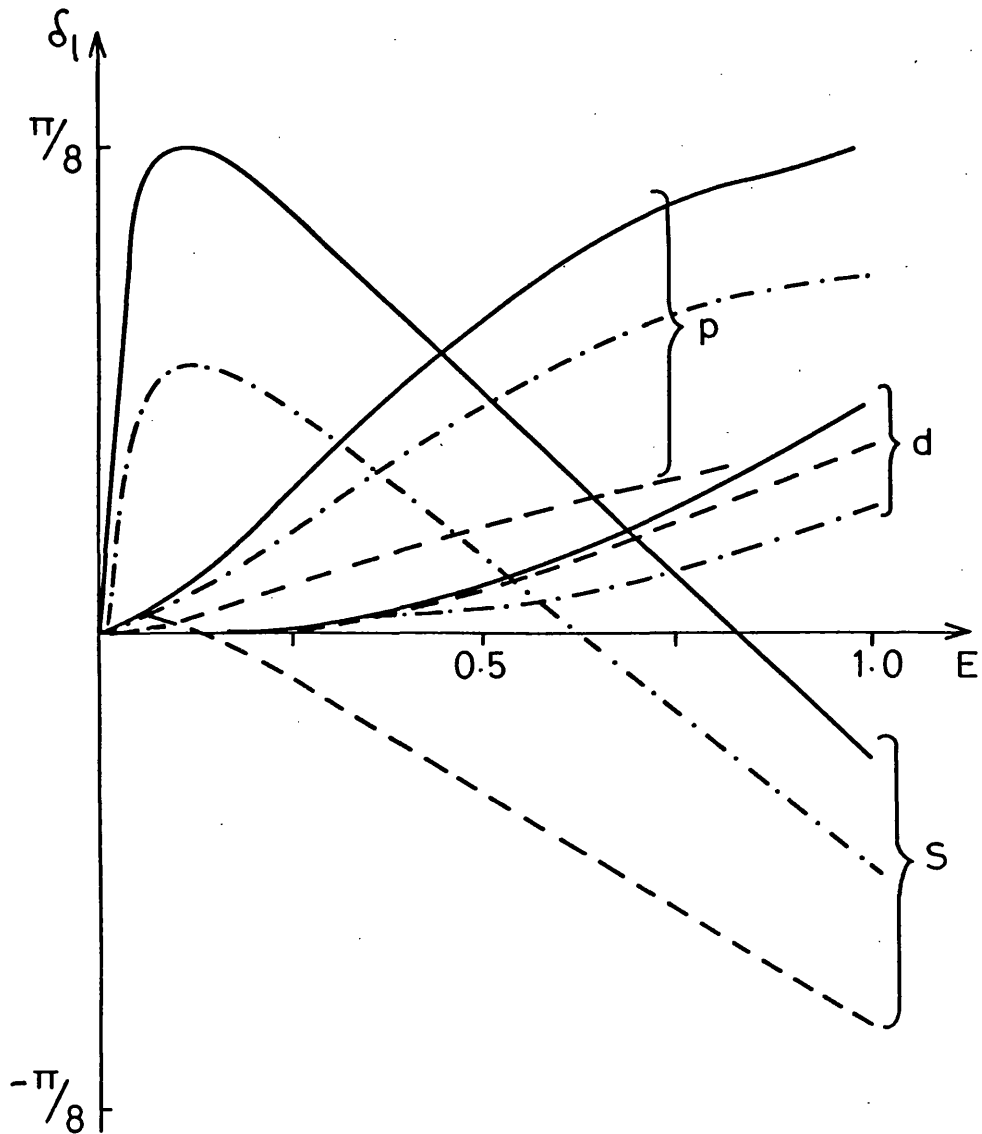


Fig. 8.4.2 Calculated phaseshifts for magnesium atoms in $Mg_x Bi_{1-x}$ for

$x = .4$ (—)

$x = .6$ (---)

$x = .8$ (-·-·-)

Energies are measured from alloy muffin-tin zero.

The addition (subtraction) of Mg to an alloy of Mg Bi is therefore comparable to the addition (subtraction) of electrons to a "liquid Bi system" since the Mg atoms do not contribute significantly to the total scattering. However, since the system remains neutral at all times, the appropriate positive charge background is also added. Of course, in addition the volume of the system also changes. The effect of the background is to contribute to changes in E_B as described by Table 8.3.2, and the effect of the addition of electrons, coupled with the volume change, is to alter the band width. Making this comparison enables an intuitive understanding of this system to be grasped more easily.

The Fermi energy can be estimated by using the Friedel (1958) sum rule which will yield exact answers in the low Bi atom density limit. For this calculation phaseshifts for the Bi atoms were used which represented a single Bi atom in a free electron environment starting from the alloy bottom of the band. The Friedel sum rule gives the excess number of states above the free electron number per Bi atom created by these potentials. Hence the Fermi energy, E_F , is approximately given by

$$\frac{(E_F - E_B)^{3/2}}{3 \pi^2 n C_{Bi}} + \frac{2}{\pi} \sum_L \tilde{\delta}_\ell(E_F) = 5 + \frac{2 C_{Mg}}{C_{Bi}} \quad (8.4.1)$$

where $\tilde{\delta}_\ell$ are the phaseshifts with respect to the bottom of the band E_B . The deduced band widths are also given in Table 8.4.2.

The Bi phaseshifts (Figure 8.4.2) look very like those of the elemental semiconductors C, Si and Ge (Figure 7.3.2). At the Fermi energy only the s and p phaseshifts are large, the s

phaseshift is large and negative, the p phaseshift is close to $\pi/2$ and both $\frac{d\delta_0}{dE}$ and $\frac{d\delta_1}{dE}$ are negative. The negative energy gradients mean that electrons at these energies are to a certain extent kept out of the muffin-tin regions. This has been discussed in detail by Greenwood (1973) who has shown that causality restricts the magnitude of this gradient.

The conductivity of a specimen is determined by its ability to impede the flow of electrons by elastically scattering them. The work of Evans et al (1973) suggests that it is the ratio of the muffin-tin density of states to the single site muffin-tin density of states $n_L^\alpha(E_F)/n_L^1(E_F)$ which appears in an expression for the conductivity. This ratio is determined by the multiple scattering of the system, being given by the imaginary part of the diagonal matrix elements of the scattering path operator:

$$n_L^\alpha(E) = n_L^1(E) \operatorname{Im} | -\sqrt{E} \tau_{LL}^{\alpha\alpha}(E)/\sin^2\delta_\ell(E) | \quad (8.4.2)$$

The bonding and energy gap within the liquid bismuth system can now be investigated by calculating $D_\ell(E)$ given by

$$D_\ell(E) = \sum_{m=-\ell}^{+\ell} n_L^\alpha(E)/n_L^1(E) \quad (8.4.3)$$

for the idealised situation in which $\delta_0 = -\frac{\pi}{2}$, $\delta_1 = \frac{\pi}{2}$, and other phaseshifts are zero. This will give a qualitative account as to how a pseudogap may arise.

For a single atom surrounded by a constant potential equal to the muffin-tin zero of energy, $D_\ell(E) = (2\ell+1)$. For two such atoms a distance R apart, bonding can take place giving $D_\ell(E)$ an energy dependence, and in this case the cluster equations are simple.

Thus, if $\tilde{M}_{L_1 L_2}$ is given by

$$\tilde{M}_{L_1 L_2} = -i (\tau^{\alpha\alpha-1})_{L_1 L_2} / \sqrt{E} = \begin{bmatrix} \alpha & 0 & \beta & 0 \\ 0 & \gamma_{-1} & 0 & 0 \\ \beta & 0 & \gamma_0 & 0 \\ 0 & 0 & 0 & \gamma_1 \end{bmatrix} \quad (8.4.4)$$

$$\begin{aligned} \text{then } \alpha &= 1 - h_0^{(+)}(\sqrt{E} R)^2 + 3 h_1^{(+)}(\sqrt{E} R)^2 \\ \beta &= 2\sqrt{3} h_1^{(+)}(\sqrt{E} R) h_2^{(+)}(\sqrt{E} R) \\ \gamma_{-1} &= 1 - (h_0^{(+)}(\sqrt{E} R) - h_2^{(+)}(\sqrt{E} R))^2 \\ \gamma_0 &= 1 + 3 h_1^{(+)}(\sqrt{E} R)^2 - (h_0^{(+)}(\sqrt{E} R) - 2h_2^{(+)}(\sqrt{E} R))^2 \\ \gamma_1 &= 1 - (h_0^{(+)}(\sqrt{E} R) + h_2^{(+)}(\sqrt{E} R))^2 \end{aligned} \quad (8.4.5)$$

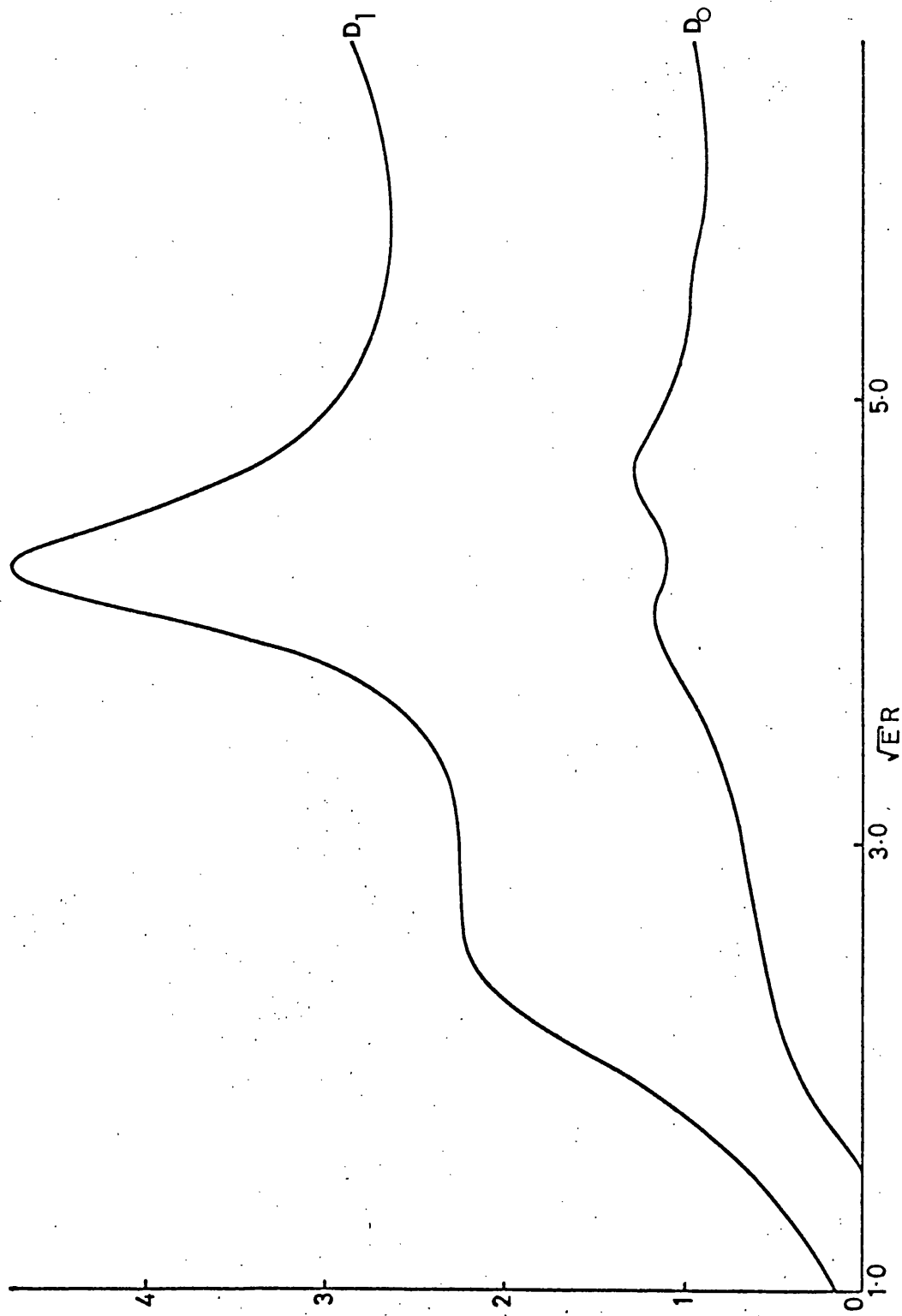
where $h_\ell^{(+)}(x)$ are spherical Hankel functions. The reciprocal of

$M_{L_1 L_2}$ gives $D_\ell(E)$ by

$$D_\ell(E) = \text{Real} \sum_{m=-\ell}^{+\ell} (\tilde{M}^{-1})_{LL} \quad (8.4.6)$$

The result is shown in figure 8.4.3. Electrons are displaced from low energies to form a band around $\sqrt{ER} = 4.26$. Note also that $D_\ell(E) = (2\ell+1)$ for $\sqrt{ER} > 2\pi$ which specifies the maximum range of the band and hence the minimum size of a cluster required in a cluster calculation.

Fig. 8.4.3. $D_0(E)$ and $D_1(E)$ for a two atom cluster of group V type atoms



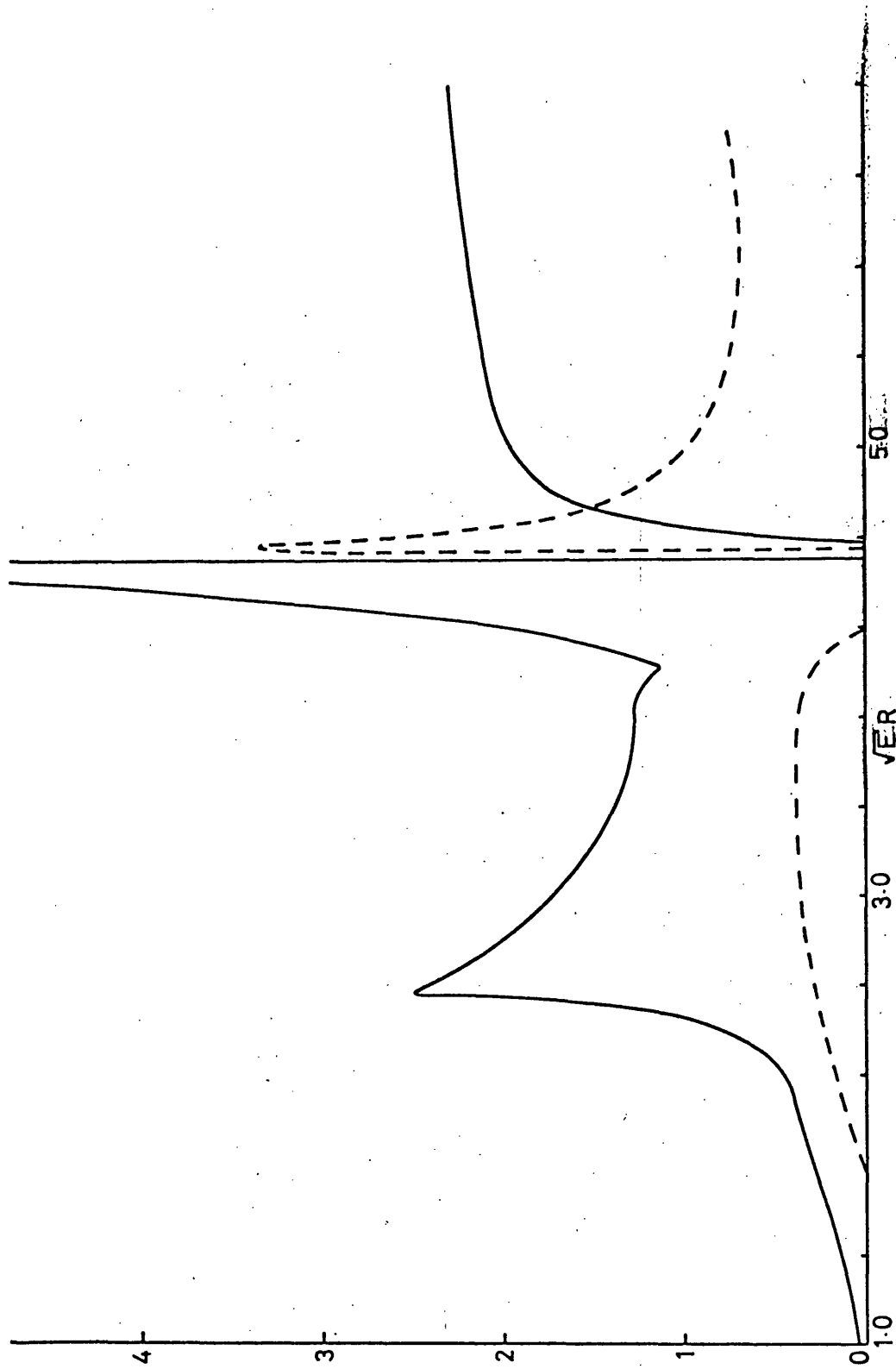
In the archetypal semiconductors such as silicon and germanium, the free atoms have four valence electrons one of which occupies an s state and three p states. In the solid all the states occupied and empty combine into hybrid, or mixed, states. Four of these are low energy bonding states with electron density heaped up between ions along four directions. In energy terms there is a gap between these states and the higher antibonding states. This energy gap is the one responsible for the semiconducting behaviour. For the Mg-Bi system one can investigate something like the same with a simple cluster calculation by recognising that the single atom pairs with the addition of further near neighbours will have bonds which interact strongly. This may be crudely modelled by increasing the strength of the second atom to represent a shell of 3.3 near neighbours with results as shown in figure 8.4.4. The interaction between the bonds produces an energy gap between $\sqrt{ER} = 4.43$ and 4.53 . Thus, for $Mg_3 Bi_2$ with $R = 5.33$ Bohr radii the gap occurs between 0.69 and 0.72 Rydbergs. This is close to the estimated Fermi energy of 0.75 Rydbergs (table 8.4.2) and energy gap of width 0.02 (Ferrier and Herrell, 1970) or 0.05 Rydbergs (Sik and Ferrier, 1974).

8.5 DISCUSSION

In an atomic representation the energy gap can be regarded as arising from the filling of the bismuth s-p band. The criteria for a semiconductor $A_x B_y$ of the same type as that of $Mg_3 Bi_2$ can be summarised as:

- (1) the phaseshifts of A are small at the Fermi energy;

Fig. 8.4.4. Representation of magnesium bismuth at critical concentration, demonstrating possible gap formation. $D_0(E)$ hatched curve and $D_1(E)$ solid curve.



- (2) the s and p phaseshifts of B are large negatively and positively at the Fermi energy respectively. Higher phaseshifts are small.

Further, if V_A and V_B are the number of valence electrons contributed by A and B respectively then the critical concentration is achieved when

$$V_A x = (8 - V_B) y$$

which is the normal condition for molecular combination.

The above criteria (1) and (2) specify certain groups within the periodic table. Most elements of groups I and II satisfy criterion (1) while most elements of groups IV, V and VI satisfy criterion (2). Indeed LiF might be regarded as an extreme case, although charge transfer complicates the issue.

In some circumstances noble metals may replace the more usual simple metal component A. In pure Cu, for instance, the Fermi energy falls above the band and at the Fermi energy all the phaseshifts are small. The d electrons are well localized (House and Smith, 1973) within the muffin-tins and therefore behave somewhat like core electrons. Hence, provided the Fermi energy does not fall when Cu is added to the other component, B, it will behave like a monovalent simple metal. Away from the critical concentration specified by equation (18), on the B rich side the alloy can still be semiconducting if B is a liquid semiconductor. One obvious way is ~~the~~ the alloy to consist of regions of $A_x B_y$ and B. However, in the example of $Cu_x Te_{1-x}$ - a semiconductor

for $x > \frac{2}{3}$ - the structural data of Hawker et al. (1974) suggests that no phase separation occurs. In the Mg_3Bi_2 case it was demonstrated in section 8.4 how the near neighbour environment determines whether a band gap exists - the same is true in the covalent semiconductors. Thus the appropriate covalent B-B bonding in local regions of excess B could ensure the semi-conducting behaviour of the AB alloy on the B rich side of A_xB_y .

In the covalent semiconductors, individual atoms have their valence requirements satisfied locally - that is, they obey the (8-v) rule. Specifically the rule states that within a covalent semiconducting alloy an element with v valence electrons has (8-v) near neighbours. Many such alloys are listed in the second column of table 8.5.1. This table is a proposed classification scheme for elements and binary alloys indicating whether the alloy is semi-conducting in the crystalline (C), amorphous (A) and liquid (L) phases.

The latter members of the group which satisfy the model requirements are known to be highly covalently bonded systems which are not semiconducting in the liquid state. As crystalline solids they crystallize in the zinc blende structure, each atom being tetrahedrally bonded. In the amorphous state their local environments are little disturbed from that found in the crystalline phase and they remain semiconductors. Such alloys can be III-V's or II-VI's and within this range there is a gradual loss of covalency. Their properties are somewhere between those of a fully covalent group IV element and a fully ionic alkali halide. In an alkali halide a very disordered local environment will not destroy the band gap

TABLE 8.5.1

Classification scheme for semiconductors satisfying model requirements (column 1), (8-v) rule (column 2). The third column lists semiconductors which satisfy neither set of requirements.

Semiconductors Satisfying												
Model Requirements	C	A	L	(8-v) Rule	C	A	L	Neither	C	A	L	
Mg_3Bi_2		✓	✓	C	✓	✓						
Li_3Bi			✓	Si	✓	✓	x	MoS ₂	✓	✓		
Mg_3Sb_2	✓	✓		Ge	✓	✓	x	NbSe ₂		✓		
$Cu_2(Se_xTe_{1-x})$			✓	As	x	✓						
Ag_2Te	✓		✓	Se	✓	✓	✓					
ZnTe	✓		✓	Te	✓	✓	x					
CdTe	✓		✓	Se_xTe_{1-x}		✓	✓					
Cu_2S			✓	S	✓		✓					
				$Ge(Se_xTe_{1-x})$	x	✓						
GaAs	✓	✓	x	Sb_2Se_3	✓	✓	✓					
InSb	✓	✓	x	Sb_2Te_3	✓		✓					
GaSb	✓	✓	x	As_2Se_3	✓	✓	✓					
InAs	✓	✓	x	As_2Te_3		✓						
InP	✓	✓										

whereas it will in the group IV semiconductors. Also a whole electron can be considered to have been transferred from the alkali ion to the halogen ion.

From the work of previous chapters it is clear that it is improbable that solid, or liquid, ordered or disordered, alloys can be ionic in the sense that an alkali halide is ionic. It is quite likely that all the alloys listed in the first column of table 8.5.1 have properties between the extremes of a group IV semiconductor and an alkali halide. We suggest that the liquid semiconductors, listed here, should be regarded as more ionic, but without an excessive amount of charge transfer, and the others as more covalent with properties requiring a tetrahedrally symmetric local environment.

8.6 BEHAVIOUR OF TRANSPORT PROPERTIES

Having discussed the origin of the band gap we are now in a position to discuss its shape and ^egeneral relevance to the transport properties. The alloy potentials constructed correspond to near neighbour environments differing, as throughout the sample, in near neighbour distance, co-ordination number and composition. These changes only have a small effect on the scattering phaseshifts and hence on the local criteria for a band gap throughout the liquid alloy. However, this does not prevent some localized regions possessing states within the energy gap for special local structural configurations. These states cannot be extended and are most probably localized in the Mott sense. The Fermi energy should reside in the gap.

At the critical concentration, heating the sample increases the conductivity according to an exponential law but also as structural disorder increases, the energy gap may narrow. ~~If the energy gap~~

~~may narrow~~. If the energy gap becomes narrower than that appropriate to minimum metallic conductivity then the alloy will become metallic as observed by Andreev, Turgunov and Alekseev (1975). Conversely, if the temperature is reduced the liquid becomes an amorphous solid which should also be semiconducting, perhaps with an even larger band gap. The temperature coefficient of resistance and thermopower (equation 1.2.3) essentially yield different aspects of the same basic information as the conductivity.

The other important transport property is the Hall coefficient, R_H , which is a measure of the charge carrier density. In a single component semiconductor the addition of a lower valence dopant would be expected to make the semiconductor p-type. However in the presence of excess Mg in a Mg-Bi alloy system, the model implies that the Fermi energy lies in the conduction band and the alloy is n type. Similarly a dearth of Mg makes the alloy p-type. This behaviour arises from the association of the density of states with the Bi atoms. It also represents another distinction between the "more ionic" and "more covalent" semiconductors in column 1 of table 8.5.1.

Thus in the general AB alloy of this type (1) the thermopower will pass through zero at A_xB_y from negative (A rich) to positive (B rich), (2) the Hall coefficient will be singular at the critical composition being negative infinite on the B rich side, (3) the temperature coefficient of resistance will be negative at the critical composition rising to a positive value on the A rich side and at least remaining negative over a wider concentration range on the B rich side.

8.7 SUMMARY

A study of the electronic properties of the liquid semiconductor Mg₃Bi₂ has been carried out. Muffin-tin potentials, phaseshifts, energies of the bottom of the bands and bandwidths were calculated across the composition range of liquid Mg-Bi. It was shown that the main roles of the Mg atoms are to influence the volume, electron density and energy of the bottom of the valence band; whereas in addition to these roles the Bi atoms are dominant in determining the density of states. As far as the scattering was concerned, the screened Mg ions betrayed their free electron character and were shown to be unimportant. Thus the system could be considered to a reasonable approximation as Bi atoms dissolved in an electron gas. A simple cluster calculation revealed that the large Bi phaseshifts were capable of creating an energy gap at the Fermi energy for the critical composition. The Bi atoms are thus solely responsible for an energy gap occurring when the s-p band is filled. No presumptions of molecular formation at the critical concentrations are made, nor do these results show that molecules form.

A general consideration of many semiconductors led to the three classifications shown in table 8.5.1. The alloys in the first column all approximately satisfy the criteria deduced for the semiconducting behaviour of Mg₃Bi₂. These were subdivided into those considered as more covalent and those considered more ionic. Alloys within these subdivisions do indeed behave differently with respect to disordering of the local environment and doping.

The analysis also reveals that the set of transport coefficients for Mg₃Bi₂ type semiconductors will behave in a distinctive manner.

CONCLUSION : PART II

By the end of chapter IV it became fairly clear that it is unlikely that the liquid semiconductors are ionic in the same sense as sodium chloride. There is strong thermodynamic evidence that chemical complexes do form, particularly in the Mg-Bi and Tl-Te systems, and the natural assumption is that since they cannot be ionically bonded they must be covalently bonded. Two separate calculations on the single hydrogen molecule in an electron gas show that the binding energy decreases with increasing electron number density. This leads one to suspect that the molecular complexes must have binding energies which decrease away from the critical composition, since there will be an electron gas environment provided by the constituent ions. This behaviour, has been modelled for the liquid Mg-Bi system, only to find that a model which assumes a constant binding energy for the $Mg_3 Bi_2$ complexes across the concentration range provides better agreement with experimental thermodynamic and electron transport data.

The final chapters have studied the liquid semiconducting Mg-Bi system adopting an approach distinctly different from that of the previous chapters. A phenomenological study of this system has demonstrated that it is possible for an energy gap in the density of states to occur at the critical composition with the filling of the s-p bands on the bismuth atoms. No presumptions of molecular formation are made. Furthermore, it does appear that this interpretation can provide a scheme, in terms of the positions of the elements within the periodic

table, to explain the occurrence of many liquid semiconductors.

BIBLIOGRAPHY

- Abramowitz, M. and Stegun, I.A., (1965), Handbook of Mathematical Functions, Applied Maths, Series 55.
- Allgaier, R.S., (1969), Phys. Rev., 185, 227.
- Andreev, A., Turgonov, T. and Alekseev, V.A., (1975), Sov. Phys. Sol. St., 16 (12), 2376.
- Animalu, A.O.E. and Heine, V., (1965), Phil. Mag. 12, 1249.
- Bhatia, A.B. and Hargrove, W.H., (1973), Nuovo Cimm. Lett., 8, 1025.
(1974), Phys. Rev. B 10, 3186.
- Bhatia, A.B. and Thornton, D.E., (1970), Phys. Rev. B2, 3004.
- Cohen, M.H. and Sak, J., (1972), J. Non. Cryst. Solids, 8-10, 696.
- Cutler, M. and Field, M.B., (1968), Phys. Rev., 169, 632.
- Cutler, M. and Mallon, C.E., (1965), J. App. Phys., 36, 201.
(1966), Phys. Rev. 144, 642.
- Cutler, M. and Peterson, R.L., (1970), Phil. Mag., 21, 1033.
- Dancy, E.A., (1965), Trans. Metall. Soc., AIME, 233, 270.
- Enderby, J.E., (1974A), J. de Physique, Colloque, C-4, 309.
- Enderby, J.E., (1974B), Amorphous And Liquid Semiconductors (J. Tauc, editor), Plenum Press, London and New York.
- Enderby, J.E. and Collings, E.W., (1970), J. Non. Cryst. Solids, 4, 161.
- Enderby, J.E., Hasan, S.B. and Simmons, C.J., (1967), Adv. Phys., 16, 667.
- Enderby, J.E. and Hawker, I., (1972), Proc. Int. Conf. on Amorphous And Liquid Semiconductors, J. Non. Cryst. Solids, 8/9, 687.
- Enderby, J.E. and Howe, R.A., (1968), Phil. Mag., 18, 923.
- Enderby, J.E. and Simmons, C.J., (1969), Phil. Mag., 20, 125.
- Enderby, J.E. and Walsh, L., (1966), Phil. Mag., 14, 991.
- Epstein, S.G., (1972), Physics And Chemistry of Liquid Metals (S.Z. Beer, editor), Marcel Dekker, New York.
- Evans, R., Gyorrfy, B.I., Szabo, N. and Ziman, J.M., (1973), The Properties of Liquid Metals (S. Takeucki, editor), Taylor and Francis, London, 319.

- Faber, T.E., (1972), Introduction To The Theory Of Liquid Metals, Cambridge University Press.
- Faber, T.E. and Ziman, J.M., (1965), Phil. Mag., 20, 125.
- Ferrier, R.P. and Herrell, D.J., (1969), Phil. Mag., 19, 853.
(1970A), J. Non. Cryst. Solids, 2, 278.
(1970B), J. Non. Cryst. Solids, 4, 338.
- Friedel, J., (1958), Nuovo Cim. Suppli., 7, 287.
- Greenwood, D.A., (1970), Electronic And Structural Properties of Amorphous Semiconductors (le Comber and Mort, editors), Academic Press, 127.
- Gunnarsson, O. and Johansson, P., (1975), submitted to Int. J. Avatit. Chem.
- Gunnarsson, O., Johansson, P., Lundqvist, S. and Lundqvist, B.I., (1975), Paper delivered at Electronic Structure and Reactivity of Metal Surfaces Conference, Nato Advanced Study Institute, Antwerp.
- Gyorrffy, B.L., (1973), Scuola Nazionale Di Struttura Della Materia: Fondamenti di Fisica Dello Stato Solido, 227.
- Hanson, H.P., (1958), Constitution of Binary Alloys, New York, McGraw-Hill.
- Harrison, W.A., (1970), Solid State Theory, McGraw-Hill.
- Haug, A., (1972), Theoretical Solid State Physics, Vol. 1, Pergamon Press.
- Hawker, I., Howe, R.A. and Enderby, J.E., (1974), Amorphous And Liquid Semiconductors (le Comber and Mort, editors), Academic Press, 127.
- Heine, V., (1968), The Physics of Metals: I, Electrons (Ziman, editor), London, CUP.
- Heine, V. and Weair, D., (1970), Solid State Physics (Ehrenreich, Seitz and Turnbull, editors), Academic Press.
- Herman, F. and Skillman, S., (1963), Atomic Structure Calculations, Prentice Hall.
- Hodges, C.H. and Stott, M.J., (1973), Phil. Mag. 26, 376.
- Hohenberg, P. and Kohn, W., (1964), Phys. Rev., 136, B864.
- House, D. and Smith, P.V., (1973), J. Phys. F3, 753.
- Howe, R.A. and Enderby, J.E., (1967), Phil. Mag., 16, 141, 467.
- Hubbard, J., (1964), Proc. Roy. Soc. (London), A281, 401.

- Hultgren, R., Orr, R.L., Anderson, P.D., Kelly, K.K., (1963),
Selected Values of Thermodynamic Properties of Metals and
Alloys, Wiley, New York.
- Inglesfield, J.E., (1969A), J. Phys. C, 2, 1285.
(1969B), Acta Metall., 17, 1395.
- Illschner, B.R., and Wagner, C.N., (1953), Acta Metall. 6, 712.
- Jewsbury, P., (1973), Ph.D. Thesis, University of Bristol.
- Joffe, A.F. and Regel, A.R., (1960), Progress in Semiconductors
(A.F. Gibson, editor), New York, Wiley.
- Jones, W. and Young, W.H., (1971), J. Phys. C, 4, 1322.
- Keller, J. and Fritz, J., (1974), Amorphous and Liquid Semiconductors,
(Stuke and Brenig, editors), Taylor and Francis, London, 2, 975.
- Keller, J. and Smith, P.V., (1972), J. Phys. C5, 1109.
- Keller, J. and Ziman, J.M., (1972), J. Non. Cryst. Solids, 8-10, 111.
- Kittel, C., (1963), Quantum Theory of Solids.
(1966), Intro. to Solid State Physics, 3rd Edition, Wiley.
- Kohn, W. and Rostoker, N., (1954), Phys. Rev. 94, 111.
- Kohn, W. and Sham, L.J., (1965), Phys. Rev., 140, A1133.
- Korringa, J., (1947), Physica, 13, 392.
- Loucks, T.L., (1967), Augmented Plane Wave Method, Benjamin.
- McGill, T.C. and Klima, J., (1970), J. Phys. C3, L163.
- Margenau, H. and Murphy, G.M., (1955), The Mathematics of Physics and
Chemistry, 2nd Edition, van Nostrand.
- Mattheiss, L.F., (1964), Phys. Rev. 134, A970.
- Miedema, A.R., (1973A), J. Less Common Metals, 32, 117.
(1973B), J. Phys. F: Metal Phys., 3, 1803.
- Miedema, A.R., de Boer, F.R. and de Chatel, P.F., (1973), J. Phys F:
Metal Phys., 3, 1558.
- Mott, N.F., (1969), Phil. Mag., 19, 835.
- Mott, N.F., (1973), Electronic and Structural Properties of Amorphous
Semiconductors (le Comber and Mort, editors).
- Mott, N.F. and Gurney, R.W., (1940), Electronic Processes in Ionic
Crystals, Oxford.

- O'Sullivan, W.J., Switendick, C. and Schirber, J.E., (1970), Phys. Rev. B 1 (4), 1443.
- Perron, J.C., (1967), Adv. Phys. 16, 657.
- Phillips, J.C., (1970A), Rev. Mod. Phys., 43 (8), 317.
(1970B), Phys. Today, 43 (2), 23.
- Ratti, V.K. and Bhatia, A.B., (1975), J. Phys. F: Metal Phys, 5, 893.
- Sanderson, E.A., (1960), Chemical Periodicity, New York.
- Sik, M.J. and Ferrier, R.P., (1974), Amorphous and Liquid Semiconductors (Stuke and Benig, editors), Taylor and Francis, London, 2, 1331.
- Slater, J.C., (1963), Quantum Theory of Molecules and Solids, Vol. 1, McGraw-Hill.
(1965), Quantum Theory of Molecules and Solids, Vol. 2, McGraw-Hill.
- Smith, J.R., Ying, S.C. and Kohn, W., (1973), Phys. Rev. Lett., Vol. 30, No. 13, 610.
- Smith, P.V. and Lloyd, P., (1972), Adv. Phys. 21, 69.
(1974),
- Soven, P., (1967), Phys. Rev. 156, 809.
- Thorpe, M.F. and Weaire, D., (1974), Amorphous and Liquid Semiconductors (Stuke and Benig, editors), Taylor and Francis, London, 2, 917.
- Varley, J.H.O., (1954), Phil. Mag. 45, 887.
- Velicky, B., Kirkpatrick, S., Ehrenreich, H., (1968), Phys. Rev. 175, No. 3, 747.
- Waseda, Y. and Suzuki, K., (1972), Phys. Stat. Sol. (B), 49, 339.
- Williams, A.R. and Morgan, J. van W., (1974), J. Phys. C7, 37.
- Ziman, J.M., (1961), Phil. Mag., 6, 1013.
(1965), Proc. Phys. Soc., 86, 337.
(1972), Sol. St. Phys. 26, I.

APPENDIX 1

The Pseudopotential and Ziman Theory

Electrons in solids have wavefunctions which are essentially smooth for most of the time but which oscillate violently close to the ion centres. Orthogonalized plane waves ($|OPW\rangle$) describe this behaviour relating plane wave states outside the atomic core ($|PW\rangle$) to the core states ($|c\rangle$):

$$|OPW\rangle = |PW\rangle - \sum_c |c\rangle \langle c|PW\rangle \quad (A1.1)$$

The strong oscillations near the ion centres give rise to a large kinetic energy which partially cancels out the effect of the strong potential. This is expressed as:

$$w_{\text{pseudo}} = v_{\text{real ion}} + \sum_c (E - E_c) |c\rangle \langle c| \quad (A1.2)$$

where $|E_c| < |E|$ and $|w_{\text{pseudo}}| < |v_{\text{real ion}}|$.

The resistivity (ρ) can be expressed in terms of the electron number density (n), the relaxation time (τ_z) and the free electron mass (m) as:

$$\rho = \frac{m}{ne^2} \frac{1}{\tau_z} \quad (A1.3)$$

The total pseudopotential $W(r)$ scatters electrons from state $|k_1\rangle$ to state $|k_2\rangle$ with matrix elements given by:

$$\langle k_2 | W(r) | k_1 \rangle = \frac{1}{V} \int_0^V \exp(-iq \cdot r) W(r) \exp(iq \cdot r) d\mathbf{r} \quad (A1.4)$$

where plane wave states of the form $(V)^{-\frac{1}{2}} e^{-ik \cdot r}$ have been taken and $q = (K_2 - K_1)$. (A1.4) is identified as the Fourier transform:

$$\langle -k_2 | W(r) | k_1 \rangle = \frac{1}{V} W(q) \quad (\text{A1.5})$$

The relaxation rate is expressed as:

$$\frac{1}{\tau_Z} = \frac{mk_F}{2\pi\hbar^3} \frac{1}{V} \int_0^\pi |\overline{W(q)}|^2 \sin\theta (1 - \cos\theta) d\theta \quad (\text{A1.6})$$

where $\overline{W(q)}$ is a time average.

The total pseudopotential is defined by:

$$W(r) = \sum_i \omega(r - R_i) \quad (\text{A1.7})$$

where $\omega(r - R_i)$ is the individual ion pseudopotential

$$\begin{aligned} W(q) &= \sum_i \int \omega(r - R_i) \exp iq \cdot (r - R_i) \exp iq \cdot R_i dr \\ &= \omega(q) \sum_i \exp iq \cdot R_i \end{aligned} \quad (\text{A1.8})$$

$$|\overline{W(q)}|^2 = |\omega(q)|^2 \sum_{ij} \exp iq \cdot (R_i - R_j) \quad (\text{A1.9})$$

Hence the resistivity may be given by:

$$\rho = \frac{m}{ne^2} \frac{mk_F}{2\pi\hbar^3} \int_0^\pi |\omega(q)|^2 N S(q) (1 - \cos\theta) \sin\theta d\theta \quad (\text{A1.10})$$

Using

$$\sin \frac{\theta}{2} = \frac{q}{2k_F}$$

$$\rho = \frac{8m^2 k_F^2}{2\pi n e^2 \hbar^3} \frac{N}{V} \int_0^1 |\omega(q)|^2 S(q) \left[\frac{q}{2k_F} \right]^3 d \frac{q}{2k_F} \quad (\text{A1.11})$$

Now

$$n = \frac{k_F^3}{3\pi^2}$$

$$\rho = \frac{4m^2 \pi^3}{h^3 e^2 k_F^2} \frac{N}{V} \int_0^1 |\omega(q)|^2 S(q) \left[\frac{q}{2k_F} \right]^2 d \left(\frac{q}{2k_F} \right)^3 \quad (\text{A.12})$$

which is usually written

$$\rho = \frac{3\pi m^2}{h^3 e^2 k_F^2} \frac{N}{V} \langle |\omega(q)|^2 S(q) \rangle \quad (\text{A.13})$$

APPENDIX 2

The Hellmann-Feynmann Theorem

Given the Hamiltonian

$$H = H_0 + g H_{\text{int}} \quad (\text{A2.1})$$

and the value of

$$E_{\text{int}}(g) = \langle \phi_0(g) | g H_{\text{int}} | \phi_0(g) \rangle \quad (\text{A2.2})$$

then the exact value of the total ground-state energy

$$E_0(g) = \langle \phi_0(g) | H_0 + g H_{\text{int}} | \phi_0(g) \rangle \quad (\text{A2.3})$$

is given by

$$E_0(g) = E_0(0) + \int_0^g \frac{1}{g} E_{\text{int}}(g) dg \quad (\text{A2.4})$$

where g is a coupling constant and H_0 the kinetic energy.

(A2.4) follows from (A2.2) and (A2.3) since

$$\frac{dE_0}{dg} = \frac{1}{g} E_{\text{int}}(g) + E_0(g) \frac{d}{dg} \langle \phi_0(g) | \phi_0(g) \rangle \quad (\text{A2.5})$$

The second term on the right-hand side is zero because the normalization is independent of g . $E_0(g)$ is the exact eigenvalue and $\phi_0(g)$ the exact eigenfunction. Hence we have a special case of the Hellmann-Feynmann theorem:

$$\frac{dE_0}{dg} = \frac{1}{g} E_{\text{int}}(g) \quad (\text{A2.6})$$

Integrating (A2.6) gives (A2.4).

ABSTRACT'The Electronic Structure Of Disordered Systems' by P. M. Dooley

A theoretical study has been carried out on the electronic structure of concentrated disordered alloys and liquid semiconductors made up of components which are metallic in the pure liquid state (e.g. Mg-Bi, Li-Bi). For the latter there is strong evidence to suggest that chemical complexes form at the critical concentration ($Mg_3 Bi_2$, $Li_2 Bi$). The nature of the bonding is discussed in depth to reveal that it is unlikely that the bonding is ionic in the same sense as sodium chloride. Two separate calculations on the single hydrogen molecule in an electron gas show that the binding energy decreases with increasing electron number density. The assumption of the covalently bonded $Mg_3 Bi_2$ complex, and the associated change in binding energy with varying electron environment away from the critical composition, does not provide good agreement with experimental thermodynamic and electron transport data. Charge transfer within disordered systems is an effect associated with interatomic bonding. Its relationship with electronegativity difference and atomic cell size is considered in detail. No simple correlation is found to exist between charge transfer and electronegativity difference.

A phenomenological study carried out on the liquid semiconducting Mg-Bi system has demonstrated that it is possible for an energy gap to occur at the critical composition with the filling of the s-p bands on the bismuth atoms. No presumptions of molecular formation are made. It does appear that this interpretation can provide a scheme, in terms

of the positions of the elements within the periodic table, to explain the occurrence of many liquid semiconductors.
